Applicability of Natural Porous Materials and Lime with Conditioning and Sorption Properties for Wastewater Treatment

Anvendelse av Naturlige Porøse Materialer og Kalk med Kondisjonering og Sorpsjon Egenskaper for Avløpsrensing

Philosophiae Doctor (PhD) Thesis

Emilio Humberto Alvarenga Castellanos

Department of Environmental Sciences

Faculty of Environmental Science and Technology

Norwegian University of Life Sciences

Ås (2016)

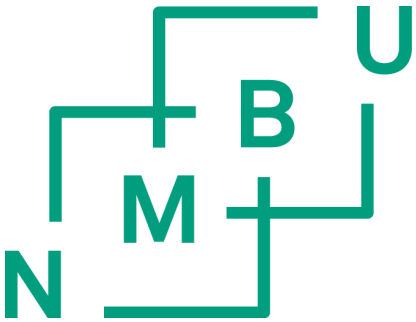

Thesis number 2016:77

ISSN 1894-6402

ISBN 978-82-575-1394-8

Supervisors

Main Supervisor:
Prof. Brit Salbu
Department of Environmental Sciences
Norwegian University of Life Sciences
P.O. Box 5003, NMBU N-1432, Ås Norway

Co-Supervisor:
Prof. Lindis Skipperud
Department of Environmental Sciences
Norwegian University of Life Sciences
P.O. Box 5003, NMBU N-1432, Ås Norway

Co-Supervisor:
Assoc. Prof. Carlos Salas-Bringas
Department of Mathematical Sciences and Technology
Norwegian University of Life Sciences
P.O. Box 5003, NMBU N-1432, Ås Norway

Co-Supervisor:
Dr. Anne Falk Øgaard
Norwegian Institute of Bioeconomy Research
P.O. Box 115, NO-1431 Ås Norway

Co-Supervisor:
Dr. Sergey Hayrapetyan
Faculty of Chemistry
Yerevan State University
A. Manoukyan St. 1, 0025, Yerevan Armenia

Co-Supervisor:
Dr. Espen Govasmark
Waste to Energy Agency of Oslo County
P.O. BOX 54 Mortensrud, NO-1215, Oslo Norway

Co-Supervisor:
Researcher Lasse Vråle
Siv. Ing. Lasse Vråle AS
Steinspranget 20
NO-3029, Drammen Norway

Evaluation Committee

First opponent:
Dr. Bernhard Drosg
Institute for Environmental Biotechnology
University of Natural Resources and Life Sciences, Vienna
Konrad-Lorenz-Straße 20
3430 Tulln an der Donau
Vienna, Austria

Second opponent:
Prof. Emeritus Per Aagaard
Department of Geosciences
University of Oslo
Sem Sælands vei 1
Geologibygningen
0371 Oslo, Norway

Committee coordinator:
Prof. Deborah H. Oughton
Department of Environmental Sciences
Norwegian University of Life Sciences
P.O. Box 5003, NMBU N-1432, Ås Norway

Acknowledgements

Firstly, I would like to express my deepest gratitude to my parents and relatives in Norway. They have given me love, guidance and support and have provided shelter during this journey.

Secondly, I would like to thank the Norwegian Institute of Bioeconomy Research (NIBIO) for giving me the opportunity to work for the first time in Norway. I had a wonderful work environment throughout these years with very kind colleagues. I would like to thank especially my leader Cand. Real. Tormod Briseid at NIBIO from the Bioresources and Recycling Technologies Department. Tormod has always been supportive towards my work and I am thankful for his valuable input and for pointing out my strengths and weaknesses in the most constructive ways.

My supervisors played a key role in this education program and I will always be deeply thankful for their help and advice. Prof. Brit Salbu as my main supervisor from the Norwegian University of Life Sciences (NMBU) encouraged me to think broader for developing ideas and new knowledge. I feel honored and grateful for that. I also would like to give acknowledgement to Dr. Sergey Hayrapetyan from Yerevan State University for his significant contributions to my work and for hosting me during my research period abroad in Armenia.

In addition, I would like to thank all the engineers and technicians from the NMBU who have worked by my side to reach the goal. You all have been kind and resourceful particularly during difficult times of this adventure.

My friends have to be mentioned as well. They created a very nice social environment for me during my studies in Ås, especially Luz Muñoz and Sergio Chávez, two persons with whom I share a deep passion for Latin America. For us three, the latter is neither a continent nor a region. It is simply a colorful cultural concept and a new way of thinking.

"I set out to discover the why of it, and to transform my pleasure into knowledge."

Charles Baudelaire (1821-1867)

To my Parents who are my infinite source of motivation and inspiration

Contents

Index of figures

Index of tables

Abbreviations

AD: Anaerobic digestion

ADR: Anaerobic digestion residue

CaO: Quick lime (as calcium oxide)

$Ca(OH)_2$: Hydrated lime

CSTR: Continuously stirred tank reactor

DB: Diatomite-bentonite

EU: European Union

FRE: FREVAR KF

GHG: Green house gas

HMM: High molecular mass

JT: Jar-tester

LD: Landfill directive

LMM: Low molecular mass

LOD: Limit of detection

LOQ: Limit of quantification

P_{inorg}: Inorganic P

P_{org}: Organic P

RAE: Relative agronomic efficiency

RR: Rotational rheometer

SLS: Separation of liquids from solids

SO: Silicon oil

TS: Total solids

ULL: Ullensaker Gardermoen

WRC: Water retention capacity

WWT: Wastewater treatment

WWTPs: Wastewater treatment plants

Symbols

$\dot{\gamma}_{avg}$: Average shear rate (s^{-1})

τ: Average shear stress (Pa)

η_{avg}: Average dynamic viscosity (Pa·s)

η: Dynamic viscosity (Pa·s)

M: Torque (N·m)

N: Rotational speed (rpm)

$\dot{\gamma}$: Shear rate (s^{-1})

q: Sorption capacity (mg g^{-1} or µg g^{-1})

Q: Flow rate (L min^{-1} or mL min^{-1})

^{238}U: Uranium isotope

Summary

Urban wastewater streams are produced in large quantities and removal of contaminants is required for compliance with environmental regulations. The water separation, concentration of particles as solid phases (e.g., flocculation) and the removal of substances of interest provides an effective waste management scheme for such purpose. Such approach for separation of liquid from solids is directly relevant to the biogas industry effluents and landfill leachates management. It implies that nutrients can be recycled from the wastewater treatment plants (WWTPs) and from biogas processes in biofertilizers whereas inorganic pollutants such as heavy metals or radionuclides, can be removed from leachates to avoid transport to the environment (e.g., run-off from agricultural soils and from landfills to water bodies).

This doctoral thesis includes and relates aspects of separation processes of liquids from solids in two main areas of focus for wastewater treatment (WWT); water separation or dewatering (**Paper I** and **II**) and retention of elements of interests by sorption (**Paper IV** and **V**). A study of recyclability of phosphorus (P) in sludge (**Paper III**) is also taken into consideration and it deals with conditioning for dewatering and sorption. The dewatering part covers sewage sludge and anaerobic digestion residue (ADR) from biogas production. On the other hand, the sorption part entails the development of sorption systems utilized for removal of potassium (K^+), and one of these systems has been utilized for removal of uranium (U(VI) or U^{6+} quantified as ^{238}U) in leachate from an alum shale landfill. Natural porous materials and lime are applied as mineral conditioners to the effluents for achieving favorable separation performance in both areas of focus. The results of this thesis are the basis for further upscaling and design of a sorption process for either recovery of nutrients such as K^+ or removal of heavy metals such as U^{6+}. Such separation unit could be used for treatment of effluents in the biogas industry and landfills. Dewatering performance prior to sorption and the regeneration of the sorbent are, however, critical for achieving a cost-effective treatment unit.

The water separation or dewatering of effluents of the biogas process requires the addition of chemical conditioners (e.g., polyacrylamide) to the treatment, which increases the operational cost of the separation. Therefore, a bentonite-based material was utilized as a mineral conditioner in **Paper I** for decreasing the dose of the polymer in the flocculation of ADR or digestate. A term defined as water retention capacity (WRC) was introduced as a dewatering performance parameter. Moreover, turbidity and capillary suction time measurements in the effluents after flocculation were taken into account for the assessment of vacuum filtration as a dewatering unit in a laboratory scale. Moreover, an empirical mathematical model for average viscosity (η_{avg}) was developed in **Paper II** due to a calibration process of a Jar-tester (JT) mixer coupled to a rotational rheometer. The standard fluid for the calibration was Newtonian and the model described the behavior of the average shear stress in a turbulent regime. A viscous and turbulent component had an effect on the η_{avg} of the fluid investigated in a turbulent regime. Thereby, the model is a first step for understanding changes in η_{avg} of wastewater or ADR and the degree of liquid to solid separation during flocculation when adding conditioners in turbulent regime as performed in **Paper I**.

Lime was used as a conditioner for increasing the plant uptake of P from sludge and ADR (**Paper III**). This investigation showed that liming of Fe-precipitated sludge and its digestate

increased the bioavailability of P, both from a chemical perspective with a modified sequential extraction scheme and with a greenhouse pot experiment with P uptake in barley.

Paper IV includes the dynamic sorption in laboratory scale of readily hydrated K^+ in a synthetic solution (2 g L^{-1} KOH) by means of a SiO_2–MnO_2–diatomite composite sorbent. The sorption system was based on cation exchange chromatography. Moreover, it was possible to recover K^+ from alum shale leachate using a bentonite-diatomite sorbent working as a cation exchanger, which was also used in the dewatering study as described in **Paper I**. The sorption process was carried out at a pH of 7.5. This pH condition increased the sorption capacity of U^{6+} about 100 times in dynamic mode (**Paper V**) compared to U in acidic leachate (pH 4.0) and at the same scale. This aspect indicated that the cation exchanger is effective for sorption of both K^+ and U^{6+} from the leachate at pH values of 7.5 or higher. Furthermore, a pilot scale trial with the bentonite-based system as described in sub-sections 5.2.7 and 6.5.2 was performed as a first step of the treatment of leachate on site. Favorable operational conditions (flow rate and pH) were determined although the sorbent was not saturated. This approach showed how beneficial the sorption unit could be for both nutrient and heavy metals removal.

This doctoral thesis was conducted at the Department of Environmental Sciences (IMV) of the Faculty of Environmental Science and Technology at the Norwegian University of Life Sciences (NMBU) and the Norwegian Institute for Agricultural and Environmental Research (Bioforsk)/Norwegian Institute of Bioeconomy Research (NIBIO), both located in Ås Norway from January 2013 to June 2016. The study comprises work packages of three different projects. The Research Council of Norway and industrial partners co-funded two of these projects: “Fixation of Nutrient Elements in Digestate” and “Sewage Sludge in Agriculture – Recycling of Phosphorus and Food Safety”. The Nordic Road Water (NORWAT) research and development program of the Norwegian Public Roads Administration (Statens Vegvesen) financed the third one in cooperation with NMBU/IMV: “Effects and Environmental Risks Associated to Interventions in Areas with Sulfide Rich Minerals (NORWAT/RV4)”. Additionally, funding for covering costs related to a five weeks research visit to the Faculty of Chemistry of Yerevan State University (Armenia) was provided by Bioforsk/NIBIO. Finally, the sorption system utilized for U separation was developed within the scope of the Centre for Environmental Radioactivity (CERAD), a Centre of Excellence of NMBU.

Sammendrag

Urbant avløpsvann blir produsert i store mengder, og for å oppfylle miljøkravene er det nødvendig å behandle dette for å fjerne forurensinger. Vannseparasjon, konsentrasjon av partikler i faste faser (f.eks. ved flokkulering) og fjerning av spesifikke stoffer er et effektivt system for vannrensing. Separasjon av stoffer fra flytende fase er også relevant for biogassanleggenes restprodukt (biorest) og utlekkingsvann fra deponier. Dette innebærer at næringsstoffer kan resirkuleres fra avløpsanlegg (WWTPs) og fra biogassprosesser til for eksempel biogjødsel, mens uorganiske miljøgifter som tungmetaller og radionuklider kan fjernes fra utlekkingsvann for å unngå overføring til vannforekomster.

Denne doktorgradsavhandlingen inkluderer og relaterer aspekter av separasjonsprosesser for flytende substrat og fokuserer på to hovedområder for avløpsrensing (WWT); Avvanning (**Artikler I** og **II**) og sorpsjon av stoffer av interesse (**Artikler IV** og **V**). En studie av effekt av utråtning av slam og kondisjonering med kalk på plantetilgjengelighet av fosfor (P) er også inkludert (**Artikkel III**). Avvanningsdelen omfatter avløpsslam og biorest (ADR) fra biogassproduksjon. Sorpsjonsdelen handler først og fremst om utvikling av sorpsjonssystemer for fjerning av kalium (K^+) og en av disse systemene ble brukt for fjerning av uran (U (VI) eller U^{6+} kvantifisert som ^{238}U) fra utlekkingsvann fra et alumskiferdeponi. Naturlige porøse materialer og kalk ble anvendt som kondisjoneringsmidler for å oppnå en effektiv separasjon i begge tilfellene. Avhandlingens resultater er grunnleggende for å kunne utvikle en oppskalert sorpsjonsenhet for enten gjenvinning av næringsstoffer som K^+ eller fjerning av tungmetaller som U^{6+}. En slik separasjonsenhet vil kunne bli benyttet for behandling av flytende restprodukter fra biogassanlegg og for avrenning fra deponier. Avvanningseffektiviteten før sorpsjon og regenerering av sorbenten er derimot kritiske faktorer for å oppnå en kostnadseffektiv behandlingsenhet.

Avvanning av flytende restprodukter fra biogassprosessen krever tilsetning av kjemiske kondisjoneringsmidler (f.eks. polyakrylamid), noe som øker driftskostnadene for separasjonen. For å kunne redusere dosering av polymeren, ble effekten av et bentonitt-basert materiale (mineralkondisjoneringsmiddel) på flokkulering av ADR undersøkt i **Artikkel I**. Vannretensjonskapasitet (WRC) ble innført som en parameter for avvanningseffektiviteten. I tillegg ble turbiditet og kapillær sugetid målt i avløpene etter flokkulering, for å evaluere en vakuumfiltreringsenhet for avvanning i labskala. Videre ble det utviklet en empirisk matematisk modell for beregning av en gjennomsnittlig viskositet (η_{avg}) i **Artikkel II** ved hjelp av en kalibreringsprosess for en Jar-tester (JT) koblet til et roterende rheometer. Standardvæsken til kalibreringen var Newtonske og modellen beskrev stoffegenskapene som blant annet den gjennomsnittlige skjærspenningen (τ) i et turbulent flytende regime. En viskøs og en turbulent komponent hadde effekt på η_{avg} i væsken som ble undersøkt i det turbulente regimet. Modellen er et første skritt mot å forstå endringer i η_{avg} i enten avløpsvann eller ADR, samt graden av avvanning ved flokkulering med kondisjoneringsmidler i turbulent regime, som undersøkt i **Artikkel I**.

Kalk ble benyttet som kondisjoneringsmiddel i **Artikkel III** for å undersøke effekten på plantetilgjengeligheten av P i slam og ADR. Resultatene viste at kalking av både Al- og Fe-felt slam og biorest økte biotilgjengeligheten av P både fra et kjemisk perspektiv med en modifisert fraksjoneringsmetode for P og i et vekstforsøk med bygg i drivhus.

Artikkel IV omhandler dynamisk sorpsjon på labskala av K^+ i en syntetisk løsning (2 g L^{-1} KOH) på kompositttsorbenten SiO_2–MnO_2–diatomitt. Sorpsjonssystemet ble basert på kationebytterkromatografi. Ved hjelp av en bentonitt-diatomitt sorbent kunne K^+ utvinnes fra utlekkingsvann fra alumskifer. Denne sorbenten fungerer som kationbytter og ble brukt i forsøket beskrevet i **Artikkel I**. Sorpsjonsprosessen ble utført ved pH 7,5. Ved denne pH-verdien var sorpsjonskapasiteten av U^{6+} omtrent 100 ganger større enn sorpsjonskapasiteten i surt utlekkingsvann (pH 4,0) (**Artikkel V**). Dette indikerte at kationbytteren er effektiv for sorpsjon av både K^+ og U^{6+} fra utlekkingsvann ved pH-verdi på minst 7,5. I tillegg ble et pilotskalaforsøk med det bentonitt-baserte systemet utført, som beskrevet i avsnittene 5.2.7 and 6.5.2. Dette var det første steget for utvikling av en stedstilpasset renseløsning. Selv om sorbenten ikke ble mettet, ble gunstige driftsforhold identifisert (strømningshastighet og pH). Disse forsøkene viste hvor effektive de undersøkte sorbentene kan være for fjerning av både næringsstoffer og tungmetaller.

Denne doktorgradsavhandlingen ble gjennomført ved Instituttet for Miljøvitenskap (IMV) ved Fakultetet for Miljøvitenskap og Teknologi (MiljøTek) ved Norges Miljø- og Biovitenskapelige Universitet (NMBU) og Bioforsk/Norsk Institutt for Bioøkonomi (NIBIO), begge i Ås, Norge, fra januar 2013 til juni 2016. Undersøkelsene inngår i arbeidspakker fra tre ulike prosjekter. Norges Forskningsråd og industripartnere finansierte to av disse prosjektene: "Fiksering av Næringsstoffer i Biorest" og "Avløpsslam til jordbruksarealer - Resirkulering av Fosfor og Mattrygghet". Statens Vegvesen, finansierte det tredje prosjektet i samarbeid hos NMBU/IMV: "Effekter og Miljørisiko Knyttet til Inngrep i Områder med Sulfidrike Mineraler (NORWAT/RV4)". I tillegg ble et femukers opphold ved det Kjemiske Fakultetet ved Jerevans Universitet (Armenia) finansiert av Bioforsk/NIBIO. Sorpsjonssystemet som ble benyttet for U sorpsjon ble utviklet ved Senter for Radioaktivitet, Mennesker og Miljø (CERAD) som er et Senter for Fremragende Forskning ved NMBU.

Resumen

Flujos de agua residual son producidos en grandes cantidades y se requiere por consiguiente remover contaminantes para el cumplimiento de regulaciones ambientales. La separación de agua, concentración de partículas en agregados sólidos (e.g., floculación) y la remoción de sustancias de interés provee un esquema efectivo de manejo de desechos para tal causa. Adicionalmente, este enfoque de separación de líquido a sólidos abarca directamente el manejo de efluentes de la industria de biogás así como también, el de lixiviados de rellenos sanitarios. De esta manera, nutrientes pueden ser reciclados en las plantas de tratamiento de agua residual (WWTPs) y en procesos de producción de biogás por medio de biofertilizantes mientras que contaminantes inorgánicos como metales pesados y radionúclidos, pueden ser separados en lixiviados para evitar su movilización en el ambiente (e.g., escurrimiento de los suelos agrícolas y de rellenos sanitarios hacia cuerpos de agua).

Esta tesis doctoral incluye y relaciona aspectos de procesos de separación de líquido a sólido en dos áreas predominantes de enfoque para tratamiento de agua residual (WWT); separación de agua o deshidratación (**Artículo I** y **II**) y retención de elementos de interés por medio de sorción (**Artículo IV** y **V**). Un estudio de reciclaje de fósforo (P) en lodos de agua residual (**Artículo III**) es también tomado en cuenta y se enfoca en acondicionamiento para deshidratación y sorción. La parte de separación de agua abarca lodos de agua residual y digestado de producción de biogás (ADR). Por otro lado, la parte de sorción comprende fundamentalmente el desarrollo de sistemas de sorción utilizados para la separación de potasio (K^+) y uno de esos sistemas fue utilizado para remover uranio (U(VI) o U^{6+} cuantificado como ^{238}U) de un lixiviado de un relleno sanitario de esquisto de aluminio. Materiales de porosidad natural y cal fueron utilizados como acondicionadores minerales de los efluentes para alcanzar alta eficiencia de separación en ambas áreas de enfoque. Los resultados de esta tesis son la base para el diseño de una unidad de sorción en una mayor escala de proceso para recuperación ya sea de nutrientes como K^+ o remoción de metales pesados como U^{6+}. Esta unidad de separación puede ser usada para tratamiento de efluentes en la industria de biogás y en rellenos sanitarios. Alta eficiencia de deshidratación y la regeneración del adsorbente constituyen no obstante, aspectos críticos de operación para alcanzar una unidad de tratamiento rentable.

La separación de agua o deshidratación de efluentes del proceso de biogás requiere agregar acondicionadores químicos (e.g., poliacrilamida) al proceso que incrementan los costos operacionales de la separación. Por consiguiente, un material basado en bentonita fue utilizado como acondicionador mineral en el **Artículo I** para reducir la dosis de polímero en la floculación del ADR. Un término definido como capacidad de retención de agua (WRC) fue introducido como un parámetro de eficiencia de deshidratación. Además, mediciones de turbidez y tiempo de succión capilar fueron hechas en efluentes después de floculación para la evaluación de una unidad de deshidratación de filtración al vacío en escala de laboratorio. Como complemento, un modelo matemático empírico para medición de viscosidad promedio (η_{avg}) fue desarrollado en el **Artículo II** como producto de un proceso de calibración de un mezclador de un Jar-tester (JT) adaptado a un reómetro rotacional. El fluido estándar de calibración tomado en cuenta para la calibración fue Newtoniano y el modelo describió el comportamiento del esfuerzo cortante (τ) en régimen de flujo turbulento. Tanto un componente viscoso como uno turbulento tuvieron un efecto en la η_{avg} del fluido investigado en régimen de flujo

turbulento. Por lo tanto, el modelo constituye un primer avance para el entendimiento de los cambios de la η_{avg} del agua residual o del ADR y del grado de separación de líquido a sólido cuando acondicionadores son agregados en régimen de flujo turbulento durante la floculación; tal y como como se llevó a cabo en el **Artículo I**.

Cal fue utilizada como acondicionador para incrementar la biodisponibilidad de P en plantas desde lodos de aguas residuales y ADR (**Artículo III**). Esta investigación mostró que al agregar cal al lodo precipitado con Fe y su respectivo digestado, se incrementó la biodisponibilidad de P, tanto con un esquema de extracción secuencial modificado como con un experimento de invernadero para biodisponibilidad de P en cebada.

El **Artículo IV** incluye un estudio de sorción de K^+ hidratado de una solución sintética (2 g L^{-1} KOH) en modo dinámico y en escala de laboratorio por medio de un adsorbente compuesto de SiO_2–MnO_2–diatomita. El sistema de sorción fue basado en cromatográfia de intercambio iónico. Además, fue posible recuperar el K^+ del lixiviado de esquisto de aluminio usando un adsorbente de bentonita-diatomita funcionando como intercambiador iónico el cual fue utilizado en el estudio de deshidratación descrito en el **Artículo I**. El proceso de sorción fue llevado a cabo a un pH de 7.5. Está condición de pH incrementó la capacidad de adsorción de U^{6+} alrededor de 100 veces en modo dinámico (**Artículo V**) con respecto a la obtenida para U en el lixiviado acídico (pH 4.0) y en la misma escala de tratamiento. Este aspecto evidenció claramente que el intercambiador iónico es efectivo para sorción de K^+ y U^{6+} del lixiviado a valores de pH mayores que 7.5. Más aún, un experimento en escala piloto fue llevado a cabo con el material basado en bentonita como un primer paso para un diseño de una unidad de tratamiento "in situ" que es descrito en los apartados 5.2.7 y 6.5.2. Condiciones favorables de proceso (flujo volumétrico y pH) fueron determinadas; no obstante, el adsorbente no fue saturado. Este enfoque mostró cuan beneficiosa puede ser una unidad de sorción para remoción tanto de nutrientes como de metales pesados.

Esta tesis doctoral fue realizada en el Departamento de Ciencias Ambientales (IMV) de la Facultad de Ciencia Ambiental y Tecnología en la Universidad de Ciencias de la Vida de Noruega (NMBU) y en el Instituto Noruego de Investigación de Agricultura y Ambiente (Bioforsk)/Instituto Noruego de Investigación de Bioeconomía (NIBIO), ambos ubicados en Ås, Noruega, desde enero del 2013 hasta junio del 2016. La investigación comprende paquetes de trabajo de tres diferentes proyectos. Dos de ellos fueron cofinanciados por el Consejo Noruego de Investigación e industrias asociadas: "Fijación de Elementos Nutrientes en Digestado" y "Lodos de Aguas Residuales en Agricultura – Reciclaje de Fosforo y Seguridad Alimentaria". El programa de investigación y desarrollo "Nordic Road Water (NORWAT)" de la Administración Noruega de Vías Públicas (Statens Vegvesen), financió el otro proyecto en colaboración con NMBU/IMV: "Efectos y Riesgos Ambientales Asociados con Intervenciones en Áreas con Minerales Ricos en Sulfuro (NORWAT/RV4)". Adicionalmente, el financiamiento para una estancia de investigación doctoral de cinco semanas en la Facultad de Química de la Universidad de Ereván (Armenia), fue proporcionado por Bioforsk/NIBIO. Finalmente, el sistema de sorción utilizado para separación de U fue desarrollado dentro del enfoque del Centro de Radioactividad Ambiental (CERAD), un Centro de Excelencia de la NMBU.

List of papers

I. **Alvarenga, E.**, Hayrapetyan, S., Govasmark, E., Hayrapetyan, L., Salbu, B. (2015) Study of the flocculation of anaerobically digested residue and filtration properties of bentonite based mineral conditioners, Journal of Environmental Chemical Engineering, Volume 3, pages 1399-1407. Published.

II. **Alvarenga, E.**, Schüller, R., Salas-Bringas, C. (2015) Calibration of a jar-tester replicated in a rotational rheometer, Annual Transactions of the Nordic Rheology Society, Volume 23, pages 199-205, ISBN 978-91-637-9104-8. Published.

III. **Alvarenga, E.**, Øgaard, A. F., Vråle, L. (2016) Effect of anaerobic digestion and liming on plant availability of phosphorus in iron- and aluminium-precipitated sewage sludge from primary wastewater treatment plants. Manuscript submitted to the Journal of Water Science and Technology.

IV. Hayrapetyan, S., **Alvarenga, E.**, Hayrapetyan, L., Gevorgyan, S., Pirumyan, G., Salbu, B. (2015) Manganese dioxide (MnO_2) - containing composite sorbents, International Conference on Advanced Materials and Technologies, Proceedings, pages 249-254. Published.

V. **Alvarenga, E.**, Hayrapetyan, S., Skipperud, L., Hayrapetyan, L., Linjordet, M., Salbu, B. (2016) Sorption properties of a bentonite based material for removal of uranium from alum shale leachate. Journal of Chemistry and Environmental Engineering, In press.

Additional scientific work performed and contributions during the PhD program:

i. **Alvarenga, E.**, Salas-Bringas, C. (2014) Separation process and test conditions for digestate using a rotational rheometer and computational flow dynamics. Proceedings of the International Water Association (IWA) Specialist Conference on Advances in Particle Science and Separation: from mm to nm Scale and Beyond, Sapporo, Japan, pages 446-448. The IWA specialist group on particle separation awarded the work with the "*Best Student Poster Award*".

ii. Hayrapetyan, S., **Alvarenga, E.**, Hayrapetyan, L., Govasmark, E., Salbu B. (2016) Some of the regularities of the changes in the measuring of particle size and Z-potential of ZETAG® 9014 polyelectrolyte with changes in pH. Nordic Polymer Days Abstracts, Helsinki, Finland, page 115.

iii. **Alvarenga, E.**, Hayrapetyan, L., Hayrapetyan, S., G. Pirumyan, Govasmark, E., Salbu, B. (2016) Influence of pH on the structuring of ZETAG® 9014 type of cationic polymer, Book: Chemical Engineering of Polymers Production of Functional and Flexible Materials, Part I: Synthesis and Application, Eds. Mukbaniani, O., Abadie, M., Tatrishvili, T., ISBN: 9781771884457. In press.

iv. **Alvarenga, E.**, Hayrapetyan, S., Govasmark, E., Hayrapetyan, L., Salbu, B. (2016) The structuring of anaerobic digestion residue particles by means of treatment with bentonite base mineral conditioners. Manuscript.

1 Introduction

There is currently a need worldwide for alternative sources of energy due to the high consumption and dependence of oil and natural gas in a global scale. These sources of carbon are non-renewable in a short term and hence there is a significant increase in greenhouse gas (GHG) emissions, which have a global impact on climate (IPCC 2007). Moreover, the global population increases continuously and the food supply and preservation of the environment become more challenging for the future generations (Cordell & Neset 2014) when natural resources such as phosphorous (P) become scarce. Such scenarios are the baseline for governments looking for new political structures and economical sustainable systems in which natural resources are effectively used and recycled. Currently, there are new trends in which fossil fuel dependent economies are shifting to more sustainable driven schemes as bioeconomies. Norway is among the countries which has set as a target to reduce the GHG emissions by 40 % by 2030 (Government.no 2015) mainly generated in the agricultural and transport sectors (Morken & Sapci 2013). With a transfer to a bioeconomical system, a circular or sustainable thinking scheme is introduced in which energy, food, health, environment and climate are connected and are of special interest for the Norwegian government (Pettersen et al. 2014). The economic sectors that play an important role in the new bio-economy are health, agriculture, aquaculture and industry.

Waste streams are produced from these aforementioned sectors. When there is wastewater generated, there is a need for treatment either for further renewable energy production (e.g., biogas), nutrient or metal recycling or removal of contaminants such as radionuclides and organic pollutants in order to achieve the GHG emissions targets and for the preservation of the environment.

On the other hand, the continuous growth of population worldwide implies an increase in the urban wastewater along with the generation of biodegradable waste. Both waste streams are defined in environmental legislation directives such as the European urban wastewater treatment (WWT) directive (91/271/EEC) and the landfill directive (LD) which aim to preserve the environment (EEA 2001). The term "biodegradable waste" includes any waste that could be decomposed by means of aerobic or anaerobic conditions in accordance with the European Union (EU)'s LD (1999/31/EC)(EUR-Lex 1993). The LD obliges the Member States of the EU to reduce significantly the amount of landfilled biodegradable waste to 35 % of the 1995 levels by 2016 (for some countries by 2020)(EC 2016). It has been forbidden in Norway to dispose such type of waste in a landfill since 2009 (Avfall Norge 2014). These increasing trends of waste generated and the stringent environmental thresholds for water discharge and landfills are shifting the waste management practices towards alternative use of resources and hindrance of transport of pollutants to the environment.

Biogas production from biodegradable waste is an alternative suitable for connecting several sectors that could reach multiple markets and business branches in a bioeconomy. Moreover, it has long-term advantages in Norway for the reduction of the GHG emissions (e.g., methane and nitrous oxide) from the agricultural sector. This reduction could occur by using anaerobic digestion residue (ADR) instead of manure as a biofertilizer with mineralized forms of N as NH_4^+. Moreover, the methane (CH_4) is recovered as an energy carrier instead of being irreversibly released to the atmosphere with untreated manure applied to agricultural fields

(Massé et al. 2011). Furthermore, the wastewater stream in the aquaculture industry does have relevance since it is one of the main industries of the country (Ward & Løes 2011). Other possible streams are food waste and garden waste (both biodegradable) as well as run-off from areas with mines or heavy metals present in mineral bedrock (non-biodegradable). There is an opportunity to use CH_4 produced from these waste sources for electricity or biofuel generation or to recycle heavy metals. Moreover, the nutrients in the ADR or digestate are mineralized during or after the biogas production and the effluent is used for the replacement of conventional mineral fertilizers and for carbon storage in soils (Al Seadi et al. 2008). Therefore, the soil quality could be improved and nutrient or heavy metal losses to the environment are decreased as well when managed effectively.

Biogas production could be linked to the wastewater treatment plants (WWTPs) for the cogeneration of energy and further stabilization of the sludge. Under such configuration, it is therefore possible to recycle nutrients along with the production of energy. In Norway, most of the total phosphorus (P_{tot}) must be removed from the water to avoid the risk of eutrophication of water bodies. It means consequently that the concentration of P_{tot} must be decreased to at least 1 mg L^{-1} for WWTPs for over 100 000 p.e. (Lovdata 1981). Moreover, P mineral resources are limited in a global scale for the increasing food production demand and thus, there is a need to recycle P through sludge or ADR land application in the agriculture sector. Such approach, however, requires that nutrients such as P must be plant available in a short term when the sludges are land applied. This aspect has relevance when the primary precipitation of the wastewater is carried out with iron or aluminium salts, which strongly bind (or act as scavenger for) nutrients like P. On the other hand, even if the P is plant available to a suitable extent, the treated sludge or ADR requires to be dewatered in order to become a cost effective nutrient concentrated by-product that could be transported over long distances for use in agriculture (Lü et al. 2015). The water separation has great relevance in order to optimize the logistics around the waste management in WWTPs. New challenges are encountered in the dewatering of ADR without reducing its fertilizer value. There is for instance, the inconvenient of the primary precipitation in the WWTPs (e.g., Fe- or Al-precipitation) where the P is strongly bound to sludge particles and thus, not available to plants in a short term. On the other hand, the efficient dewatering of ADR from food waste or similar biodegradable waste is of special interest for the industry. In other words, the fertilizer value must be maintained without using chemical agents for dewatering that are known to restrict the P plant uptake. Furthermore, water could be recycled and sent back to the inlet stream of biogas plants when the biodegradable waste has a low water content (e.g., food waste). However, other nutrients as nitrogen in ammonium form (NH_4^+) need to be removed as well in order to avoid its accumulation and further inhibition of the anaerobic digestion (AD) (Yenigün & Demirel 2013). Moreover, K^+ usually follows the liquid stream after dewatering of the ADR and thus, there is a potential to separate K^+ along with NH_4^+ to a solid phase by means of sorption processes (Hayrapetyan et al. 2015; Kizito et al. 2015) in order to achieve a by-product with a fertilizer value that could replace mineral fertilizers.

Separation of colloids, particles, and chemical substances (either nutrients or pollutants) has been an area of focus in the WWTPs in the further treatment of sludge or ADR. Water management and its treatment could be more effective if particles and substances of interest are concentrated in solid phases. Water volumes are therefore reduced significantly and the solids management or disposal becomes an alternative more convenient for compliance with environmental regulations and for recycling schemes of both nutrients and metals. The

combination of chemical and mechanical separations and additional treatments allows achieving a stabilized by-product; dewatered, odorless and pathogen free sludge. The centralized WWTPs in Norway operate with primary precipitation as a chemical treatment due to the stringent threshold for P (Henze & Ødegaard 1994). Filtration, heat exchangers and centrifuge units are utilized for the mechanical removal of water, whereas the stabilization of the sludge is achieved commonly by thermal treatments, AD or liming (Ødegaard et al. 2002).

The mechanical removal of water is, however, dependent on the conditioning of the sludge. Thickeners are used for that purpose in the WWTPs, where mineral conditioners and polyelectrolytes alone or in combination are commonly added to the sludge in order to increase the dry matter content of the sludge drastically (Alvarenga, Hayrapetyan, et al. 2015). Particle aggregation and sorption (adsorption or absorption) of substances of interest (e.g., nutrients) is thus enhanced. The performance of the separation units is increased when the sludge becomes porous either to let the water go through the structure or to fix dissolved nutrients. However, the dosage of mineral and chemical conditioners implies changes of dynamic viscosity in both laminar and turbulent regimes of the wastewater (WW) effluent that affect the further separation of particles. Hence, well-defined rheological properties provide information for optimization of conditioning and dewatering operations (Örmeci 2007; Alvarenga, Schüller, et al. 2015).

Additionally, there is a need for removal of pollutants in water outside the traditional urban wastewater streams. For instance, the final disposal of rock material from mining and milling, road and tunnel construction etc. is of major concern, due to leachate of naturally occurring radionuclides and metals to the aquatic environments. In Norway, alum and black shales can increase levels of both radionuclides and metals in run-offs due to construction work. These type of sulphide-bearing rocks are distributed unevenly in Norway, and are mainly abundant in Oslo region (Jeng 1991) and can become a problem when they are exposed to air (oxygen) and the metal-sulphides are oxidized. Uranium is a naturally occurring radionuclide in most soils and rocks and the release of U species is a main concern due to weathering of alum and black shales in the construction sector. U can be toxic, acting as a heavy metal if accumulating in living organisms and will also emit radiation during disintegration from ^{238}U to daughter nuclides such as radium (^{226}Ra), radon (^{222}Rn), lead (^{210}Pb) and polonium (^{210}Po), being α- and beta- emitters (WHO 2001). Especially the α-emitting Ra and Po-isotopes are considered highly radiotoxic. Therefore, sorption of these pollutants in the membranes of the landfills is required in order to avoid transport to aquatic environments. Alternatively, the water or leachates of the landfill could be treated "in situ" by means of industrial processes for particle and pollutants removal.

There are different water- and sludge treatment needs as described in the previous paragraphs. Separation processes of liquid from solids can analogously be applied beyond the centralized schemes of WWT for increasing dewatering performance, particle separation and removal of substances of interest. These features are considered in this doctoral thesis with the application of natural porous materials such as bentonite for the recovery of macronutrients (e.g., K^+) and for the removal of heavy metals (e.g., U^{6+}) from an alum shale leachate. On the other hand, lime was investigated as a mineral conditioner for sludge, influencing the plant uptake of P from sludge and ADR to barley (*Hordeum vulgare*).

2 Objectives of the study and hypotheses

The overall aim of this doctoral thesis was to find naturally abundant materials that could be utilized for different WWT needs, with focus on separation of liquids from solids (SLS), in particular bentonite based materials and lime.

The sub-objectives were:

- To separate the water (dewatering) from ADR by means of flocculation combined with vacuum filtration.
- To increase the plant availability of P in Fe- and Al-precipitated sludge using liming as a post-treatment.
- To study the sorption of water-soluble K (from a synthetic solution and alum shale leachate) and U (from alum shale leachate) to silica and bentonite based materials.

On one hand, the separation of particles in ADR was considered with pre-treatments of the colloidal suspension adapted from the wastewater industry. The understanding of the dewatering process of the ADR and its further optimization was the starting point to convert the digestate into a product meant to be used as a biofertilizer. In addition, a mathematical model is introduced in the thesis for understanding the changes in average viscosity (η_{avg}) in a Jar-tester (JT). Such device is commonly used in the WWT industry for optimizing or correcting dosages of conditioners. The P plant availability in sludge, produced after chemical WWT, was evaluated after AD and liming treatments to reach the aforementioned objective. On the other hand, the sorption of water-soluble ions to organic and inorganic precipitants/surfaces for both recovery of macronutrients and/or removal of heavy metals, remains as the main link between the different types of wastewater or industrial liquid waste effluents investigated. A common material diatomite-bentonite (DB) combined system was considered for the wastewater treatment as a mineral conditioner for aggregating ADR particles and for sorption of cations in a landfill leachate. Moreover, diatomite was used as a base material for a composite sorbent for cation removal from a synthetic solution. Both the dewatering and the sorption separation processes were studied in a laboratory scale, aiming to upscale the process by understanding changes in physical and chemical properties of the wastewater effluents.

The hypotheses that were taken into account for the development of this research work were:

- The use of bentonite based mineral conditioners maintains effective dewatering performance of ADR (**Paper I**).
- The η_{avg} has an impact on the separation of liquids from solids of WW (**Paper II**).
- Liming as a post-treatment increases largely but differently the desorption of P from Fe- and Al-precipitated sludge (**Paper III**).
- A higher effect of liming on the plant uptake of P is achieved for Fe- and Al-precipitated sludge if combined with AD (**Paper III**).
- K^+ is adsorbed from a synthetic solution with a SiO_2–MnO_2–diatomite sorbent (**Paper IV**) and from alum shale leachate with a bentonite based material in basic pH range.
- The sorption capacity (q) of a bentonite based material for U^{6+} decreases by decreasing pH of the leachate (**Paper V**).

3 Overview of the study

The overview of the study is shown in Figure 1.

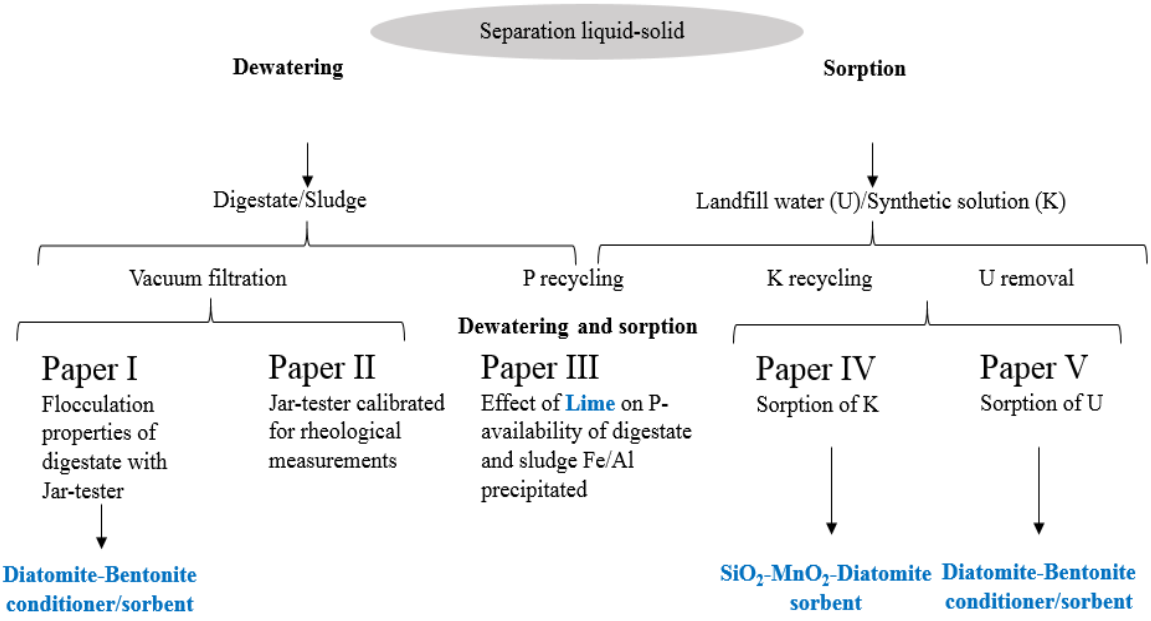

Figure 1: Schematic description of the articles and the materials (marked in blue) used for their experimental parts

There are two focuses of this study, which are dewatering and sorption as separation processes of substances from liquid to solid. Figure 1 shows the schematic description of the study of this thesis.

The natural diatomite-bentonite (DB) system has been applied either as a mineral conditioner (**Paper I**) or as a sorbent (**Paper V**). This system was produced in the Republic of Armenia. Lime on the other hand, could be applied as a mineral conditioner for dewatering of sludge or ADR and desorption of P from limed Fe/Al sludge (**Paper III**). .

Papers I and **II** are orientated towards dewatering performance. Aggregation of particles in WWT implies the addition of shear to the fluid or substrate of interest. Hence, the JT paddle geometry and the operating mixing conditions prior to the separation were relevant. Dosing of conditioners along with fast mixing (coagulation phase) and slow mixing (flocculation phase) rotational speeds were targeted for optimization of the particle separation and understanding of flow behavior and changes in η_{avg} during flocculation with a JT.

Papers IV and **V** include the main sorption block in which the properties of the SiO_2–MnO_2–diatomite and DB sorbent were studied in a dynamic configuration. Sorption of K^+ and U^{6+} as UO_2^{2+} in water was the focus. Treatments were required to enhance mass transfer for both materials (SiO_2–MnO_2–diatomite and DB) by means of ion exchange mechanisms. On the other hand, binders for the DB sorbent were considered in order to achieve a particle size for favorable

permeability and flow resistance of the granules inside of the columns. This aspect was applicable for both treatment scales.

4 Background

Firstly, the separation processes of liquids from solids connected to the aim of the study (Chap. 2) as well as some process steps currently implemented in the wastewater industry for particle separation and purification of effluents or leachates are described. Secondly, recycling perspectives for nutrients are considered for such separations. In addition, radionuclides and heavy metals removal from liquid phases are included. However, challenges continuously occur from a process performance angle. Both approaches, for nutrient and inorganic pollutants, cover a set of separation methods applicable in either small or large scale. Albeit, mathematical tools and understanding of chemical and physical properties of suspensions could improve the separation methods at laboratory scale for further upscaling. These opportunities are also described in this chapter.

4.1 Liquid-solid separation for water treatment (waste management)

The SLS is relevant in industrial processes and these are used for water treatment or recovery and processing of solids (Svarovsky 2000). Recovery of either one or both of the phases is usually targeted for the waste management and possible recycling or reuse of the separated streams of the industrial processes. On the other hand, the compliance with environmental regulations for the final disposal of either one or both phases is also aimed (Svarovsky 2000). A sequence of steps is followed in the process configuration of SLS. These stages are pre-treatment, solids concentration, solids separation and post-treatment.

It is certainly feasible to remove particles by other means than gravity when the sedimentation rates of the suspended material are unpractically slow. Filtration as a physical straining is implemented in the solids separation and classified in two main categories for particle separation; those in which cakes are formed and those in which the particles are captured in the depth of the filter medium (Wakeman 2011). In principle, these differ in the way the particles are collected. Depth filters collect the particles in the bottom of the unit whereas cake filters compress the solid phase. However, both phases could require additional purification. Further separation of particles or refinement with lower particle sizes require the use of post-treatments of the filtered solution.

4.2 Application of liquid-solid separation in wastewater treatment (particle removal)

The need to reach standards for water quality have orientated the treatment towards particulate efficiency separation, organic matter and other dissolved substances removal. These materials originate from waters such as wastewater from soil erosion and dissolution of minerals in run-off waters and from domestic and industrial waste streams. In water or wastewater, these waste discharges may include suspended and/or dissolved organic and/or inorganic matter and a variety of biological forms such as bacteria, algae, and viruses (Bratby 2006d). However, most

of these materials are present in water and wastewater in the nm to mm range, including low molecular forms, colloids, pseudocolloids and particles.

In environmental chemistry, lower size range particles are defined as entities having diameters larger than 0.45 µm (Salbu 2009). These particles are expected to settle in undisturbed water due to gravity. On the other hand, particles that do not sediment due to mutual repulsion and Brownian movements (random) are defined as colloids or pseudocolloids (Salbu 2009). These entities are localized heterogeneities ranging in size from about 1 nm to 0.45 µm. Therefore, chemical species with nominal molecular mass less than 1-10 kDa (diameter lower than 1 nm) should be referred as low molecular mass species (LMM) (Salbu et al. 2004; Salbu 2009). Colloids and particles settle according to the sedimentation coefficient K_s, given by the product (density × diameter) (Salbu 2009). Hence, small dense particles settle together with larger less dense particles.

Figure 2 shows the separation types that are suitable for a size spectrum of dispersed material. Nonetheless, it is unpractical and not feasible from an industrial point of view to apply directly the sorption and filtration as unit operations (e.g., due to filter blinding or clogging). There are processes that could favor SLS and are a common practice in the water or wastewater industry where fine particulate, colloidal or dissolved material are turned into a form suitable for separation from the dispersion (Bratby 2006d). These processes could achieve either,

1- To increase the adsorptivity of particles to a given filter medium by altering the surface properties of the particles, or by aggregating dispersed small particles into aggregates.

2- Chemical precipitation of dissolved materials (exceeding solubility constants) in order to create suitable particle size for feasible filtration.

Thereby, a stable dispersion can reach an unstable stage known as destabilization. The processes that enhance such destabilization of particulate and dissolved matter in water are referred to as coagulation and flocculation (both terms defined in sub-section 4.4.1).

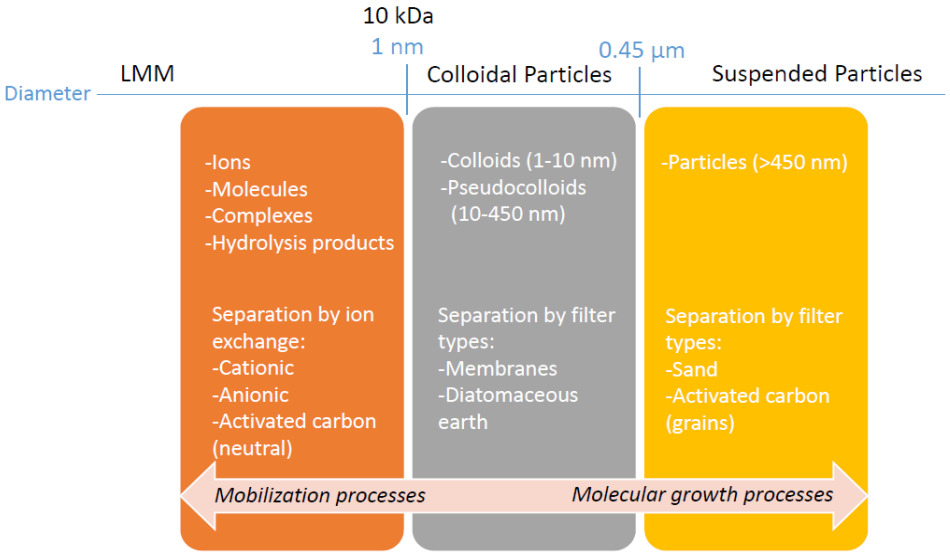

Figure 2: Size classes of water dispersions and filter types for particle separation (adapted from Salbu et al. (2004) & Salbu (2009))

4.3 Overview of a wastewater treatment process

There are several treatment technologies in WWT and there is a broad set of process configurations for particles and pollutants removal. For the purposes of this thesis, the process steps described in the following sub-sections are the ones that have a connection with the study described in Chap. 2 and 3.

4.3.1 Conventional wastewater treatment process

Although there is not a standard plant design due to the broad variation in composition of wastewater, a typical treatment sequence used (primary, secondary and tertiary) is shown in Figure 3, although, such configuration is not a typical Norwegian WWTP. The wastewater chemical treatment plants in Norway were implemented in 1972 and had neither secondary treatment nor AD (Ødegaard et al. 1973). Some modern Norwegian WWTPs are nowadays usually coupled to a biological processes for sludge treatment such as AD for stabilization of the sludge. In such context, stabilization refers to a sludge, which is pathogen free and with reduced odor (Ødegaard et al. 2002). The baseline in Figure 3 comes from the experience in municipal WWT that could be adapted to other industrial liquid wastes (Theodore et al. 1999a). However, it is of great relevance for plant design, the understanding in temporal variations in industrial WW strength, flow and waste components and their impact in the process operation. For that purpose, laboratory and pilot studies are required so the WWT could be cost effective when upscaled.

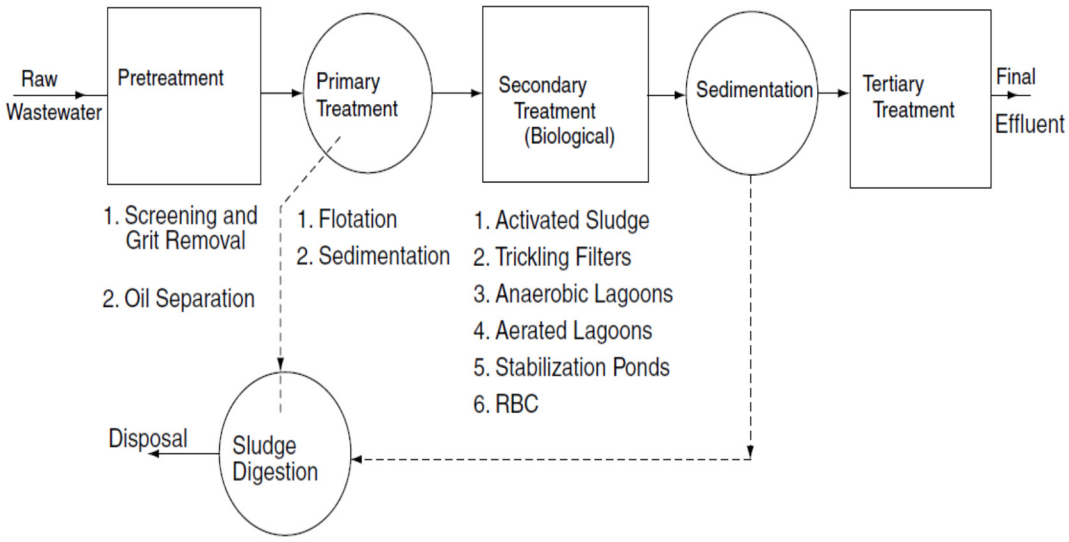

Figure 3: Typical wastewater treatment plant (WWTP) processing steps. The plant design is not typical for plants in Norway (Bewtra & Biswas 2006)

The chemical co-precipitation reactions of the primary treatment of wastewater can be seen from Table 1. Its performance by means of lime ($CaOH_2$ or CaO) or Fe- and Al-salts is critical for the removal of organic matter and P for the further separation units. In other words, the sludge is conditioned or precipitated either physically or chemically for the next processing steps by means of coagulation and flocculation. When the pH is changed for enhancing flocculation, it is important to achieve hydrolysis and polymerization of the Fe- and Al-species. Thereby, polymerization produces scavengers (e.g., $Fe(PO_4)_x(OH)_{3-3x}(H_2O)$) for co-precipitation of dissolved inorganic substances. Additional treatments like sorption and/or ion exchange could follow for removal of organic and inorganic pollutants (or nutrients) to a greater extent (Theodore et al. 1999b) as defined and described in sub-section 4.5.

Table 1: Metal coagulants and chemical reactions for coagulation and flocculation (Anzalone et al. 2006).

Coagulant	Chemical Added or naturally present in the wastewater stream	Chemical Reaction	Favorable pH for Flocculation	Floc Charge Positive	Floc Charge Negative
Aluminium sulphate	HCO_3^-	$Al_2(SO_4)_3 \cdot xH_2O + 3Ca(HCO_3)_2 \longrightarrow 2Al(OH)_3\downarrow + 3CaSO_4 + xH_2O + 6CO_2$	Approximately pH 7	<pH 7.6	>pH 8.2
	$Ca(OH)_2$	$Al_2(SO_4)_3 \cdot xH_2O + 3Ca(OH)_2 \longrightarrow 2Al(OH)_3\downarrow + 3CaSO_4 + xH_2O$			
	PO_4^{3-}	$Al_2(SO_4)_3 \cdot xH_2O + 2PO_4^{3-} \longrightarrow 2AlPO_4\downarrow + 3SO_4^{2-} + xH_2O$	pH range: 5.5-6.5	-	-
Ferrous sulphate and lime	-	$FeSO_4 \cdot 7H_2O + Ca(OH)_2 \longrightarrow Fe(OH)_2 + CaSO_4 + 7H_2O$ $4Fe(OH)_2 + O_2 + 2H_2O \longrightarrow 4Fe(OH)_3\downarrow$	pH range: 3-13	pH range: 3-6.5	pH range: 8-13
Ferric chloride	HCO_3^-	$2FeCl_3 + 3Ca(HCO_3)_2 \longrightarrow 2Fe(OH)_3\downarrow + 3CaCl_2 + 6CO_2$	pH range: 8-8.3	-	pH range: 8-13
	$Ca(OH)_2$	$2FeCl_3 + 3Ca(OH)_2 \longrightarrow 2Fe(OH)_3\downarrow + 3CaCl_2$			

The pH is a determinant factor in cationic exchange of P in the sludge. There is competition of hydrogen ions (H^+) and other cations. For instance, at low pH values the P_{inorg} is strongly associated to the sludge particles surface (Fe- and Al-binding) whereas the increase of the pH solubilizes the P_{inorg}. In this case, there is a competition between hydroxide ions (OH^-) and P_{inorg} as $H_2PO_4^-$. The solubilization or desorption of P_{inorg} takes places by anionic exchange with OH^- and HCO_3^- ions. The process of co-precipitation of P_{inorg} with Fe- and Al-precipitates can be illustrated as follows:

$$(Fe,Al)\text{-}OH_2^+ + H_2PO_4^- \rightleftharpoons (Fe,Al)\text{-}O\text{-}PO(OH)_2 + H_2O \quad (1)$$

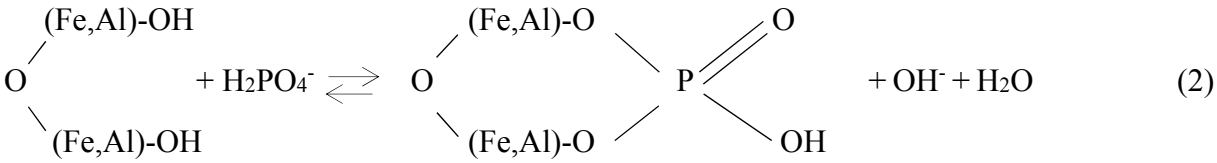

(2)

The P_{inorg} ($H_2PO_4^-$) would be more plant available by increasing the pH in Eq. 1. Firstly, less positive Fe/Al-hydroxides would be obtained in the sludge and secondly, an increase in the concentration of OH^- in Eq. 2 would shift the equilibrium towards the left.

Alternatively, Ca can precipitate P for pH values above 9. The type of insoluble Ca-phosphates can be seen from Eqs 3 to 6 (Bratby 2006e).

$$CaHPO_4(s) \rightleftharpoons Ca^{2+} + HPO_4^{2-} \quad (pH\sim8,0) \quad (3)$$

$$\log K_{25^oC} = -6.6$$

$$Ca_4H(PO_4)_{3(s)} \rightleftharpoons 4Ca^{2+} + 3PO_4^{3-} + H^+ \quad (pH\sim9,0) \quad (4)$$

$$\log K_{25^oC} = -46.9$$

$$Ca_{10}(PO_4)_6(OH)_{2(s)} \rightleftharpoons 10Ca^{2+} + 6PO_4^{3-} + 2OH^- \quad (pH>12) \quad (5)$$

$$\log K_{25^oC} = -114$$

$$Ca_{10}(PO_4)_6(OH)_{2(s)} + 6H_2O \rightleftharpoons 4[Ca_2(HPO_4)(OH)_2] + Ca^{2+} + 2HPO_4^{2-} \quad (pH>12) \quad (6)$$

$$\log K_{25^oC} = -17$$

The sludge processing prior to its disposal could include stabilization of biodegradable organics, concentration (thickening or flotation) of solids or substances and dewatering. Ultimately, the disposal of the stabilized and the dewatered material is followed in a waste management scheme. Such final disposal could be incineration, land application and landfilling. Land application of treated sludge is the trend in the EU, as mentioned before in Chap. 1 concerning EU's LD. Norway follows the same direction with 60 % of the sewage sludge used in the agriculture sector (Hamilton et al. 2015). Moreover, the landfilling of biodegradable waste is forbidden (EUR-Lex 1993).

At this stage of treatment or processing, the sludge could contain pollutants along with chemical residuals from the previous treatment steps; e.g., metal sulfides, heavy metal hydroxides and carbonates, heavy metals organic complexes, radionuclides, Ca carbonate,

soaps and detergents, biomass and precipitated phosphates among others (Theodore et al. 1999b). Soluble pollutants as ammonia, other pollutants and non-biologically degradable chemical oxygen demand from these compounds could be present in the sludge since the concentration and dewatering remove the water only to a certain extent. The sludge as a final product has still more than 50 % by weight water (Theodore et al. 1999b).

4.3.2 Stabilization of the sludge

The stabilization of biodegradable organics is achieved by means of aerobic digestion and AD. The latter is preferred because it allows a high degree of reduction of organic matter with small increments in the bacterial biomass compared to the aerobic process. In the AD, a broad range of microorganisms metabolizes the organic matter in anoxic conditions. The four processes involved in this treatment are hydrolysis, acidogenesis, acetogenesis and methanogenesis. The biogas product is a mixture of CH_4 (55-70 %) and carbon dioxide (CO_2) (30-45 %) with water and other traces of gases which is used for electricity production and for the transport sector (Boyle 2004).

The anaerobic digesters are usually tanks with hydraulic retention times (HRTs) from 10 to 30 days dependent on the feeding substrate organic matter content (Theodore et al. 1999c). The process operates in a mesophilic temperature range (30-42°C) or a thermophilic one (50-60°C). In addition, the pH is a critical parameter for the performance when the sludge has a high content of protein. Therefore, the alkalinity could increase to concentration values over 5000 mg L^{-1} and the bacteria would be inhibited due to the pH over the operational range (6.5-7.5) (Theodore et al. 1999c). Thickening of the feeding sludge or biodegradable waste is required in order to reduce the tank volume. Thereby, longer HRTs are achieved. Conversely, the AD process decreases the dry matter content to 3-6 % solids before its further processing (e.g., dewatering) (Theodore et al. 1999c).

Liming with CaO dosage is used for sanitation and the sludge is maintained stable at pH 12 temporarily or above (Theodore al. 1999c). Such treatment implies temperature increase $\geq$ 55°C due to the exothermic chemical reaction of CaO and water in the sludge (Ødegaard et al. 2002). Moreover, it adds porosity to the sludge for further dewatering (Deneux-Mustin et al. 2001). The lime could be dosed in different steps of the sludge processing either as a solid or as a suspension. For instance, it could be added prior or after the thickeners for conditioning before the dewatering of the sludge. Alternatively, it could be dosed after the dewatering up to 50 % TS (Norsk Vann 2010).

4.3.3 Dewatering of the sludge

Although the process terms dewatering and concentration might sometimes be confused, they confer different properties to the sludge. The latter still leaves the sludge with the properties of a liquid whereas the former produces a rather fragile solid (Theodore et al. 1999c). When the dry matter content of the sludge is increased to 20-30 %, it forms a porous solid called cake (Theodore et al. 1999c). The water is adsorbed and chemically combined in the sludge structure

and hence, not free in the cake. The dewatering commonly follows the concentration and/or biological stabilization even though it could be used in other steps of the sludge management process. In spite of being a mechanical process, physical and chemical conditioning are usually used as aids for dewatering to increase the separation efficiency. A wide number of physical and chemical conditioners are utilized in the WWTPs. Among these, lime ($Ca(OH)_2$ as a slurry), aluminium and various ferrous or ferric salts have been used for conditioning of the sludge prior to dewatering (Theodore et al. 1999c). Lime as a mineral conditioner creates a network of calcium carbonate crystals, which holds the sludge particles apart, and allows hence, the water to flow during dewatering. Aluminium- and Fe-salts contribute to form the inorganic matrix and these chemical conditioners help to remove water bonded to hydrophilic organics. The conditioning of the sludge prior to dewatering is critical for avoiding filter cake blinding or clogging as shown in Figure 4 where colloidal particles can obstruct the porous channel structure of the cake. Moreover, The mass of the resulting sludge is increased by 10 to 25 % by chemical conditioning; depending on the properties of the individual sludges (Theodore et al. 1999c) and the water removal by means of conditioners as polyacrylamide (e.g., nonionic, cationic or anionic) (Alvarenga, Hayrapetyan, et al. 2015). Some examples of the types of polyacrylamide can be seen in Figure 5. Furthermore, fine particles and soluble substances can be sorbed to chemical precipitates as for the case of P removal in the primary treatment of the WWTPs.

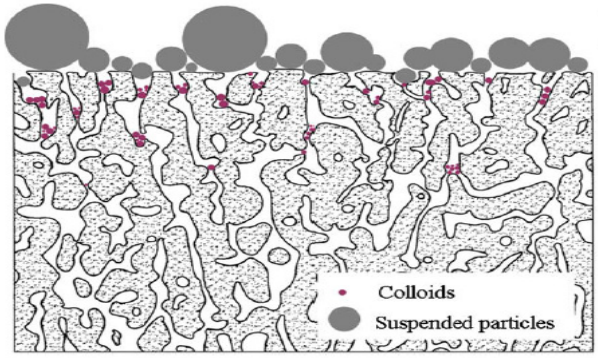

Figure 4: Hypothetical porous structure of a cake with colloids blocking the water flow within its channels (adapted from van Halem et al. (2009))

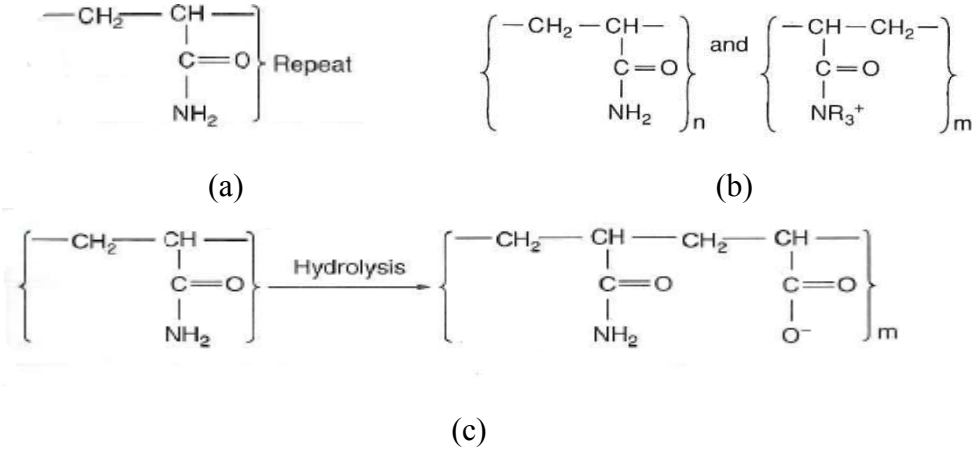

Figure 5: Some general types of polyacrylamide (a) nonionic, (b) cationic and (c) anionic, where R is usually a CH_4 or CH_3CH_2 derivative (adapted from Bratby (2006a))

The supernatant after dewatering could contain suspended solids, organics and pollutants. Further addition of polymers (as chemical conditioners) prior to, during or after the dewatering might contribute to decrease the concentration of pollutants in the supernatant (Theodore et al. 1999c).

4.4 Primary treatment for wastewater

4.4.1 Coagulation and flocculation

Coagulation is defined as the process whereby destabilization of a suspension occurs by means of overcoming the conditions that enhance stability in a given system (Bratby 2006d). Its aim is to remove particles and P as phosphates. On the other hand, flocculation is a process that follows coagulation and it aims aggregation of destabilized particles.

The two widely accepted flocculation mechanisms for particle removal are (Alvarenga, Hayrapetyan, et al. 2015),

- Surface charge neutralization
- Particle-particle bridging (enhanced by polymers)

Other processes that could occur for particle removal are compression of double layer, sorption and sweep floc or entrapment.

The forces acting on particles in a colloidal suspension are repulsive and attractive. The former is a result from the charged surface of the electrical double layer (Coulomb repulsion of same charge) and the latter comes from van der Waals forces of intermolecular attraction (van der Waal attraction of masses). Typically, hydrophobic colloids exhibit a negative surface charge. Near to the surface of the colloidal particle, there is a rigid Stern layer by attraction of positively charged particles. Further, a diffuse layer of counter-ions develops as seen in Figure 6 (Egan 2015). The ions in the diffuse layer follow the Maxwell-Boltzmann potential energy distribution (Bratby 2006b) as shown in Figure 7 (Egan 2015).

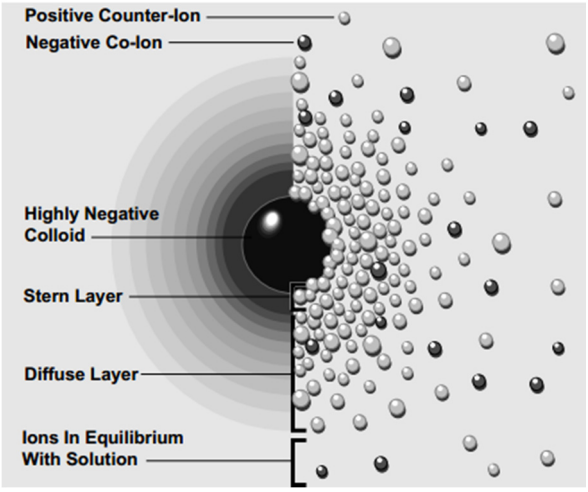

Figure 6: Conceptual representation of the electrical double layer (Egan 2015)

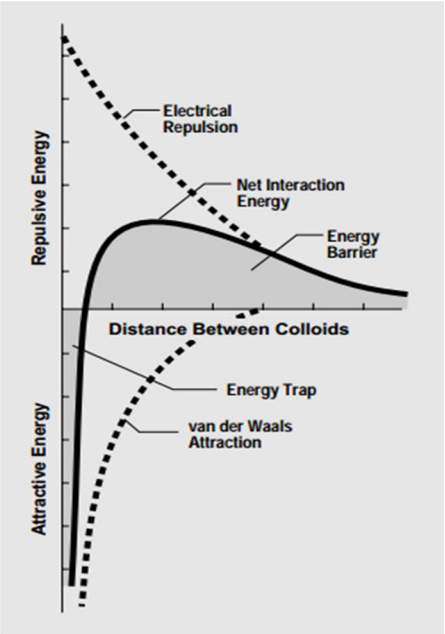

Figure 7: Potential energy of interaction between two particles. The resulting net interaction curve is formed by subtracting the attractive curve from the repulsion one (Egan 2015)

The charge neutralization mechanism occurs when coagulant addition lowers the highly negative surface charge from Figure 6. Thereby, the repulsive energy curve drops and the energy barrier decreases substantially. The energy barrier in Figure 7 could be completely eliminated by adding more coagulant.

On the other hand, in the particle bridging mechanism, the polyelectrolyte or polymer chain is sorbed to the colloid surface forming loops, trains and tail configurations as seen from Figure 8. Bridges are formed when two particles come together because of the loops and tails of one particle that attach themselves to bare patches on the other particle (Napper 1983). This mechanism predominates when dosing organic coagulants.

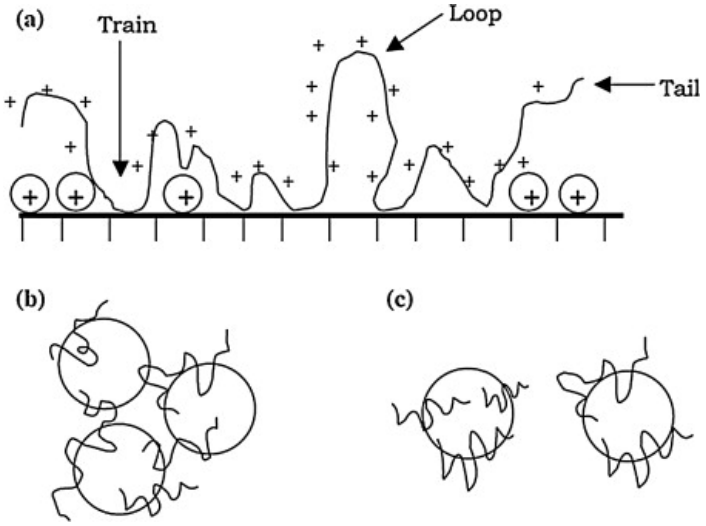

Figure 8: (a) Sorption of the polymer and formation of loops (b) bridging flocculation (c) floc breakup (restabilization of the colloidal system) (Lee et al. 2014)

The compression of the double layer increases by for instance, increasing the ionic strength of the solution and the repulsive energy in Figure 7 will decrease and therefore, particles tend to aggregate. Compression of double layers can for instance be obtained by increasing the conductivity of solutions. Further compression would certainly suppress the energy barrier. The sweep floc process occurs when there is sufficient coagulant dosage to reach oversaturation. Metal hydroxide species are thus generated as precipitates and the colloids are enmeshed in the growing aggregates (Bratby 2006f). This process is dominant when using inorganic coagulants.

4.4.2 Addition of filter aids

Filter aids (or flocculants) are defined as chemicals or substances added to a destabilized suspension in order to rapidly increase the rate of flocculation, or to improve the floc strength over the flocculation (Bratby 2006d). In addition, these chemicals are employed as physical or chemical conditioners that favor further thickening and dewatering because of the strength given to the flocs (Thapa et al. 2009; Alvarenga, Hayrapetyan, et al. 2015). Both types of conditioners were used for dewatering in **Papers I** and **III**.

4.4.3 Challenges

The challenges encountered in the chemical precipitation of the primary treatment for wastewater are according to Bratby (2006g),

- Very low P after pre-precipitation that influences the performance of the activated sludge unit.
- Low pH that influences biological treatment processes.
- Strong binding of P to Al/Fe- or Ca-salts with poor accessibility of P to plants (sludge applied as a biofertilizer).
- Overproduction of sludge and difficult further processing.
- The cost of the coagulants (e.g., Fe^{2+}- vs. Fe^{3+}-salts)

4.5 Sorption and ion exchange processes and mechanisms for post-treatment of wastewater

The sorption (ad/absorption) and ion exchange processes share many common features concerning batch and fixed bed process configurations and thus these treatments can be grouped as sorptive processes (LeVan et al. 1999). Sorption is defined as the accumulation (or depletion) of solute molecules or ions in a gas-solid or liquid-solid interface (LeVan et al. 1999). Highly porous solids with very large internal surface area per unit volume are preferred. Such materials are natural or synthetic of amorphous microcrystalline structure (LeVan et al. 1999). Moreover, these materials can be regenerated (e.g., with inorganic acids) in order to be used several times. In ion exchange processes (e.g., chromatography), a cationic mechanism occurs when cations are adsorbed to resins and hydrogen ions are released to the eluted solution (LeVan et al. 1999).

Thereby, the pH decreases drastically for aqueous solutions as shown in **Papers IV** and **V**. On the other hand, sorption of anions on the solid surface enhances release of hydroxide ions in an aqueous system and thus, the pH tends to increase (LeVan et al. 1999). These processes usually occur throughout a polymeric solid or a porous material (LeVan et al. 1999).

Sorption and ion exchange are processes, which are considered as physico-chemical treatments. These types of treatments are more expensive than biological ones; nonetheless, they remove pollutants that are difficult to separate by biomass means (Theodore et al. 1999b). These tertiary treatments are usually used in series with the secondary ones; though these could be applied as stand-alone units as well.

Sorption can be classified as physical, chemical and ion exchange. The physisorption is defined as a binding to a surface by London-van der Waals forces (LeVan et al. 1999). Thereby, the sorption process is reversible (e.g., by means of regeneration with inorganic acids) and the sorption capacity is not destroyed (LeVan et al. 1999). Conversely, the chemisorption involves chemical bonding (monolayer model) and the process becomes irreversible and generally, the capacity of the sorbent is destroyed (LeVan et al. 1999). In ion exchangers, ions of positive charge (e.g., cations) and negatively charged (e.g., anions) in an aqueous solution replace other ions of the same charge originally present in the solids (LeVan et al. 1999). Thus, the electrostatic sorption mechanism confirms a monolayer model, and the process is reversible for cationic or anionic species. The DB sorbent investigated in this thesis acts as a cation exchanger for K^+ (sub-section 6.4.2) and U^{6+} removal (**Paper V**).

The most widely used physico-chemical treatment is sorption. The main target of this treatment is to remove soluble organics with activated carbon as sorbent. This is physical sorption acting on neutral masses. It can be applied as powder to basins or as granules in packed counter-flow columns. The latter can be more expensive but it can be regenerated thermally or with solvents whereas the former is discarded after use (Theodore et al. 1999b). Pretreatment for suspended solids removal (e.g., flocculation) is often required prior to the sorption process. However, backwash systems are included in the columns for the particles that are not removed by the pre-treatment and that could clog the unit.

On the other hand, ion-exchange processes have been employed as sorptive separations for many years for treatment of industrials water inlets in contrast to the applicability for WWT. However, selectivity has been improved for removal of specific pollutants such as heavy metals and radionuclides, even though their concentration might be rather low compared to other inorganic substances (Theodore et al. 1999b). The process configuration for an ion exchanger is by counter-flow through a series of columns containing specific resins. In practice, pre-treatment for particles and organics removal is performed along with pH adjustment.

The removal capacity of an ion exchanger is a function of the regeneration. Such cleaning of the ion exchanger resin is crucial for the economical feasibility of the treatment. They main challenge is to optimize the amount of regenerant to be applied since significant amounts are required. The bulk of the economic costs of ion exchangers is mainly attributed to the regeneration and the further disposal of the regenerant (Theodore et al. 1999b). The advantage is that the resin can be used several times after regeneration by maintaining a good separation efficiency. When the latter decreases drastically, the resin must be replaced. Cation removal exchangers are most often regenerated with mineral acids (Theodore et al. 1999b).

Although sorption and ion exchange processes are frequently considered as treatments after particle removal, they already occur in the primary treatment of wastewater. This fact is attributed to the surface charge of colloidal particles that interacts with ions and molecules nearby. There is a sequence of three processes for sorption of an ion or molecule on the surface of a solid as suggested Stumm and Morgan (1962),

- Removal of the ion from the solution
- Removal of the solvent from the solid surface
- Binding of the ion to the surface

Thermal motion allow the ions and molecules to move continuously. Consequently, the colloidal particles are in contact with molecules because of random movement known as Brownian motion. There are three possible scenarios for such interactions (Bratby 2006c):

- The molecule or ion can be held to the surface by chemical bonding (e.g., ionic, covalent, hydrogen, dipolar). On the contrary, sorption could arise from forces of attraction (e.g., London-van der Waals).
- Electrostatic repulsion could occur before the previous scenario takes place (Coulomb).
- The molecule could be released to the solution due to the Brownian motion even though it was already binded.

Empirical expressions are used for describing the adsorptivity of a given system. These are termed as isotherms and they relate the amount of adsorbate per unit mass of adsorbent to the concentration of the adsorbate remaining in solution. Langmuir and Freundlich models have been extensively used as isotherms (Bratby 2006c).

Equation 8 shows the Langmuirian sorption behavior (monolayer model) for a system,

$$\frac{C}{x/m} = a + \frac{C}{b} \tag{8}$$

where *C* represents the concentration of adsorbate or solute (molecules or ions) remaining after sorption. The mass of solute adsorbed per unit of mass of sorbent is given by the *x/m* ratio. The constants *a* and *b* are constants of a given system. Examples of Langmuirian sorption behavior in the context of water or WWT, are the destabilization properties usually observed with hydrolyzed Fe (Fe^{3+}) coagulants and with polyelectrolytes (Black et al. 1965; Stumm & O'Melia 1968; Report 1971). Furthermore, Langmuir isotherms were employed for the U^{6+} sorption behavior in **Paper V**.

The model suggested for Freundlich isotherm (multilayer model) is given by,

$$\log\left(\frac{x}{m}\right) = \left(\frac{1}{a}\right)\log C + \log b \tag{9}$$

Black and Chen (1967) have reported a Freundlich sorption behavior for destabilization characteristics of diluted clay suspensions by hydrolyzed Al sulphate. This is an indication of the complexity of aluminium hydrolysis products formed when using Al-based coagulants instead of Fe- coagulants or polyelectrolytes as studied in **Paper III**.

4.6 Perspectives for recycling and environmental remediation

Nutrients, radionuclides, heavy metals and trace elements can potentially be remobilized to the environment when present in soils naturally (e.g., alum shale) or applied as fertilizers (e.g., ADR or sludge). Alum shale, usually containing a series of heavy metals and radionuclides, may represent an environmental hazard as uptake of such inorganic pollutants could occur in plants or other living organisms (Skipperud et al. 2016); analogously as it could also occur when sludge containing heavy metals and/or radionuclides is used as a fertilizer.

4.6.1 Nutrient recycling

Phosphorus is a macronutrient that is a building "stone" for life. It is needed along with N and K by all plants. The P concentrations in plants vary from 0.1 to 0.4 % and it has been proven that P stimulates root growth and accelerates plant ripening (Ott & Rechberger 2012). Phosphorus is thus essential for food production. However, the mineral resources of P are finite and these are located in a few countries. Therefore, food supply is jeopardized due to the increasing world population (Rittmann et al. 2011).

In Norway, 6.2 kg $year^{-1}$ per capita of P were imported from the period 2009-2011. The agriculture sector imports mineral-P as well as the aquaculture one with fish feedstuff with 1.7 and 1.94 kg P $year^{-1}$ per capita accordingly (Hamilton et al. 2015). The P potentially recycled from the wastewater industry accounts only for 0.64 kg P $year^{-1}$. The figure in Europe (EU-15) is comparable with a net per capita of 4.7 kg P $year^{-1}$ consumption with only 0.77 kg P $year^{-1}$ recycled (Ott & Rechberger 2012). The main losses are the accumulation in agricultural soils, landfill disposal of biodegradable waste and run-off to water recipients (Ott & Rechberger 2012). There is therefore need for optimizing fertilization, recycling of P-rich wastes, household centralizing WWT, and implementing other WWT for P removal (e.g., sorption) (Ott & Rechberger 2012).

Anaerobic digestion treatment is a suitable alternative to recover nutrients and energy. It has the advantage to convert P_{org} to inorganic P (P_{inorg}) by metabolizing the organic matter in biodegradable waste. Animal waste and wastewater (e.g., black water) contain a significant amount of P. A strategy to recycle P from animal waste for use in agriculture is shown in Figure 9 (Rittmann et al. 2011).

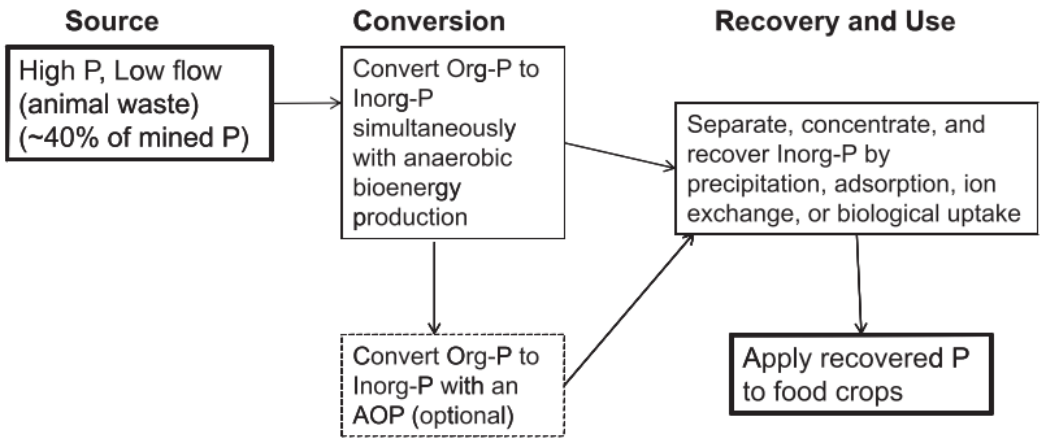

Figure 9: Strategy for recycling the losses of phosphorus (P) from animal waste in the agriculture sector. The term AOP refers to advanced oxidation processes (Rittmann et al. 2011)

Such strategy could be applied for the WWTPs. However, challenges are encountered for both types of waste streams when the AD reduces the P plant availability as investigated by Kahiluoto et al. (2015). Such effect is comparable to the one obtained on P plant uptake when sludge is Fe- or Al- precipitated (Rittmann et al. 2011). Liming as a post-treatment for sludge is studied in **Paper III** as an alternative for increasing P plant uptake in anaerobically digested sewage sludge. It favors a better P mobility in soil when used as a fertilizer (Krogstad et al. 2005).

Another challenge in the nutrient recycling approach is the recovery K^+ remaining in solution in the primary and secondary treatment of the WWTPs as shown in Figure 3. In spite of being specifically attracted to a solid surface, K^+ ions remain in solution because they are readily hydrated in aqueous solutions. Less hydrated ions like for instance Cs^+ and $CuOH^+$ are preferably sorbed by solid surfaces (Bratby 2006c). **Paper IV** describes a manganese dioxide (MnO_2) composite sorbent that is able to remove K^+ from an aqueous system. Moreover, there are results included in Chap. 6 sub-section 6.4.2 for K^+ recovery from the same wastewater type used for U^{6+} removal in **Paper V**.

4.6.2 Radionuclides, heavy metals and trace elements

Inorganic pollutants like radionuclides (e.g., ^{238}U, ^{137}Cs, ^{90}Sr, ^{60}Co), heavy metals (e.g., Ba, Pb, Zn, Mn among others) and trace elements (present in levels < 0.1% in minerals) can potentially be transported to the environment by anthropogenic activities. The latter includes mining and milling, roads and tunnels construction where these pollutants are mobilized to water bodies by means of natural weathering of rocks. Among them, alum shales are particularly abundantly present in Oslo area and the Mjøsa district and Hedmark County in Norway (Jeng 1991). Therefore, many environmental issues have been addressed and connected to the weathering of shales.

Alum shales contain sulphides that could be combined with Fe, Cu, Zn, Pb and Ni (Jeng 1991). The pH values of leachates from Oslo region can range from 5.28 to 6.40. Nevertheless,

the pH can be even lower due to hydrolysis of Fe^{3+} or Al^{3+}. The sulfuric acid produced by oxidation of sulphides (e.g., from pyrite) reacts with the silicates of the mineral and thereby, it dissolves the pollutants aforementioned. Although several reactions can undergo depending of the environmental conditions, two general pathways for pyrite are characteristic under highly acidic conditions (pH < 3) due to oxidation. These are accordingly,

Path 1:

$$FeS_{2(s)} + 7/2O_2 + H_2O \longrightarrow Fe^{2+} + 2SO_4^{2-} + 2H^+ \quad (10)$$

$$Fe^{2+} + 1/4O_2 + H^+ \longrightarrow Fe^{3+} + 1/2H_2O \quad (11)$$

Path 2:

$$FeS_{2(s)} + 14Fe^{3+} + 8H_2O \longrightarrow 15Fe^{2+} + 2SO_4^{2-} + 16H^+ \quad (12)$$

The chemical species of a particular inorganic pollutant have a great relevance in connection with the safety analysis of the type of final disposal of the waste (e.g., landfills). Uranium, which is naturally present in the Norwegian alum shale, can for instance solubilize and form complexes with different ligands, depending of the alkalinity and pH of the water (Gavrilescu et al. 2009)(Choppin et al. 2013). Figure 10 shows a speciation diagram of uranium present as uranyl (UO_2^{2+}) species in a surface water under normal atmospheric pressure of CO_2 ($pCO_2 \sim 3.2 \times 10^{-4}$; $\log [CO_3^{2-}] = 2pH - 18.1 + \log(pCO_2)$) (Choppin et al. 2013). Such speciation diagram is obtained from mass balances due to hydrolysis or complexation and from their chemical equilibrium constants. In oxic water environments, U is present as U^{6+} and it strongly binds to carbonates as a complex although its solubility could be limited due to formation of UO_2^{2+} silicate species. A DB system (from the Republic of Armenia) as a source of silicates and consisting mostly of montmorillonite, was utilized in **Paper V** for U^{6+} sorption from a leachate from an alum shale landfill. In this case, U was present as colloid and LMM particles.

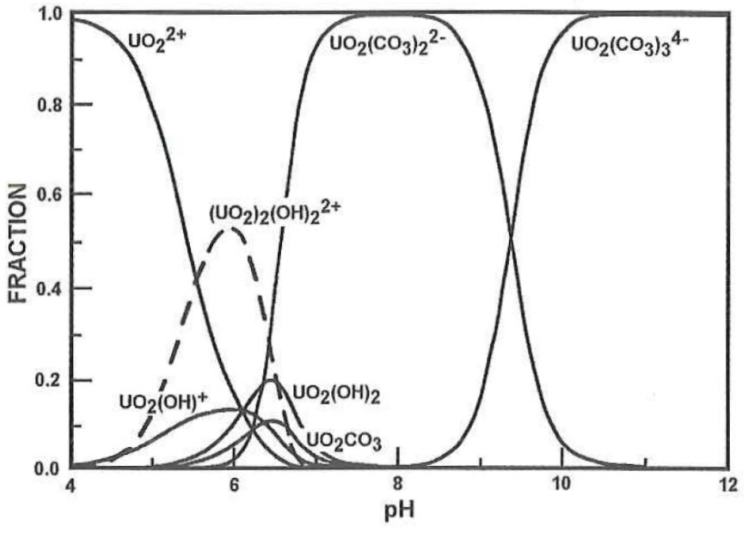

Figure 10: Speciation of uranium (U) in water with natural carbon dioxide (CO_2) content at different pH values. The diagram shows hydrolysis and carbonate (CO_3^{2-}) complexation (Choppin et al. 2013)

4.7 Improvement methods for separation of liquid from solids

4.7.1 Optimization of dewatering

Jar-testing units are commonly employed in the industry for performing adjustments of coagulants and flocculants dosage in WWTPs. In spite of the laboratory scale of the JTs, as shown in Figure 11, changes can be carried out in the process scale considerably in advance and prior to the dewatering of sludge after primary and/or secondary treatment. This particular feature is mainly derived from the mechanical features associated to the geometry of the paddles and the container in the mixing process. Moreover, there are controlled rapid mixing conditions for coagulation over time as well as for the slow mixing for flocculation. An analogous behavior to the plant scale is therefore expected by performing such tests in the laboratory scale (Teefy et al. 2011). Albeit, the use of JTs usually leads to time-consuming adjustments of the process. This aspect is due to a theoretical and empirical baseline that must be considered by process operators in order to have the best approximation to the real process conditions. Furthermore, this baseline is inherent to every WWTP and iterations are required to match the baseline conditions. The latter aspect leads to a time-consuming correction in the process (Teefy et al. 2011).

Figure 11: Jar-tester (JT) flocculator produced by Raypa®

A study of optimization of dewatering of ADR is presented in **Paper I** where a JT unit was used for mixing alternative coagulants and commonly used flocculants. It was possible to determine an optimal dose for both the physical and the chemical conditioner employed. Diatomite was used as a porosity carrier of the physical conditioner.

4.7.2 Rheology and fluid dynamics

A deeper understanding of flow behavior can contribute to improve the efficiency of particle separation in liquid substrates. Removing solutes and particles from water does represent a more favorable approach for sustainable waste management in the industry (Örmeci 2007; Boger 2009). Such scope is applicable for water recycling, nutrient recovery and inorganic/organic pollutants removal.

Rheology is the science that studies the deformation and flow of matter (Steffe 1996b). This science essentially studies the way in which materials respond to applied stresses or strain (Steffe 1996b). The effect of the shear history is for instance of relevance for flocculated systems like sludge. The flocs in the flocculated dispersions are weakly held aggregated by interparticle forces. Therefore, their structure will be directly affected by flow, whereas the flow structure will in turn have an effect on the flow behavior (Mewis & Wagner 2012). This physical interaction between microstructures and the fluid usually results in a non-Newtonian flow behavior. In other words, a small amount of fine aggregates can induce significant rheological changes (Fisher et al. 2007; Boger 2009; Mewis & Wagner 2012). Hence, it is important from a process perspective to understand the rheological properties of the materials that are transported in the WWTPs. Thereby, a stagnated fluid (fluid at rest) is avoided at low stresses (or low $\dot{\gamma}$) and hence, problems could be avoided in the overall SLS equipment performance (Mewis & Wagner 2012).

A Newtonian fluid has a constant viscosity (η) independent of shear rate ($\dot{\gamma}$) and influenced only by temperature. The η can be calculated for a Newtonian fluid from Eq. 13 (Steffe 1996a). On the contrary, a non-Newtonian fluid has a variable η with respect to $\dot{\gamma}$ and some with time (Steffe 1996a). For instance, a fluid's η can decrease by increasing the $\dot{\gamma}$ and thus the fluid has a pseudoplastic or shear thinning behavior (Steffe 1996a). While in other fluids, an increase in η with increased $\dot{\gamma}$ can show dilatant or shear thickening course (Steffe 1996a). In addition, changes in η in some fluids over long time lead to a phenomenon called thixotropy. Flow-induced changes in microstructure could for instance enhance such behavior (Mewis & Wagner 2012).

$$\eta = \frac{\tau}{\dot{\gamma}} = \frac{K_1 M}{K_2 N} \tag{13}$$

where,

η: Dynamic viscosity [Pa·s]
τ: Shear stress [Pa]
$\dot{\gamma}$: Shear rate [s^{-1}]
K_1: Shear stress constant [m^{-3}]
K_2: Shear rate constant [dimensionless]
M: Torque [N·m]
N: Rotational speed [rpm]

Instruments such as a rotational rheometer (RR) can measure rheological properties of fluids. These type of rheometers can operate at different shear values (variable angular velocity) or in

an oscillatory configuration (dynamic mode). The RR is used to investigate time-dependent behavior of fluids. Rotational instruments such as mixers or paddles like in a JT can be calibrated for measurements of rheological properties such as η_{avg} or sometimes referred as Newtonian equivalent η (Salas-Bringas et al. 2006; Alvarenga & Salas-Bringas 2014; Alvarenga, Schüller, et al. 2015). A calibration procedure of a replicated JT adapted to a RR was carried out in **Paper II** for understanding flow behavior of the fluid composition under JT conditions. The determination of the location of the $\dot{\gamma}_{avg}$ in the replicated JT is necessary to enable the determination of η and to understand how shear affects the fluid behavior during the flocculation process in the JT. The obtained $\dot{\gamma}_{avg}$ can be used to downscale or upscale flocculation processes.

5 Materials & methodology utilized

5.1 Materials

5.1.1 Anaerobic digestion residue

The ADR employed for the dewatering study of **Paper I** was sampled from the rejected water stream or centrate of the centrifuge at Lindum AS biogas plant in Drammen (Norway) as seen from Figure 12. Sludge (from different counties and WWTPs), garden and food waste are co-digested in the biogas process. The dewatered ADR produced by Lindum AS is meant to be employed as a biofertilizer in the agriculture sector (Lindum n.d.).

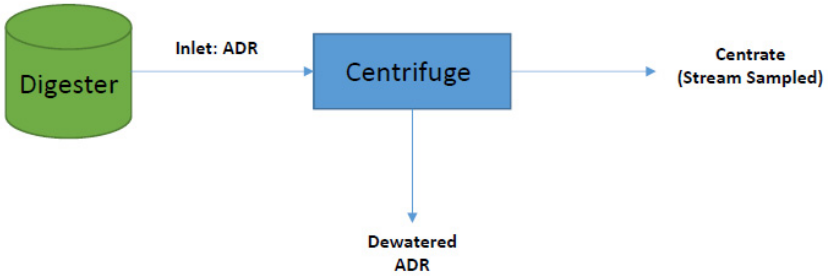

Figure 12: Dewatering flow diagram of Lindum AS biogas plant. The inlet of the centrifuge is anaerobic digestion residue (ADR) from the digester

The physical-chemical parameters of the ADR sampled are shown in Table 2 and were analyzed in accordance to the standard methods for the examination of water and wastewater (APHA 2012).

Table 2: Physical-chemical parameters of the anaerobic digestion residue (ADR)

Parameter	Value or Concentration
pH[a]	8.3 ± 0.2
TS	0.8 ± 0.1 %
SS	0.4 ± 0.07 %
VS	99.90 ± 0.01 %
Conductivity	7.65 ± 0.02 mS/cm
Turbidity	4700 ± 50 FTU
P_{total}	83 ± 5 mg/L
ortho-P	2.5 ± 0.2 mg/L
K	350 ± 20 mg/L
NH_4	50± 3 mg/L
COD	2500 ± 70 mg/L

a: measured at 25°C.

The pH of the ADR substrate was measured in a Thermo Orion pH-meter model Dual Star and the conductivity was determined in a Mettler Toledo instrument model Seven Multi with an electrode Inlab 730. The total solids (TS), suspended solids (SS) and volatile solids (VS) were determined by a gravimetric method at 105°C until constant weight. The P_{total} and the K concentrations were measured by inductively coupled plasma mass spectrometry (ICP-MS). The ortho-P was measured by a UV-spectrophotometry. The ammonia concentration was determined by the ion selective electrode (ISE) method by a Thermo Scientific Orion electrode model 9512HPBNWP connected to the Thermo Orion device model Dual Star.

5.1.2 Iron and aluminium precipitated sewage sludge and inoculum

The sewage sludge samples were taken from the inlet of the thermophilic biogas process of FREVAR KF (FRE) (60°C) and Ullensaker Gardermoen (ULL) (55°C) WWTPs (**Paper III**). These samples were stored at 4°C. The inlet of the AD digesters is Fe-precipitated sludge with $FeCl_3$ for FRE whereas ULL has one precipitated with $Al_2(SO_4)_3$. Both substrates were thickened in the WWTPs for achieving the TS content required for the AD. Accordingly, the inoculum was sampled from the digester (for both sludges FRE and ULL) in the WWTPs and stored at 37°C before the continuously stirred tank reactor (CSTR) experiment (sub-section 5.2.3). Thereby, adapted microorganisms from each biogas process (FRE and ULL) were used in the CSTRs.

The physical-chemical parameters of the sludges sampled are shown in Table 3 and were analyzed in accordance to the standard methods for the examination of water and wastewater (APHA 2012). The pH of the sludges was measured with a Thermo Orion pH-meter model Dual Star and the conductivity was determined in a Mettler Toledo instrument model Seven Multi with an electrode Inlab 730. The TS and VS were determined by a gravimetric method at 105°C and 550°C respectively until constant weight. The P_{total}, Fe, Al, Ca, K, Na and Mg and heavy metals (Cr, Cu, Mn, Ni, Cd, Pb and Zn) contents in all the dry sludges were determined by microwave digestion and inductively coupled plasma optical emission spectrometry (ICP-OES). Organic P was estimated by solubilizing the inorganic P with 12 N H_2SO_4 in a water bath at 70°C for 10 min and subtracting the value from P_{total} (Møberg & Petersen 1982).

Table 3: Physical-chemical parameters of the primary sludges

Parameter	FRE	ULL
Total dry solids (TS, %)	9.5 ± 0.06	5.9 ± 0.04
Volatile solids (VS, % of TS)	71 ± 0.65	72 ± 0.45
pH (25°C)	6.2 ± 0.2	5.9 ± 0.2
Conductivity (mS/cm)	9.64 ± 0.02	4.53 ± 0.02
	g/kg TS	
Fe	115 ± 0.1	7.5 ± 0.1
Al	11 ± 0.1	60 ± 0.1
Ca	9.6 ± 0.08	5.9 ± 0.2
K	5.5 ± 0.1	3.5 ± 0.1
Na	3.8 ± 0.03	0.91 ± 0.01
Mg	1.9 ± 0.1	2 ± 0.1
P_{total}	8.8 ± 0.1	12 ± 0.1
P_{org}*	0.6 ± 0.14	1.9 ± 0.1
N	14 ± 0.1	24 ± 0.1
Cr	0.05 ± 0.002	0.022 ± 0.001
Cu	0.074 ± 0.0008	0.076 ± 0.0008
Mn	0.079 ± 0.0007	0.15 ± 0.0002
Ni	0.014 ± 0.002	0.013 ± 0.001
Cd	0.0004 ± 6e-5	0.0005 ± 6e-5
Pb	0.013 ± 0.001	0.035 ± 0.0002
Zn	0.25 ± 0.01	0.24 ± 0.01

*: Organic P

5.1.3 Alum shale landfill leachate

The leachate was sampled from the superficial water of an open alum shale landfill as shown in Figure 13. The water was pumped to a container. The landfill was constructed by the Norwegian Public Roads Administration (Statens Vegvesen) next to a construction site of a road and a tunnel in Gran County, Norway. The sample was stored at 4°C prior to the sorption experiments of U^{6+} with the DB sorbent in **Paper V**.

Figure 13: Sampling of leachate from the alum shale landfill located in Gran County Norway

The physical-chemical parameters of the leachate were analyzed in accordance to the standard methods for examination of water and wastewater (APHA 2012) and can be seen from Table 4. The pH of the leachate was measured with a Thermo Orion pH-meter model Dual Star and the suspended solids were gravimetrically obtained (105°C). The total organic carbon was measured by catalytic oxidation (680°C) in a TOC-L TOC Shimadzu Analyzer. The alkalinity was determined by titration to a pH of 8.3. The turbidity was measured in a Hanna turbidimeter and the sulfate (SO_4^{2-}) content was determined by barium sulphate precipitation in a colorimeter. The total nitrogen (N_{total}) was measured by means of the Kjeldahl method. All the other elements (including U) were measured by ICP-MS.

Table 4: Physical-chemical parameters of the leachate

Parameter	Unit	Value or concentration
pH (25°C)	-	7.5
Total organic carbon	mg/L	1.2
Alkalinity (pH = 8.3)	mmol/L	<0.15
Turbidity	FNU	26.4
Suspended solids	mg/L	26.1
S	mg/L	116
SO_4^{2-}	mg/L	309
N_{total}	mg/L	27.5
P_{total}	mg/L	0.03
Cl^-	mg/L	25.4
Ca	mg/L	110
Fe	µg/L	327
K	mg/L	12.2
Mg	mg/L	14
Na	mg/L	110
Al	µg/L	213
As	µg/L	5.4
Ba	µg/L	140
Cd	µg/L	0.5
Co	µg/L	0.3
Cr	µg/L	0.2
Cs	µg/L	0.7
Cu	µg/L	0.6
Hg	µg/L	<0.002
Mn	µg/L	48.4
Mo	µg/L	800
Ni	µg/L	10
Pb	µg/L	0.7
Si	mg/L	7.1
Sr	µg/L	1900
Zn	µg/L	33
V	µg/L	10.2
B	µg/L	85.5
Th	µg/L	<0.04
U	µg/L	150

5.1.4 Conditioners for dewatering and sorbents

The code "DB" refers to a diatomite-bentonite combined system and it was selected from among other tested materials such as olivine and nepheline (produced by Sibelco AS, Norway), Drammen blue clay (from Norway) and commercial Polyclays (provided by Nordisk Vannteknikk AS, Norway). The DB conditioner/sorbent was previously characterized and tested by Dr. Sergey Hayrapetyan from Yerevan State University (Armenia) and therefore, it was selected for importing knowledge and experience with the system to Norwegian local materials.

The diatomite (a naturally occurring siliceous rock) is amorphous silica (SiO_2) with a SiO_2 content between 85-90 %. It adds porosity to the system while the bentonite (a clay consisting of 60-70 % montmorillonite, $Al_2[Si_4O_{10}](OH)_2 \cdot nH_2O$) provides the structure for functional groups (e.g., CaO and PO_4^{3-}). The bentonite is produced by the Ijevan Bentonite company and a diatomite is elaborated by the Diatomite company, both from the Republic of Armenia. The Armenian diatomite has a pore size between 150-200 nm and a pore volume of 2 $cm^3\ g^{-1}$. In addition, the diatomite was used in a SiO_2–MnO_2–composite sorbent (7.4 $\%_{w/w}$ MnO_2) to remove K^+ in **Paper IV** from a mono component synthetic solution of 2 g L^{-1} of potassium hydroxide (KOH). Typically, the specific surface area measured for the bentonite by means of nitrogen gas gives results in the range of 20–100 $m^2\ g^{-1}$ of clay regardless of the preparation technique and the montmorillonite content (Eisenhour & Reisch 2006). The diatomite on the other hand, is the silica-containing component, which provides the structure for increasing porosity and rigidity in the mineral conditioner as well as for enhancing mass transfer for sorption. These properties provide favorable filterability as well as sorption in order to avoid clogging during filtration (Novak et al. 1988).

The DB natural porous system was used as a mineral conditioner in **Paper I** to decrease the amount of the chemical conditioner ZETAG 9014® (a cationic polyacrylamide produced by BAFS SE, Germany) for maintaining effective dewaterability of the ADR whereas in **Paper V**, it was utilized as a sorbent for U^{6+}.

Lime stabilization (with CaO and $Ca(OH)_2$) and conditioning (with $Ca(OH)_2$) of untreated and anaerobically digested Fe- and Al-precipitated sludges was performed in **Paper III**. The company Miljøkalk AS from Norway produced both types of lime.

5.1.5 Soil and crop for the greenhouse experiment

A nutrient-deficient soil from Norway consisting of 1 % clay, 2 % silt and 97 % sand was taken into account for the greenhouse experiment of **Paper III**. The crop employed as a reference was a variety of barley (*Hordeum Vulgare L. cv. Heder*).

5.1.6 Jar-tester (JT) prototype and silicon oil

Jar-testers were utilized for dispersing conditioners in the ADR or Fe- and Al-precipitated sludges (**Papers I** and **III**). The substrates were conditioned thereby for dewatering. The JT employed in **Paper I**, a Kemira™ Flocculator 2000, was replicated in a CAD program, SolidWorks® as seen in Figure 14 (a) and (b). The prototype was used in **Paper II** and was printed in an ABS 3D printer Mojo® as shown in Figure 15. The paddle was printed in two sections and it includes a lid for the container. The black square surface is a holder of the printer.

(a) (b)

Figure 14: (a) Kemira™ Jar-tester (JT) unit and (b) replicated system in SolidWorks®

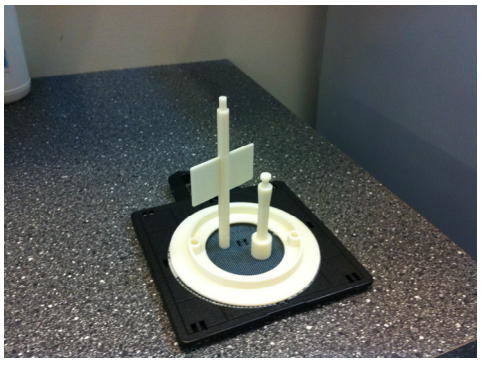

Figure 15: Prototype and lid of the Jar-tester (JT) printed in an ABS 3D printer Mojo®

A calibration procedure of the prototype (**Paper II**) described in sub-section 5.2.2, was performed with a standard Newtonian silicon oil (SO) labelled as 1000 cP and produced by Brookfield Engineering Laboratories Inc. in USA.

5.2 Methodology

The two main parts of this thesis are dewatering and sorption, as mentioned in Chap. 3. The conditioning and further dewatering of ADR was optimized in **Paper I**. The parameters analyzed were the turbidity of the separated liquid phase and the capillary suction time of the ADR during flocculation. Moreover, the weight of the dry and wet sludges after SLS was monitored. Stabilization of sludge (with AD or liming) and mineral conditioning with $Ca(OH)_2$ of ADR was carried out in **Paper III** for desorbing P_{inorg} from sludge and ADR. The parameters controlled for the AD were pH, and concentrations of CH_4, NH_4^+, volatile organic acids and alkalinity as total inorganic carbon. The P_{tot} content was determined in the chemical characterization of the sludges and ADR as well as in the crop of the greenhouse experiment.

The changes in Torque (*M*) were measured by means of rotational rheometry over a broad set of rotational speeds (*Ns*) and temperatures for the calibration of the JT prototype in **Paper II**. Such physical parameters allowed obtaining flow curves. Moreover, a mathematical expression for the prediction of the η_{avg} of a Newtonian fluid was found in terms of *M* and *N* at different temperatures and in laminar and turbulent flow regimes. Such approach provided a calibrated system for measurements of η_{avg} by means of a JT prior to the dewatering of sludge or ADR (**Paper I** and **Paper III**).

Dynamic sorption was considered in **Papers IV** and **V**. Removal of K^+ and U^{6+} were monitored with changes in their concentration over the sorption process along with the pH and the temperature. Additionally the flow rate (*Q*) was controlled in both laboratory and pilot scales.

5.2.1 Dewatering with a diatomite-bentonite system

The physical conditioner was DB-12Ca and it was added to the ADR and dispersed at 300 rpm for 300 s. The code "12" refers to the weight ratio of bentonite:diatomite (2:1). A slurry of CaO was prepared and added to the DB system in order to fix Ca to the surface of the bentonite. The chemical conditioner was ZETAG 9014® and it was dosed at t = 300 s in accordance with the design of the dewatering batch experiments presented in Table 5 (Alvarenga, Hayrapetyan, et al. 2015). The dispersion time was 180 s at 300 rpm. A slow flocculation phase followed at 30 rpm for 600 s. The dewatering of the ADR was carried out with a laboratory scale vacuum filtration assembly as seen from Figure 16 (Dahlstrom et al. 1999). The term "water retention capacity (WRC)" was introduced for evaluating the dewatering performance. It was defined as follows,

$$\mathrm{WRC} = \frac{[\text{Mass of wet sludge(g)} - \text{Mass of dry sludge (g)}]}{\text{Mass of dry sludge (g)}} \tag{14}$$

Table 5: Design for the dewatering batch experiments and doses for 1L of anaerobic digestion residue (ADR) (Alvarenga, Hayrapetyan, et al. 2015)

Experiment	Dose of DB-12Ca (g/g of TS)	Dose of ZETAG® 9014 (mg/g of TS)
1	0.8	19
2	0.8	38
3	0.8	75
4	0.8	150
5	1.6	19
6	1.6	38
7	1.6	75
8	1.6	150
9	3.1	19
10	3.1	38
11	3.1	75
12	3.1	150
13	4.7	19
14	4.7	38
15	4.7	75
16	4.7	150

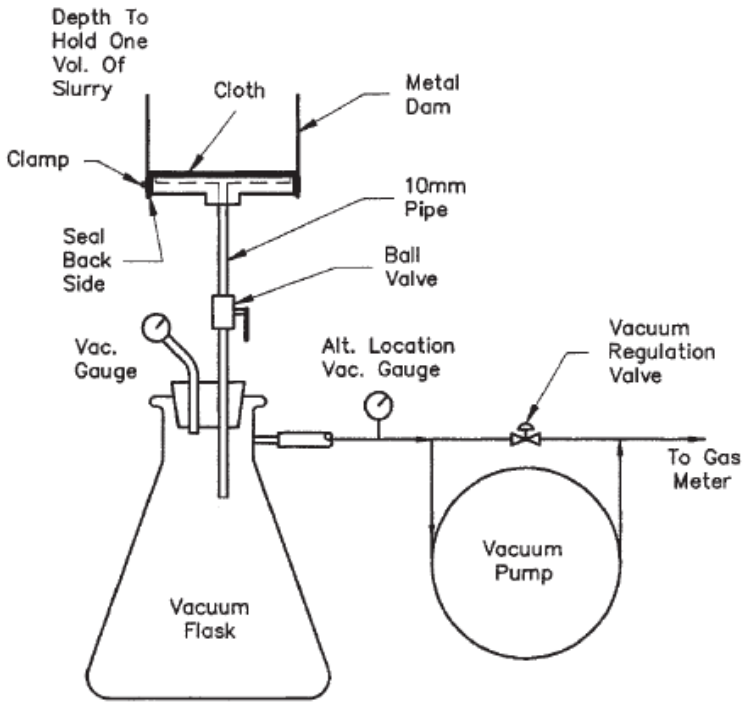

Figure 16: Vacuum filtration assembly for the dewatering of anaerobic digestion residue (ADR) (Dahlstrom et al. 1999)

5.2.2 Calibration procedure of the Jar-tester (JT) prototype

The JT replicated paddle (of a Kemira™ JT, **Paper I**) was adapted to a rotational rheometer Paar Physica UDS 200 as seen from Figure 17. The prototype was calibrated using a 1000 cP SO. Moreover, the temperature was controlled with a water bath. The slow mixing range (for laminar regime) considered was between 10 to 50 rpm; whereas the fast mixing (or turbulent regime) was between 100 to 500 rpm (**Paper II**). For both flow regimes, the volume of the SO considered was 725 mL.

The actual viscosity of the silicon oil was measured by means of a cone-plate geometry (50 mm diameter, 1^0, 50 µm gap) at constant shear rate (5 s^{-1}) in an Anton Paar rheometer MCR-301. The temperature range from 20 to 60^0C with 10^0C ramping steps was taken into consideration for the actual viscosity measurements.

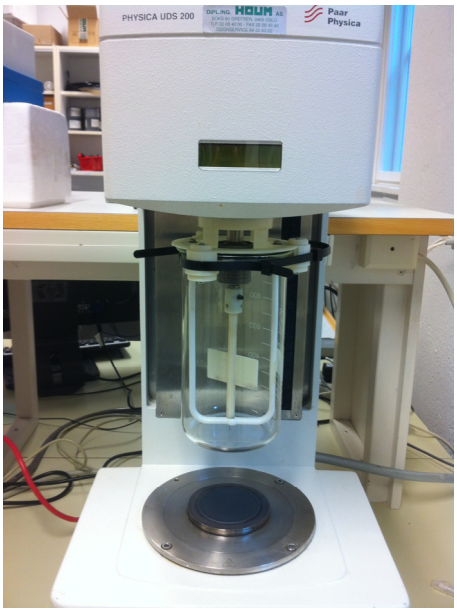

Figure 17: Replicate of the Jar-tester (JT) assembled to a Paar Physica UDS 200 rotational rheometer

In the laminar regime (from 10 to 50 rpm), the calibration procedure was based on a coaxial analogue method which has been already tested for other geometries and screw type of probes (Salas-Bringas et al. 2006; Salas-Bringas 2011). In such geometry, Eq. 13 can be expressed as,

$$\eta = \frac{15\delta}{\pi^2 r^3 h} \cdot \frac{M}{N} \tag{15}$$

Where, M/N is the slope between Torque (M) (N·m) and rotational speed (N) (rpm) and h (m) is the height of the radius of the analogue cylinder. This slope can be obtained with a Newtonian standard of known η by measuring both M and N in the rheometer. It is therefore possible to

estimate by an iterative process the radius r (m) of the analogue cylinder and the gap δ (m) or "r_{cyl} -r" between the concentric cylinders.

The turbulent regime required the inclusion of an additional term in Eq. 13. A mathematical expression was defined as,

$$M = A \cdot N^B \cdot \eta + C \cdot N^D \quad (16)$$

Where A, B, C and D are constants and coefficients determined by means of the function *fminsearch* in MatLab® from MathWorks Inc.. The script was based on the work performed before by Schüller et al. (2010) and it is included in the Appendix. The first term of Eq. 16 is fundamentally Eq. 13 when $B = 1$. The second term was considered as a turbulent component, which provided a non-linear response in the rheometer for M from 100 to 500 rpm (**Paper II**). The model is based on the assumption that the η_{avg} depends only on temperature (Steffe 1996c).

5.2.3 Anaerobic digestion treatment and liming of the iron and aluminium precipitated sludges

The four CSTR biogas reactors were produced by the Dep. of Mathematical Sciences and Technology of the Norwegian University of Life Sciences. These are shown in Figure 18 and they had a start-up phase based on the experiment of Estevez et al. (2014) with 9 L of inoculum and with a gradual increase of their organic load rate from 1 to 3 g of VS $L^{-1}d^{-1}$ over three weeks. There were two replicates per substrate (FRE and ULL) considered for such treatment in order to evaluate the repeatability of the measurements. These CSTR units were continuously monitored for the parameters mentioned before. The nominal working volume was 15 L. The configuration was thermophilic (55 and 60°C) and a HRT for the sludges of 22 days for FRE and 15 days for ULL (**Paper III**) was taken into account.

Figure 18: Biogas continuous stirred tank reactors (CSTRs) in thermophilic configuration with two replicates for FRE and two for ULL

The untreated sludges and the ADR after the biogas process were limed with $Ca(OH)_2$ to a final concentration of 26 % (0.35 g $Ca(OH)_2$ g^{-1} TS). Additionally, the untreated sludges were limed with CaO up to 27 % (0.39 g CaO g^{-1} TS). A JT equipment from Phipps & Bird™ was used as a tool for the dispersion of the lime with a rotational speed of 100 rpm for 10 min in 800 mL of sludge or ADR. The resulting limed products were decanted and dried at 105°C.

5.2.4 Characterization of phosphorus (P) in the fertilizers (sludges and ADR)

All the untreated and treated substrates by AD or liming were chemically analyzed for P_{tot} and characterized by means of a modified sequential extraction scheme for P (Hedley et al. 1982; Sharpley & Moyer 2000). One g of dry sample was sequentially extracted with 200 mL of deionized water for 1 h followed by 200 mL of 0.5 M $NaHCO_3$ (labile-P), 0.1 M NaOH (Al/Fe-bound P) and 1 M HCl (stable Ca-P) each for 16 h. The residual P was determined after an acid digestion in a high performance microwave reactor model IV from MLS GmbH for 4 h at 260°C and 50 bar. The P_{tot} was analyzed in the fertilizers and in the different fractions using an ICP-OES Perkin-Elmer model 5300 DV.

5.2.5 Greenhouse experiment for phosphorus (P) recycling

The pot experiment was carried out in a greenhouse as seen from Figure 19. Ten fertilizers were obtained in total from the treatments described in sub-section 5.2.3. The relative P plant uptake in the sludges was compared to the fractions obtained in the characterization described in sub-section 5.2.4. Moreover, each treatment had three replicates (pots).

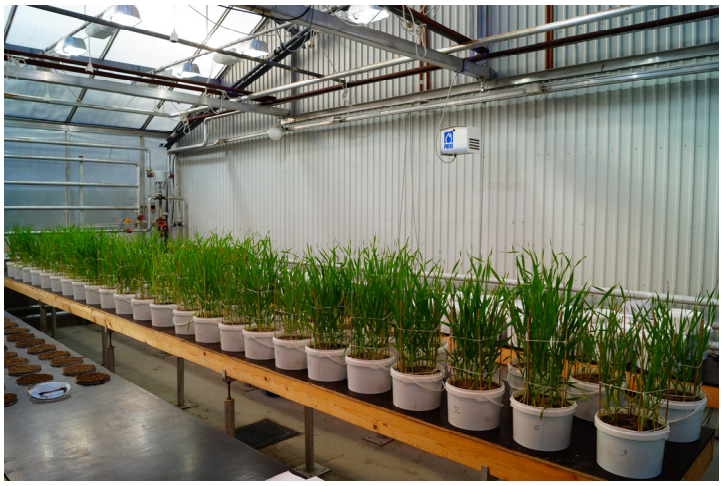

Figure 19: Greenhouse phosphorus plant uptake experiment (48 pots)

A soil with nutrient deficiency consisting of a limed mixture of sand and 4 weight-% sphagnum peat was added to 3 L pot to a final weight of 3.5 kg. The P plant available content of the soil was low with 11 mg kg^{-1} measured by the ammonium lactate extractable P method (Egnér et al. 1960). The sludge (untreated and treated) amounts that were applied, were based on a total P content and 90 mg P pot^{-1}, equivalent to 60 kg P ha^{-1} (assuming 20 cm topsoil depth). The P fertilization effect of the sludges was compared to the treatment with no P added and mineral control treatments where $Ca(H_2PO_4)_2$ was applied at a rate of 45 and 90 mg P pot^{-1}, equivalent to 30, 60 kg P ha^{-1}. All other nutrients were applied in amounts regarded as sufficient for ensuring that only P would be the limiting nutrient for plant growth. Nitrogen was applied as $Ca(NO_3)_2$ (300 mg N pot^{-1}), K as K_2SO_4 (300 mg K pot^{-1}) and Mg as $MgSO_4$ (37.5 mg Mg pot^{-1}). In addition, micronutrients (Fe, Mn, Cu, Mo, B and Zn) were applied. All mineral nutrients were added in solution. The controls had two pH levels (6.5 and 6.9) to account for possible pH effect on P uptake. Whereas, the sample pots had only one initial pH level of 6.5. The pH was adjusted by means of solid calcium carbonate ($CaCO_3$) reagent grade for all the pots, 0.3 g $CaCO_3$ per kg soil mixture for the pH 6.5 and 0.8 g $CaCO_3$ per kg soil mixture for the pH 6.9. There were three replicates per treatment.

The relative P fertilization effect or agronomic efficiency (RAE) for the treatments of the sludges was calculated from Eq. 17.

$$\% \text{ RAE} = \frac{P_{uptake} - P_{uptake\ (control\ 0\ mg\ P\ per\ pot)}}{P_{uptake\ (control\ 90\ mg\ P\ per\ pot)} - P_{uptake\ (control\ 0\ mg\ P\ per\ pot)}} X100 \quad (17)$$

The sand and peat mixture was mixed homogenously with the sludges, except a top layer of approximately 2.5 cm without sludge. The latter was carried out for avoiding negative effects on the germination associated to fertilization. Holes of 1 cm depth were done where 18 seeds of barley were sown. The number of plants was adjusted to 15 after the germination.

Deionized water was applied three times a week to about 60 % of water holding capacity. The light was provided by 18 fluorescent lamps of 400 W (model Osram Powerstar HQI-BT®) in a 40 m^2 room. The photosynthetic flux in the room was 200 µmol m^{-2} s^{-1} at plant height with a 16 h/8 h day/night cycle. Heating was provided if the temperature dropped bellow 18°C during the day (16 h) and 15°C at night (8 h). The plants were harvested approximately 7 weeks after sowing, when the plants were at start of heading. The plants were cut roughly 2.5 cm above the soil surface, stored in a paper bag per pot and dried at 60°C until constant weight. The plant samples were afterward grounded and digested in the high performance microwave reactor equipment for the further analysis of the P_{tot} by ICP-OES.

5.2.6 Dynamic sorption experiments of potassium (K^+) with a SiO_2–MnO_2–diatomite composite sorbent (laboratory scale)

The sorbent was prepared with 0.2 L of water glass (390 g L^{-1} SiO_2, silicate modulus M = 3.0) and 35 g of $KMnO_4$. A 0.5 L slurry of diatomite (**Papers I** and **V**) of 200 g L^{-1} was added to the system in order to fixate to its surface the functional group of MnO_2 as well as for adding porosity for the enhancement of mass transfer. The mixture was filtered and dried at room temperature followed by a further drying at 105°C. Thereafter, the system was grounded to obtain a powder consistency.

The specific surface area as m^2 g^{-1} was measured for the sorbent with the BET method (Brunauer et al. 1938) by means of a Gemini VI® instrument manufactured by Micromeritics USA Ltd. The value obtained was 422 m^2 g^{-1} for SiO_2–MnO_2–diatomite.

The sorption process configuration was in dynamic mode were a column with dimensions 200 mm X 1.0 mm was filled with 8 g of the sorbent. A synthetic solution of KOH 2 g L^{-1} was passed through the columns from the top to the bottom at a Q of 1 mL min^{-1}. The Q was controlled by gravity and the separation of K^+ (**Paper IV**) was carried out at room temperature (20°C). Volume samples were taken until reaching saturation of the sorbent. Aliquots were taken from the volumes samples and analyzed by ICP-MS model Agilent Tech. 8800 Triple Squad.

5.2.7 Dynamic sorption experiments of uranium (U^{6+}) with a diatomite-bentonite sorbent (laboratory and pilot scale)

The sorbent coded as DB-12P-HP was prepared with the same base materials as in **Paper I**. The code "DB" refers to the diatomite-bentonite combined system. A 1 L bentonite slurry of 200 g L^{-1} was prepared and mixed with of a 100 ml 10 $\%_{v/v}$ solution of phosphoric acid (H_3PO_4). The volume ratio of bentonite to H_3PO_4 was 10:1. The mixture was left in contact and undisturbed overnight. Afterward, a 0.5 L slurry of diatomite of 200 g L^{-1} was added to the aforementioned mixture. The code "12P" refers to the DB weight ratio of bentonite:diatomite = 2:1 and the H_3PO_4 treatment. The system was then filtered and the resulting solid was dried at room temperature; followed by a drying at 105°C. The system was grounded in order to obtain a homogeneous powder consistency. The term "HP" refers to a further treatment with H_3PO_4.

The specific surface area as m^2 g^{-1} was measured for DB-12P-HP with the BET method (Brunauer et al. 1938) by means of a Gemini VI® instrument manufactured by Micromeritics USA Ltd. The value obtained was 209 m^2 g^{-1} for DB-12P-HP.

A granulation process was carried out manually for the laboratory and pilot scales by adding gradually the 10 $\%_{v/v}$ H_3PO_4 solution (approximately 50 mL) to a container with DB-12P-HP system as powder with an amount lower than 50 g. Granules where obtained by shaking the mixture with circular movements until the system was aggregated. The wet granules were sieved in a 3 to 4 mm mesh and the process was repeated until obtaining a particle size between 3 to 4 mm. It was possible to granulate 400-500 g of DB-12P-HP per batch with approximately 50 mL of the H_3PO_4 solution. These batches were dried at room temperature followed by a heat treatment of 500°C for 4 h for improving its porosity and further resistance to water flow.

An amount of 24 g of granulated sorbent was added to the column in the small scale as seen in Figure 20 (**Paper V**). An initial regeneration with 0.1 L of a 7.5 $\%_{v/v}$ hydrochloric acid (HCl) solution was performed prior to the first sorption experiment. The column was then washed with deionized water for removal of the remaining acid. Afterward, the sample (leachate) was introduced without any pH adjustment (pH 7.5), from the top of the column at a Q of 3 mL min^{-1} by gravity. The temperature was 10°C over the whole sorption experiment. Volume samples were collected from the bottom of the columns. In addition, aliquots of 5 mL were taken for each of the volumes sampled for quantifying the concentration of U^{6+} after contact with the sorbents. For that purpose, an ICP-MS model Agilent Tech. 8800 Triple Squad was used.

After reaching saturation of the sorbent at pH 7.5, a second regeneration was carried out with the 7.5 $\%_{v/v}$ HCl solution. Samples were taken during the regeneration in order to determine the amount of acid required for "cleaning" the sorbents. After regeneration and washing with deionized water, the pH of the sample was adjusted to 4.0 with concentrated HCl and then a second sorption experiment was performed at the same temperature and Q as the previous one.

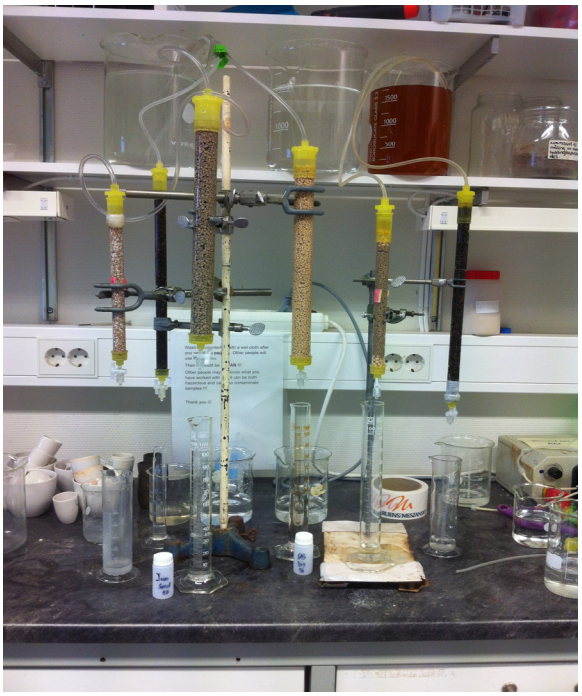

Figure 20: Experimental assembly of the dynamic sorption of uranium (U^{6+}) with DB-12P-HP

An amount of 12.3 kg of the granulized sorbent DB-12P-HP was packed in a 20 L ion exchange column model LC 010 and produced by the company Novatek AS in Norway as seen in Figure 21. Such column works in a counter flow configuration. The sorbent was regenerated/washed once with 20 L of a solution of HNO_3 10 $\%_{v/v}$. Deionized water was pumped after to remove the excess of acid in the column. The leachate was passed through the column with a peristaltic pump model Masterflex® L/S and manufactured by Cole-Parmer Instrument Company at two *Q*s; 1.5 L min^{-1} firstly and then at 0.5 L min^{-1}. The sorption trial was carried out at 10°C in a cooling room with a controlled temperature. The volume passed through the column was measured and aliquots were taken for the further analytical determination of U^{6+}. Moreover, the pH was measured in every aliquot for determining a set of operation conditions (pH and *Q*) for effective removal of U^{6+}. The saturation of the sorbent was not achieved in this case. The samples taken were analyzed using ICP-MS.

(a) (b)

Figure 21: Experimental assembly of the dynamic sorption in pilot scale showing (a) the sample (alum shale leachate) in the biggest container and the columns (in blue) and (b) the pump before the inlet of the counterflow columns

6 Main results and discussions

The main results of all the **Papers** (**I** to **V**) are included in this Chapter. Additionally, results of rheological measurements from the testing of the JT prototype (**Paper II**) during flocculation of ADR are shown in sub-section 6.2.3. Finally, preliminary results for U^{6+} sorption in pilot scale are included in sub-section 6.5.2.

6.1 Effect of bentonite based conditioners on dewatering of anaerobic digestion residue (ADR) (Paper I)

The substrate considered was ADR and it was characterized as described in sub-section 5.1.1. The DB surface has SiO_2 (mainly from the diatomite), Al_2O_3 (from the bentonite) and other minor oxides (CaO, MgO, Fe_2O_3, TiO_2 Na_2O, K_2O etc.) as structure forming oxides. The functional group of the DB-12Ca mineral conditioner was CaO. The DB-12Ca material was treated with a slurry of CaO so its content of Ca could be increased to 5 % in order to enhance sorption (taken into account for **Paper V**) and flocculation of the ADR particles (e.g., colloidal). The composition of the DB-12Ca conditioner from three x-ray fluorescence (XRF) spectrums is shown in Figure 22 and it can be seen from Table 6. The equipment was calibrated with a backscattered electron detector calibration standard for scanning electron microscopy.

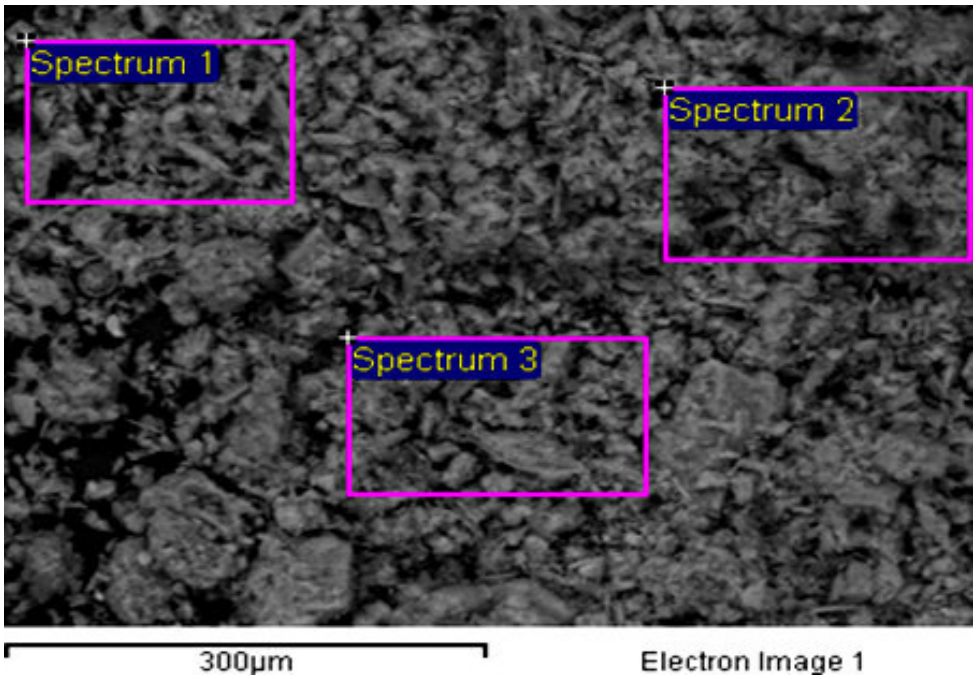

Figure 22: Spectrums selected for the scanning electron microscopy of the mineral conditioner, DB-12Ca.

Table 6: X-ray fluorescence (XRF) data of the mineral conditioner or sorbent (results are semiquantitative and in weight %)

Spectrum	Elements										
	O	Na	Mg	Al	Si	P	K	Ca	Ti	Fe	Total
1	63.3	0.5	0.6	2.9	22.3	3.7	0.3	4.8	0.1	1.5	100
2	65.4	0.6	0.7	3.0	23.1	3.9	0.3	5.0	0.1	1.5	100
3	68.5	0.6	0.7	3.1	24.2	4.0	0.4	5.2	0.1	1.6	100
Mean	65.7	0.6	0.7	2.9	23.2	3.9	0.3	5.0	0.1	1.6	100
STD dev.	2.6	0.02	0.03	0.12	0.9	0.1	0.01	0.2	0.004	0.06	-

The findings in **Paper I** proved that the WRC of the ADR was increasing linearly by increasing the chemical conditioner ZETAG 9014® amount in the flocculation, whereas with the DB-12Ca dose an opposite trend was obtained as seen from Figure 23 (a) and (b). In other words, dewatering rates of ADR are slower when flocculating with a polymer than with a physical conditioner as investigated by Thapa et al. (2009) for lignite. Therefore, the mineral conditioner has a tendency to weaken the water retention properties of the polymer (Thapa et al. 2009). On the other hand, excess of polymer would cause gelation of the sludge or ADR and further pressing would be required to increase the dewatering efficiency of the process.

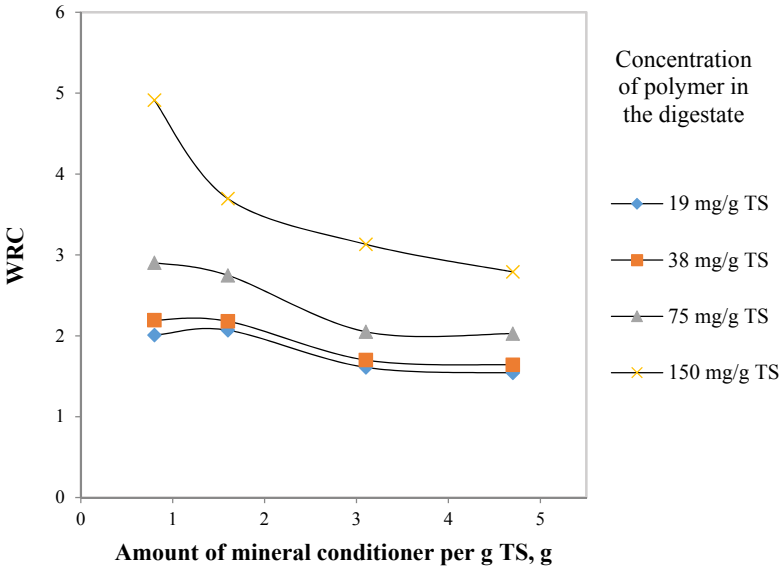

(a)

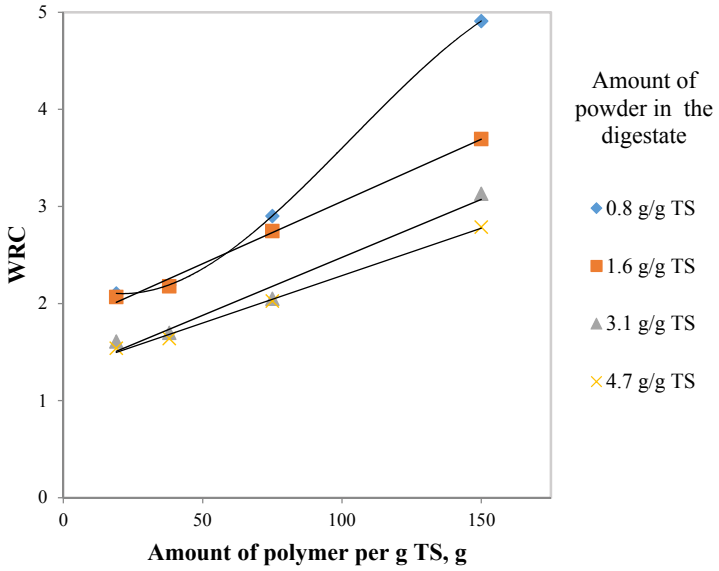

(b)

Figure 23: Influence in the water retention capacity (WRC) with filter powder (a) and polymer addition (b)

The mineral conditioner contains 5 % Ca that reacts with dissolved organics (fulvic and humic acids) in the ADR by an ion exchange process as formerly studied by Li (2014) for the mechanism of clogging in landfill leachates by means of $CaCO_3$. However, a synergy effect occurs when using additionally a polymer for flocculation of ADR. Thereby, it was possible to

determine a filterability region of WRC in terms of the relative fraction (%) of polymer in the dry cake as shown in Figure 24. Two critical points were determined in order to achieve favorable filterability (marked in gray color) without clogging the system (lowest point) as well as for the gelation of the system (highest point).

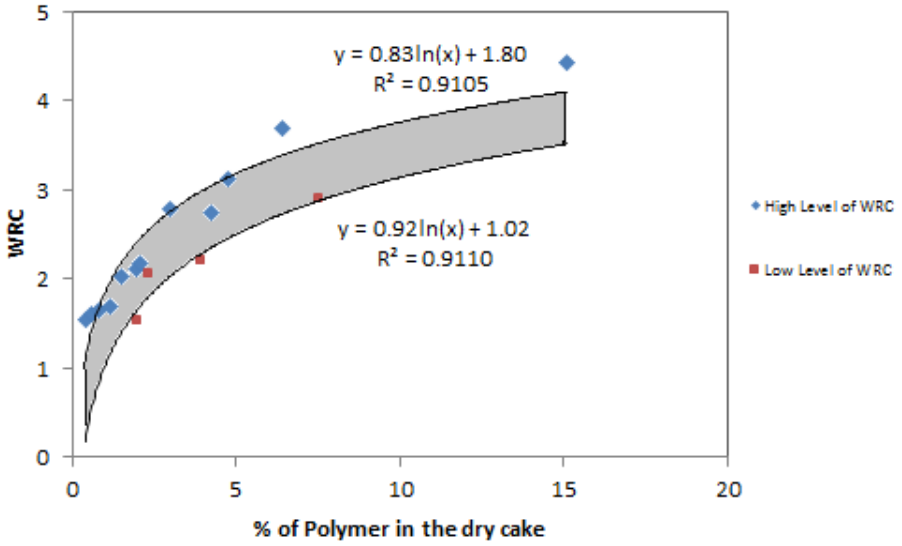

Figure 24: The influence of polymer content on the water retention capacity (WRC)

The doses of both conditioners were optimized with the assessment of the flocculation and filtration properties of ADR such as turbidity. The optimal doses of the dewatering process obtained were 19-25 mg of polymer and 0.8-1.6 g of mineral conditioner per g of TS of ADR. Figure 25 presents the effect of the amount of DB-12Ca and concentration of ZETAG 9014® on the turbidity of the effluent of the ADR after the dewatering.

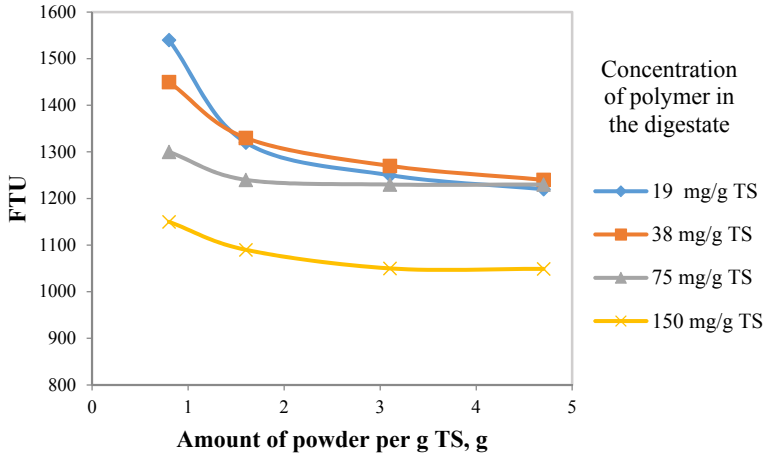

Figure 25: Turbidity of the anaerobic digestion residue treated by mineral conditioner and polymer

6.2 Jar-tester (JT) conditions and their influence in the separation from liquid to solid of anaerobic digestion residue (ADR) (Paper II)

A Newtonian SO was used and physically characterized (with the measurement of the actual viscosity) as described in sub-section 5.2.2. Results of the actual viscosity of the SO are included in Table 7.

6.2.1 Estimation of the average viscosity of a Newtonian fluid with a Jar-tester (JT) in laminar regime

A good prediction of the average viscosity (η_{avg}) was obtained from the linear fit of Torque (M) and rotational speed (N) from the UDS 200 rheometer for **Paper II**. The linear relationships for the SO at different temperatures and the variation of the slope (M/N) can be seen from Figure 26. Moreover, the slope (M/N) considered the effects associated with viscous shear.

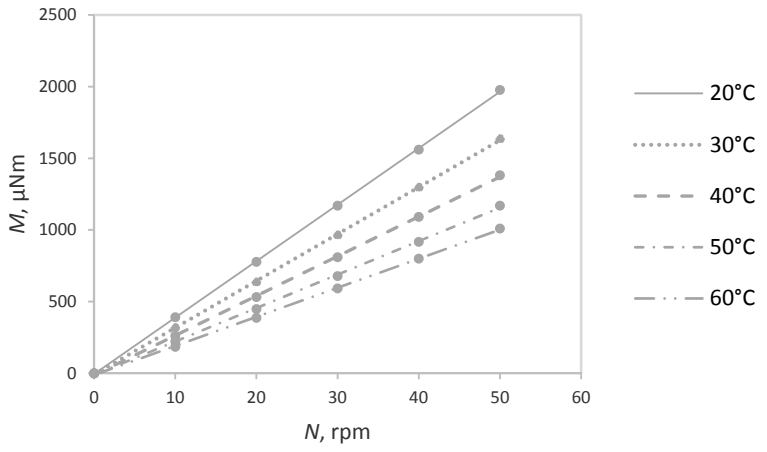

Figure 26: Linear relations between average Torque, M (Nm) and rotational speed, N (rpm) over the whole temperature range. The measurements were performed in a Paar Physica UDS200 rheometer

The variation of the slope (M/N) along with the predicted η_{avg} are included in Table 7. The function Goal Seek from Excel® was utilized for the iterative calculation of the analogue radius (r = 0.03056 m) from Eq. 15 (Salas-Bringas 2011; Alvarenga & Salas-Bringas 2014). The constants K_1 and K_2 obtained for the calculation of the shear stress (τ) and the shear rate ($\dot{\gamma}$)were 5902.7 m^{-3} and 0.213 (dimensionless) respectively. It was hence possible to predict the η_{avg} of the Newtonian SO with the JT mixer prototype in laminar regime.

Table 7: Variation of slope (Torque/Rotational speed, *M/N*) within the temperature range and the inclusion of the predicted viscosity and the relative error (*E*)

T (°C)	Slope (*M*/*N*) Viscosity	Actual Viscosity (Pa·s)	Predicted Viscosity (Pa·s)	*E*
20	0.000039241	1.110	1.088	0.020
30	0.000032465	0.913	0.9	0.014
40	0.000027326	0.759	0.757	0.002
50	0.000023043	0.641	0.639	0.004
60	0.000019978	0.549	0.554	0.009

6.2.2 Modelling of the average viscosity of a Newtonian fluid and the effect of the rotational speed of a Jar-tester (JT) on the location of the average shear rate in turbulent regime

The flow regime was considered turbulent for a Reynolds number above 10 000 (Sinnott 2013) for SO at 20°C (**Paper II**). The transition of the flow regime from laminar to turbulent was determined at $N = 100$ rpm. Such flow regime gave a non-linear response of M vs. N as shown in Figure 27.

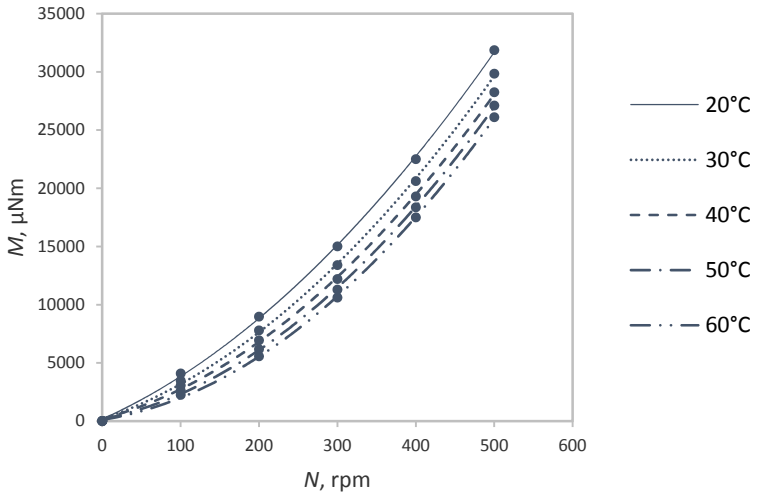

Figure 27: Non-linear relations between average Torque, M (µNm) and rotational speed, N (rpm) over the whole temperature range. The measurements were performed in a Paar Physica UDS200 rheometer

The function *fminsearch* from MatLab® allowed linearizing the relationship of M vs. N by minimizing the prediction error to the largest possible extent. The coefficients and constants calculated in MatLab® for Eq. 16 were,

$$M = 100.9 \cdot N^{0.75} \cdot \eta + 0.032 \cdot N^{2.15} \quad (18)$$

A good correlation was obtained by plotting the predicted *M* from Eq. 18 against the experimental *M* as shown in Figure 28.

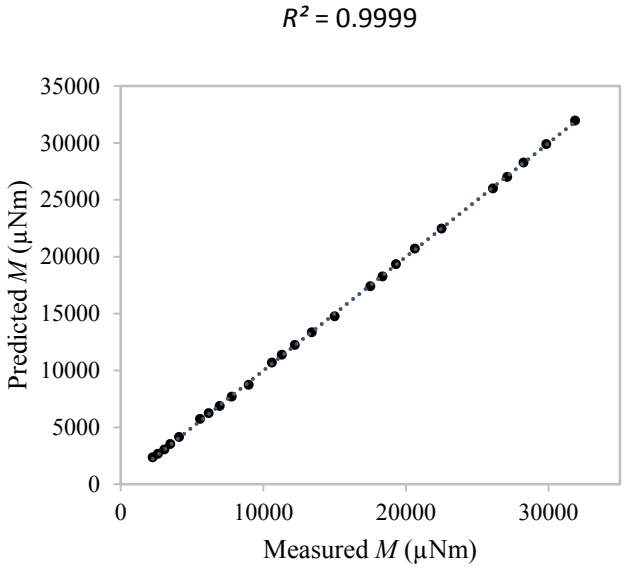

Figure 28: Linear relationship between the experimental and the predicted Torque for all the rotational speeds (100-500 rpm) over the whole temperature range (20-60^{0}C)

Equation 18 shows that there is a viscous contribution to the *M* (or the shear stress) of the fluid along with a turbulent effect. The latter causes the non-linear behavior of the experimental data in spite of using a Newtonian fluid for the measurements. The turbulence induced by the JT propeller influenced the response of the rotational rheometer (*M*) with a coefficient of 2.15 in Eq. 18. The model from Eq. 18 takes as an input the temperature and the *N* and it "linearizes" the response of the rotational rheometer. Furthermore, Eq. 18 considers the effect associated with turbulence over the whole calibration range (10-500 rpm). There is most likely that laminar regions are present in the layer close to the mixer surface or to the wall of the JT (with fluid velocities close to zero) whereas turbulent effects prevail in other sections of the JT with higher $\dot{\gamma}$ (Zhang et al. 2012). Thereby, the location of the average shear rate ($\dot{\gamma}_{avg}$) in the JT depends on the *N*.

6.2.3 Degree of separation from liquid to solid in a flocculation process of anaerobic digestion residue (ADR)

A calibrated system for rheological measurements as the one from **Paper II** was preliminary tested for the flocculation of ADR (9 % by weight of TS). The results show in Figure 29 (Alvarenga & Salas-Bringas 2014) that there is a significant effect on *M* when adding the polymer during the fast mixing of the flocculation. The device utilized was the JT and the conditioners investigated in **Paper I**. After reaching a maximum, *M* starts to decrease but the reason was undetermined.

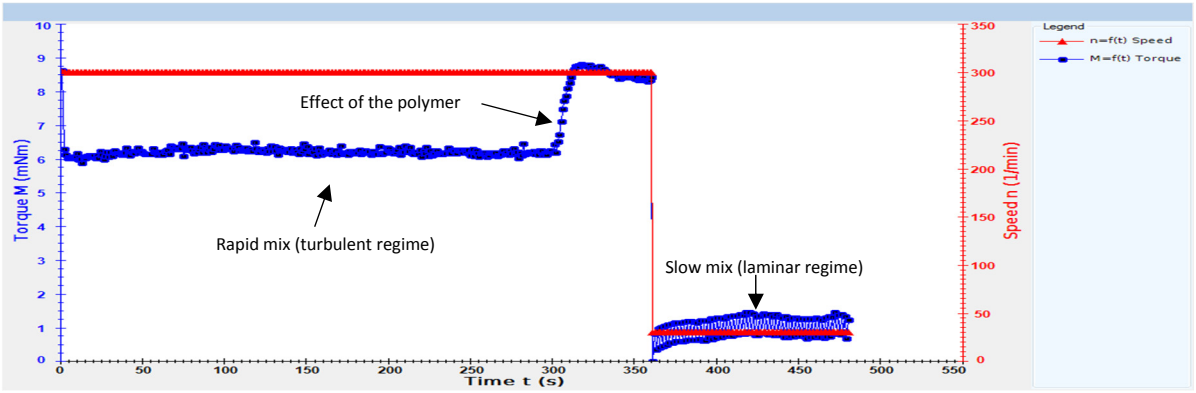

(a)

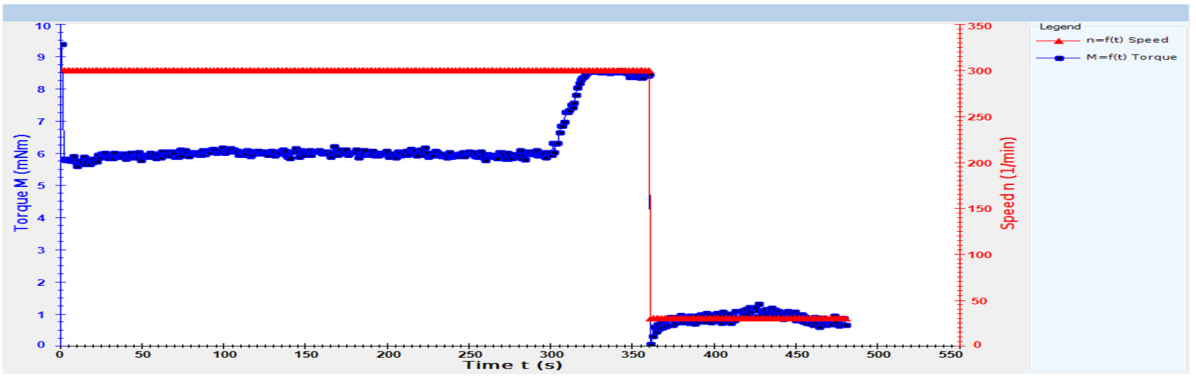

(b)

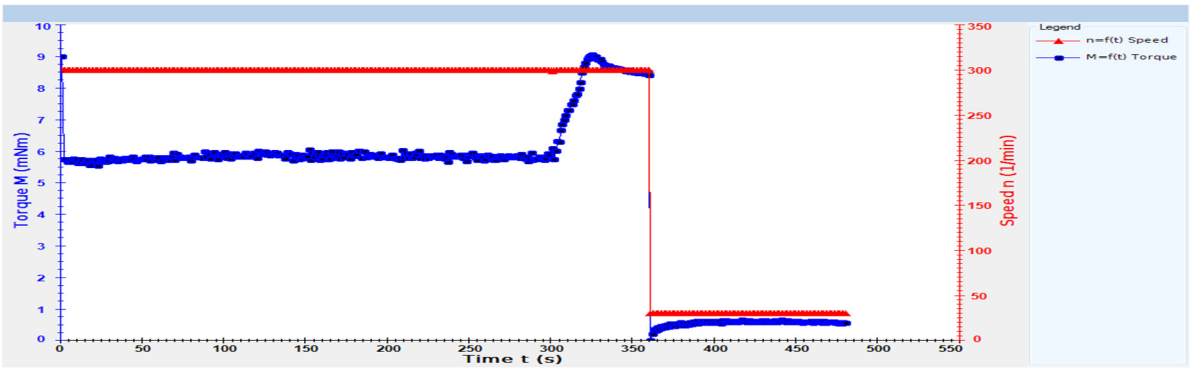

(c)

Figure 29: Flocculation of digestate at 40^{0}C with 20 g of physical conditioner (DB-12Ca) and three polymer (ZETAG 9014®) doses: (a) 6.9, (b) 8.7 and (c) 10.4 g L^{-1} of digestate. The physical conditioner was added at t = 0 s and the polymer doses at t = 300 s (adapted from Alvarenga & Salas-Bringas (2014))

On the other hand, the slow mixing phase of the JT provided information of the degree of separation of the ADR. The three points plotted in Figure 30 is the average *M* during the slow mixing for each polymer dose and this trend provided the extent of the separation during the flocculation of ADR with the JT (Alvarenga & Salas-Bringas 2014). Therefore, the optimization of conditioner doses could be done and assessed from a physical point of view by

means of changes in *M* or shear stress that represent how thin or thick is the fluid during the mixing phase at constant *N*. However, more research is required in order to understand the fluid behavior particularly when there is a transition from Newtonian to non-Newtonian fluid during the aggregation of a colloidal suspension such as the ADR (Mewis & Wagner 2012).

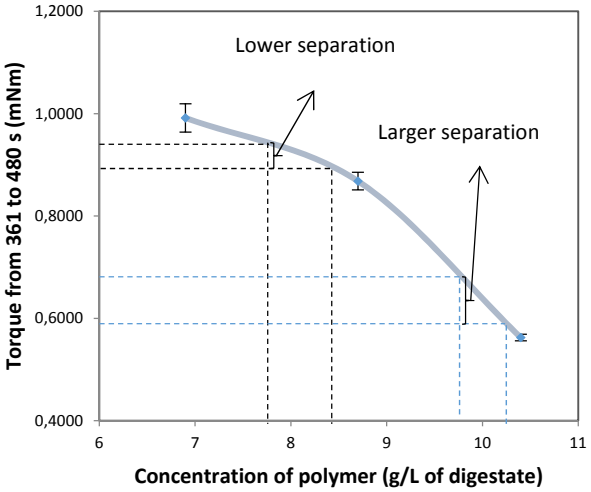

Figure 30: Ranges of separation at low shear rate ($\dot{\gamma}$ = 0.51 s^{-1}) or laminar regime (slow mixing at 30 rpm)(Alvarenga & Salas-Bringas 2014)

The information given by this physical approach from Figure 30 is interpreted as follows: the lower the *M*, the thinner the fluid is and the larger the degree of separation. In other words, the liquid and solid fractions are separated to a greater extent. On the contrary, the higher the *M*, the more viscous is the composition, showing that the solid fraction is disperse in the fluid, increasing therefore its η.

6.3 Effect of anaerobic digestion and lime treatment on recyclability of phosphorus (P) (Paper III)

The contribution of both stabilization treatments on P plant availability was studied in **Paper III**. A sequential extraction scheme was followed for the chemical characterization of the sludges as a fisrt approach to determine the P plant availability (Hedley et al. 1982; Sharpley & Moyer 2000). Figure 31 shows the distribution of P in pools of different solubility. Water soluble P, labile P ($NaHCO_3$-P), Al-/Fe-bound P (NaOH-P) and stable Ca-bound P (HCl-P) are distinguished by sequential extractions.

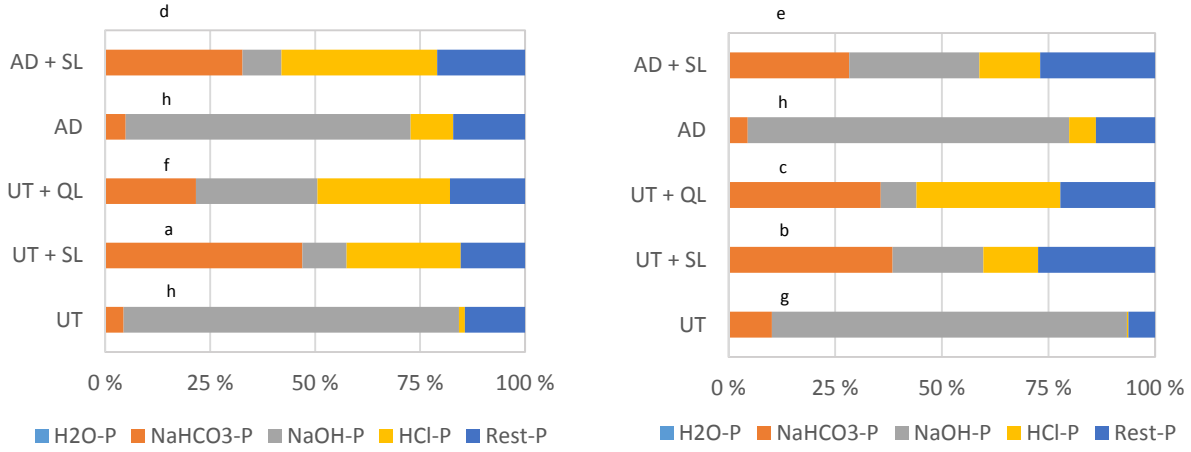

(a) (b)

Figure 31: Distribution of total P (P_{tot}) into different P fractions for the (a) FRE and (b) ULL untreated and treated sludges. The terms UT refer to raw sludge, AD to anaerobic digestion, SL to slaked lime ($Ca(OH)_2$) and QL to quicklime (CaO) accordingly. The different lower case letters above the bars indicate significant differences between treatments ($p < 0.05$) for the P-labile fraction ($NaHCO_3$-P) fraction.

It can be seen from Figure 31 (a) and (b) that the H_2O-P (loosely bound P) concentration for all the untreated and treated sludges was low. Both the raw sludge and the non-limed AD treated sludge showed a considerable low labile P fraction ($NaHCO_3$-P). Moreover, the P-Fe/Al (NaOH-P) fraction was the highest for both of these substrates.

The lime treatment was positive with respect to increase the labile P for both the SL and QL. However, the positive impact on the P availability was higher for SL than QL. This difference was more pronounced for FRE than ULL, where SL increased the labile P share more than twice compared to non-limed treatments. Furthermore, the limed FRE substrates (either UT or AD) have a higher labile P extractable amount that the ones for ULL. The statistical analysis shows that by comparing terms of treatment means with the Tukey's HSD test, there are significant differences between treatments. The letters above the bars in Figure 31 show that a variation between treatments for the labile P fraction is significant in relation to the variation of each treatment.

The second approach for the assessment of the recyclability of P included a growth experiment with barley and the P relative uptake for all the treatments can be seen from Figure 32 (a) and (b).

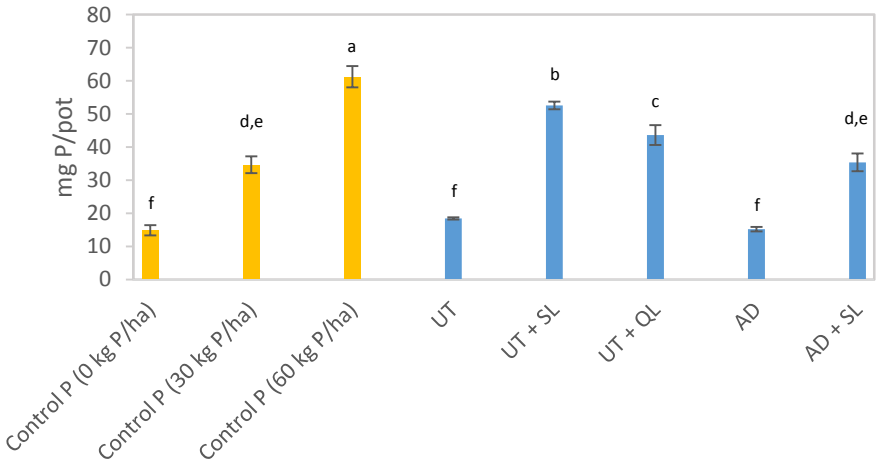

(a)

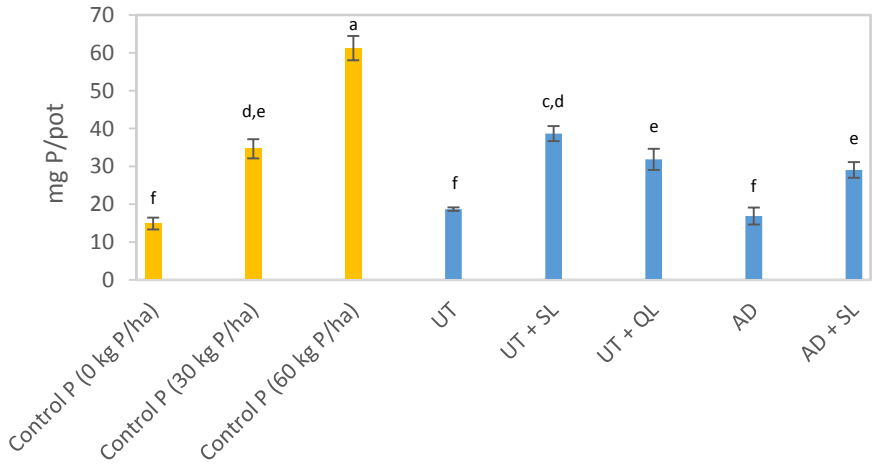

(b)

Figure 32: Average P plant uptake per pot for the (a) FRE and (b) ULL untreated and treated sludges. The terms UT refer to raw sludge, AD to anaerobic digestion, SL to slaked lime ($Ca(OH)_2$) and QL to quicklime (CaO) accordingly. The different letters above the bars indicate significant differences between treatments ($p < 0.05$).

The P plant uptake results confirm that the treatments with the highest availability of P are the ones that were limed (Krogstad et al. 2005) as shown for the P-fractionation as well. A poor effect on P-plant uptake was achieved with the AD without liming. The P-plant uptake was not significantly different from the untreated sludge and the control 0 kg P ha^{-1}. In this case, the negative effect of the AD treatment on the P-plant uptake applies only to AD combined with liming as seen from Figure 32 (a) and (b). AD has hardly any P fertilizer effect.

Anaerobic digestion shows very low RAE values as seen from Table 8. On the other hand, liming increased the RAE values substantially. The highest RAE was obtained by Fe-precipitation and liming (UT + SL) compared to AD and liming (AD + SL).

Table 8: Relative (%) phosphorus (P) fertilization effect for the primary precipitated sludges and their treatments

Treatment	RAE (%)	
	FRE	ULL
UT	7.7	8.2
UT + SL	81.3	51.3
UT + QL	62	36.6
AD	0.7	4.3
AD + SL	44.2	30.6

Liming of sludge led to increased concentrations of labile P and Ca-P and reduced concentration of P-Fe/Al as shown by the sequential P-fractionation. This favored the P-plant availability and P-plant uptake compared to sludges where the main part of P was bound to either Fe or Al. This can be explained by increased pH values of the soils with limed sludge (Table 9). Thereby, Fe/Al (hydr)oxides were less positively charged and the solubility of P-Fe/Al increased with increasing soil pH (Lindsay 1979). Simultaneously, the Ca concentration was raised by liming, resulting in a shift of Fe/Al binded P to Ca binded P in the sludges. Such binding in the pH range from 7.6 to 8.4 released the Fe/Al associated P to a most likely non-crystalline type of Ca phosphate in the sludges (Øgaard & Brod 2016). However, the complexity of Al hydrolysis products release seemingly previously adsorbed P at a lower rate than Fe hydrolysis products as the pH raises from 6.1 to 7 and onwards in the soil (Haynes 1982; Singh et al. 2005; Achat et al. 2016).

Table 9: pH of the soil after seven weeks of pot experiment

Fertilizer	pH of the soil at the end of the pot experiment
FRE	
Raw sludge	6.1 ± 0.06
UT + SL	8.2 ± 0.05
UT + QL	8.3 ± 0.06
AD	5.8 ± 0.04
AD + SL	7.3 ± 0.03
ULL	
Raw sludge	6.1 ± 0.05
UT + SL	7.6 ± 0.06
UT + QL	8.4 ± 0.03
AD	5.8 ± 0.04
AD + SL	7.1 ± 0.02

6.4 Recovery of potassium (K^+) with SiO_2–MnO_2–containing composite sorbents (Paper IV) and bentonite based materials

6.4.1 Synthetic solution of potassium (K^+)

The composition in weight % of the SiO_2–MnO_2–Diatomite sorbent is shown in Table 10.

Table 10: X-ray fluorescence (XRF) data of the sorbent SiO_2–MnO_2–Diatomite (results are semiquantitative and in weight and atomic %)

Element	Weight%	Atomic%	Weight%	Atomic%	Weight%	Atomic%	Average value Weight%
	Spectrum 1		Spectrum 2		Spectrum 3		
C*	4.5	7.4	7.9	13.0	9.3	14.8	
O	52.9	65.2	55.6	68.4	52.0	61.7	53.5
Na	4.5	3.9	5.1	4.3	3.7	3.1	4.5
Al	0.2	0.1	0.1	0.1	0.2	0.1	0.2
Si	27.5	19.3	22.9	16.1	24.3	16.4	24.9
S	0.5	0.3	0.3	0.2	0.2	0.1	0.4
K	1.9	1.0	1.5	0.7	1.6	0.8	1.6
Ca	0.1	0.05	0.1	0.05	0.2	0.1	0.1
Mn	7.5	2.7	6.4	2.3	8.4	2.9	7.4
Fe	0.3	0.1	0.2	0.05	0.2	0.07	0.2
Totals	100		100		100		

*: From the carbon film of the XRF sample holder

Diatomite was used as a wide porous carrier. Such approach was utilized as well for the sorbent preparation of **Paper V** and the mineral conditioner of **Paper I**. The aim of the diatomite was to enhance mass transfer for maximizing the recovery of K^+. However, the MnO_2 on the surface of the sorbent is most likely the most important factor for the sorption process. Moreover, a uniform distribution on the surface of the porous system has relevance as well due to the availability of functional groups (e.g., MnO_2) that would influence the sorption capacity (q) of the system. The saturation curve of the sorbent can be seen from Figure 33 in which equilibrium is reached after 1200 mL at a pH of 12.6 (20°C).

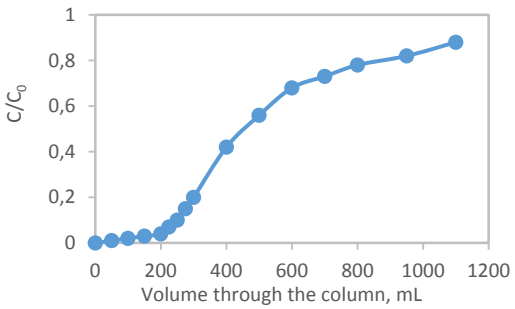

Figure 33: Sorption of potassium (K^+) on the sorbent SiO_2–MnO_2–Diatomite. Ref. concentration (C_0) potassium hydroxide (KOH) – 2 g L^{-1}.

The SiO_2–MnO_2–Diatomite sorbent is able to remove K^+ from a basic pH solution in a satisfactory way. The sorption capacity (q) capacity can be approximately estimated when reaching 0.3 L in the saturation curve (Figure 33). The amount of removed K^+ is 0.6 g. An amount of 10 g of the sorbent in the column would for instance have an approximate q of 60 mg g^{-1} of SiO_2–MnO_2–diatomite sorbent. In spite of such a highly expected q, this system is more expensive compared to the DB-12P-HP one.

6.4.2 Alum shale landfill leachate

The composition in weight % of the sorbent DB-12P-HP can be seen from Table 11.

Table 11: X-ray fluorescence (XRF) data of the DB-12P-HP sorbent (results are semiquantitative and in weight %)

Sorbent	**Element**									
	O	**Na**	**Mg**	**Al**	**Si**	**P**	**K**	**Ca**	**Ti**	**Fe**
DB-12P-HP	63.5	0.5	0.7	2.6	21.6	9.0	0.3	0.4	0.2	1.2

The sorption isotherms are included in Figure 34 where the sorption process is well described by both Langmuir and Freundlich models. The results of K_L, K_F, n and q_0 (from the linear regressions) can be seen from Table 12 along with their correlation coefficients (R^2). The difference with the sorbent from **Paper IV** is that the silicagel and the MnO_2 were replaced by bentonite and the H_3PO_4. In spite of performing the sorption process with a multicomponent system, the q achieved for K^+ was between 1.4-1.6 mg g^{-1}. This result confirms that the bentonite based sorbent DB-12P-HP is effective for K^+ recovery at a pH of 7.5 (10ºC) regardless of the readily hydrated form of K^+ in aqueous solutions (Bratby 2006c) and the fact that there is competition for the sorption sites. Thereby, the DB-12P-HP could be studied for recovery of K^+ in other colloidal suspensions such as ADR (**Paper I**) or sewage sludge (**Paper III**).

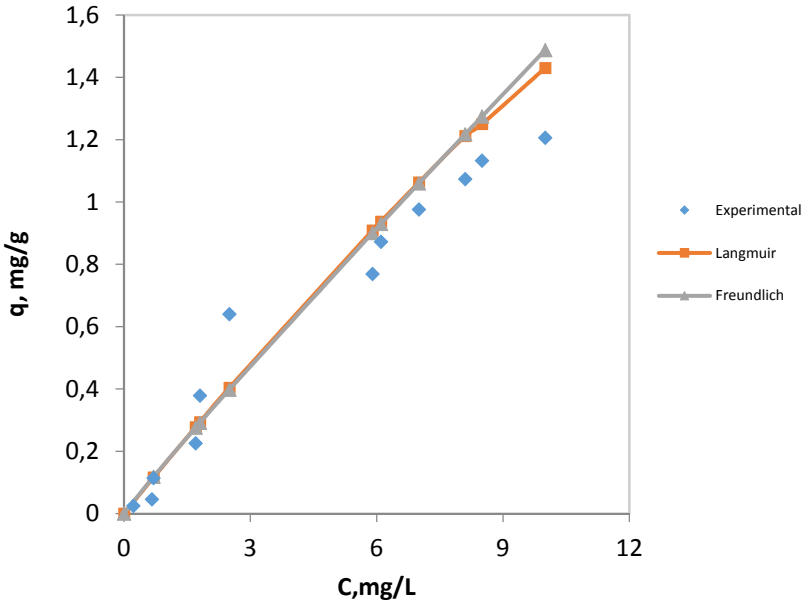

Figure 34: Sorption isotherms (pH = 7.5, 10^0C) for potassium (K^+) from alum shale leachate with DB-12P-HP

Table 12: Values of the constants of the Langmuir and Freundlich isotherms at the studied pH (potassium, K^+ recovery)

pH	Langmuir			Freundlich		
	R^2	q_0	K_L	R^2	n	K_F
7.5	0.9609	11.42[a]	0.0147[b]	0.9998	1.0512	0.1664[c]

[a]: mg/g
[b]: L/mg
[c]: mg $L^{1/n}$/g $mg^{1/n}$

6.5 Effect of pH on the sorption capacity of uranium (U^{6+}) with bentonite based materials (Paper V)

6.5.1 Laboratory scale

The sorption capacity (q) of U^{6+} with DB-12P-HP (**Paper V**) was significantly decreased by adjusting the pH of the alum shale leachate to 4 as shown in Figure 35. The sorbent was saturated with approximately 50% of the volume passing through the column at pH 7.5. At the latter pH value, there was a significant amount of leachate passing through the column due to the slow increase from C/C_0 = 0.4 to 0.6 and thus, the sorption capacity was higher than at pH 4.0. The q is quantified later in this sub-section by means of isotherm equilibrium models.

However, the saturation curve gives information about the pH where the *q* is higher or in other words, where the sorbent works more efficiently.

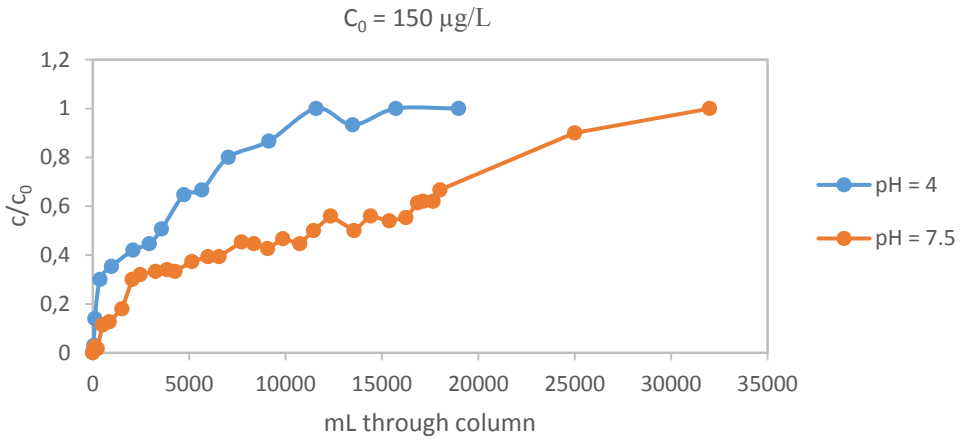

Figure 35: Saturation curves for uranium (U^{6+}) sorption with DB-12P-HP at 10^0C and Q = 3 mL min^{-1}

Such behavior can be explained by the species of U^{6+} in solution and the presence of other inorganic ligands such as sulphate, carbonate and phosphate, forming complexes (Cheng et al. 2004; Guo et al. 2009; Galindo et al. 2010; Singh et al. 2010). Moreover, the competition of U^{6+} for sorption sites with SO_4^{2-} ions (from the alum shale's weathering process) is higher at lower pH values. Furthermore, the formation of uranyl-sulphate complexes could potentially influence the sorption process as well at values lower than pH 7.5. This result is in accordance with the findings of Bachmaf et al. (2008) for a bentonite as a sorbent were the predominant species of U^{6+} in the solution (0.01 M NaCl + 0.005 M Na_2SO_4 and [U] = 5×10^{-5} M) were UO_2OH^+ and $(UO_2)_3(OH)^{5+}$ at pH values between 4 and 5. These hydrolyzed species of U, readily form ligands with the phosphate groups fixated to the surface of DB-12P-HP.

The *q* was determined by means of fitting the experimental data into the equilibrium isotherm models of Langmuir and Freundlich as seen from Figure 36. The results of K_L, K_F, n and q_0 (from the linear regressions) can be seen from Table 13 along with their correlation coefficients (R^2). The sorption process is better described in both pH's with the Freundlich isotherm due to the higher R^2 fitting values. Moreover, there is a substantial difference in magnitude between pH 4 and pH 7. The latter showing a higher degree of sorption for U^{6+} with a *q* of 30 µg g^{-1} compared to 0.6 µg g^{-1} as seen from Figure 36.

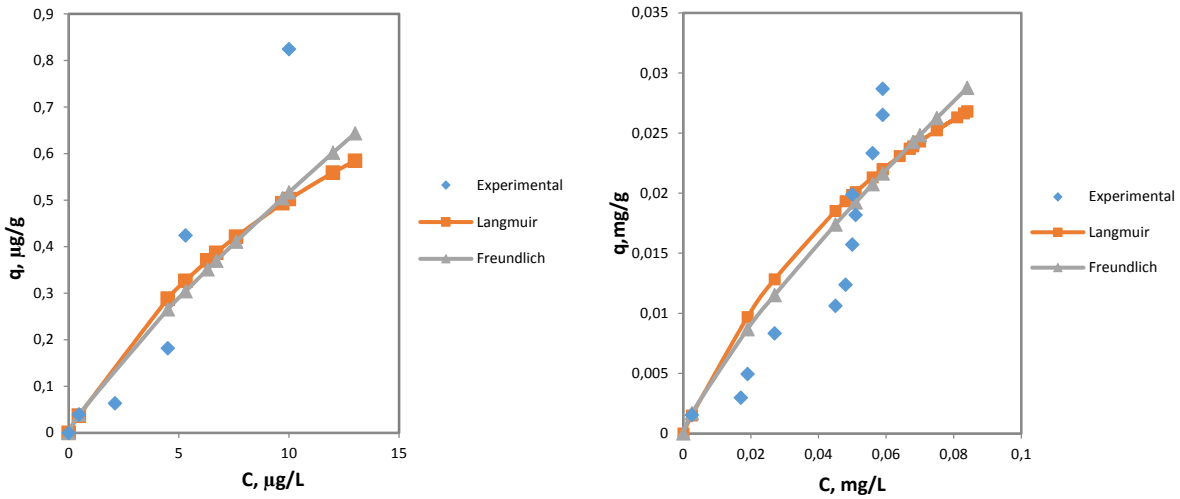

(a) (b)

Figure 36: Equilibrium isotherms for uranium (U^{6+}) (a) pH = 4 and (b) pH = 7.5 for DB-12P-HP at 10°C

Table 13: Values of the constants of the Langmuir and Freundlich isotherms at the studied pH's (uranium, U^{6+} removal)

pH	**Langmuir**			**Freundlich**		
	R^2	q_0	K_L	R^2	n	K_F
4	0.8369	1.28[a]	0.0646[c]	0.9935	1.1970	0.0755[e]
7.5	0.953	0.055[b]	11.16[d]	0.9906	1.2418	0.2113[f]

[a]: µg/g
[b]: mg/g
[c]: L/µg
[d]: L/mg
[e]: µg $L^{1/n}$/g $µg^{1/n}$
[f]: mg $L^{1/n}$/g $mg^{1/n}$

The q of DB-12P-HP at pH 7.5 is comparable to the one of hydrous lanthanum oxide (38 µg g^{-1}) for U removal from seawater (Alexandratos 2010). Such sorbent represents an alternative to the expensive and freshly prepared hydrous titanium oxide, with a capacity 1550 µg g^{-1} (from seawater as well) (Alexandratos 2010). Khalili et al. (2013) have found q-values as high as 62 mg g^{-1} for U^{6+} removal from a synthetic solution of U and Th with a bentonite at pH 3 and T = 25°C with a C_0 of 100 ppm. Such a broad difference in capacity from those studies shows clearly the effect of the competition for sorption sites on the surface of the natural bentonites in multicomponent systems as seawater or leachates for instance.

The variation of pH in the columns (at 10°C) suggest that there is a cationic exchange mechanism for DB-12P-HP as seen in Figure 37. The leachate before passing through the column had a pH 4. A sorption test with NaCl 0.1 N with an initial pH of 5.5 was carried out to

confirm the type of mechanism. The pH inside of the column sharply decreased to 2.6 as seen in Figure 37 (a) due to the production of H^+ ions from the cation exchange. It gradually increases and it stabilizes to a value of 4 in both Figure 37 (a) and (b) in the column. Moreover, the pH started to change after 7 L (Figure 37b) confirming the sorption mechanism. Therefore, the cationic exchange behavior suggests that DB-12P-HP works more efficiently at pH higher than 7, as seen from the results from the previous sub-section (6.4.2). A sorbent as DB-12P-HP would hence be more effective for removal of U^{6+} and K^+ from alum shale leachate at pH values higher than 7 due to the cation exchanger nature of the sorption process and the U species in solution.

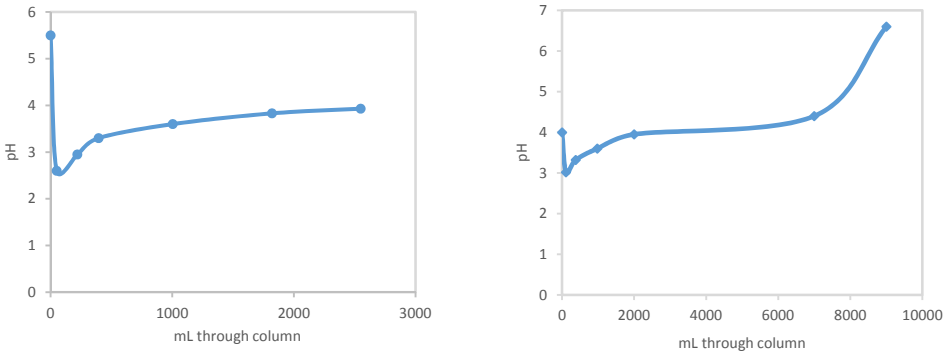

(a) (b)

Figure 37: pH variation at 10^0C in the sorption column for (a) sodium chloride (NaCl) 0.1 N and (b) leachate in a laboratory scale

6.5.2 Pilot scale

The upscaling of the sorption experiment showed that the Q was critical to control the pH inside of the column as seen from Figure 38. Thereby, cation exchange maintains the pH around 4 due to the release of hydrogen ions at Q = 0.5 L min^{-1} in spite of a pH of 7.5 in the leachate. Nonetheless, the pH would most likely increase in order to achieve an efficient separation of U^{6+} at higher pH values inside of the column, as seen before in the laboratory scale trial. Moreover, the channeling effect in the sorbent seems to be overcome compared to the low efficiency removal at Q = 1.5 L min^{-1}. Therefore, stability of the pilot assembly was achieved after passing 0.6 m^3 of landfill water under those experimental conditions with an effective flow resistance of the sorbent granules.

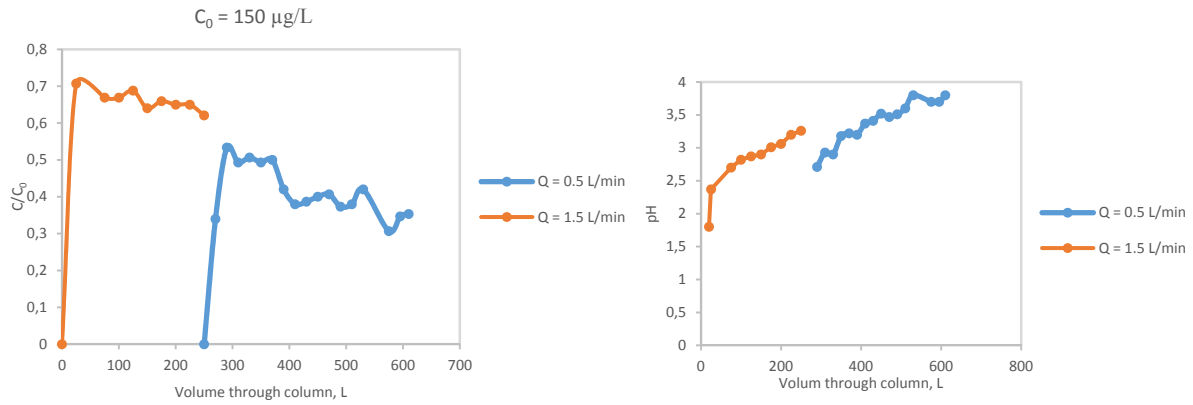

(a) (b)

Figure 38: Variation of (a) uranium (U^{6+}) removal by sorption and (b) pH inside of the column in the pilot scale assembly at 10^0C

7 Uncertainties

The optimization study in **Paper I** included the trends and correlation coefficients (R^2) as statistical assurance. In addition, the term WRC was introduced as a dewatering performance parameter. The uncertainties considered for **Paper II** were based on the same statistical evaluation as in **Paper I**. However, the relative error was taken into consideration for the assessment of the predicted η_{avg} in both laminar and turbulent regimes. In addition, the actual viscosity of the SO (reference material) was measured in an Anton Paar rheometer MCR-301 (sub-section 5.2.2) with a sensitivity of 10 nNm for Torque.

In **Paper III**, the AD treatment had two replicates per untreated sludge for assessing the performance of the reactors. Three replicates were taken into account for the fertilizer, plant and soil analyzes with the inclusion of the standard deviation as a quality assurance of the data. Analysis of variance (ANOVA) was performed to study the effect of sludges on P uptake. To perform multiple comparisons, the Tukey's honestly significant difference multiple comparison test was used ($\alpha = 0.05$). The calibration curves of the ICP-OES were constructed with analytical grade standards. The detection limit (LOD) and the quantification limit (LOQ) for the P concentration in the sludges were 0.005 g kg^{-1} and 0.016 g kg^{-1}. In the P fractionation scheme, the LOD and the LOQ were 0.026 mg L^{-1} and LOQ 0.087 mg L^{-1} accordingly. For the plant analyzes, the LOD and LOQ for P determination were 2e-4 g kg^{-1} and 7e-4 g kg^{-1}. In all the cases (extraction aliquots, plants and sludges), three blanks were analyzed with the rest of the samples along with certified reference materials NIST 1643H® and NIST 1567a® for the extraction samples and the plants respectively and ACLASS Lot. 17359® for the sludges.

In **Papers IV** and **V** an internal standard of 20 mg L^{-1} (Ge, In, Sc, Rh and Bi) was added "on line" to all the samples and the three blanks to asses and correct the drift of the response of the ICP-MS. Moreover, a certified reference material NIST 1643H® was analyzed with the rest of the samples as an additional control sample. The calibration curves of the ICP-MS were constructed with analytical grade standards. The LOD and LOQ for K^+ were 0.06 mg L^{-1} and 0.19 mg L^{-1} accordingly. For ^{238}U, the LOD was 0.01 µg L^{-1} and the LOQ was 0.037 µg L^{-1}.

For all the experiments, it is assumed that the samples involved (digestate, sludge and alum shale leachate) were representative of the bulk, and that the bulks were representative of the problems in question. Uncertainties of the representativeness of the samples have therefore not been evaluated.

8 Conclusions

The work performed in this thesis shows how natural porous materials can be applied for wastewater treatment purposes, and could be utilized for a suspended and colloidal (**Papers I** and **II**) to a LMM (**Papers IV** and **V**) particle separation. Moreover, lime improved desorption of P in sludge when the latter nutrient was strongly binded to Fe- or Al-precipitated sludge (**Paper III**).

The bentonite-based mineral conditioner proved to be suitable for decreasing the polymer dose to as low as 19-25 mg per g TS of ADR (0.8 % TS) (**Paper I**). Moreover, the term for the characterization of the water retention by the mineral conditioner and the polymer –water retention capacity– WRC showed to be an effective dewatering parameter for the optimization of the dose of the polymer. Thereby, it was possible to determine that a concentration over 5 % of the polymer in the dry cake would reduce the dewatering performance of the ADR by vacuum filtration. Such bentonite-based materials could therefore be applied as mineral conditioner with a synergic effect with the chemical conditioner, which allowed favorable water separation from the ADR. This advantage was due to the chemical interaction of the surface of the mineral conditioner with particles along with the diatomite, which created a porous structure in the cake.

The changes in average viscosity of the ADR during flocculation showed that there is an effect of such property on the dewatering performance. The empirical mathematical model of **Paper II** allowed measuring the average viscosity of the ADR in a JT prior to its dewatering for both laminar and turbulent regimes for a standard with known viscosity. However, the behavior of the fluid in turbulent regime showed that the location of the $\dot{\gamma}_{avg}$ was changing with rotational speed. Furthermore, the shear stress in turbulent regime was affected by a component that provided a non-linear response of the rotational rheometer. The degree of separation or dewatering could be obtained in ADR, in spite of such behavior of the fluid, in turbulent regime. Therefore, the viscosity model was a first step to understand the extent of the dewatering from a physical perspective. Such information can thus complement knowledge on how the conditioners are dosed in order to find the optimal conditioner combination as performed in **Paper I**.

The anaerobic digestion had a negative effect for Fe- and Al-precipitated sludges on the P availability (**Paper III**). Lime in both hydrated ($Ca(OH)_2$) and quick (CaO) forms contributed to reverse this negative trend when added as a physical conditioner to the ADR (as in **Paper I**) and untreated sludges. This mineral conditioner has clearly an application for further increase of desorption of P_{inorg} in the soil solution when limed substrates are used as biofertilizers. However, this effect is higher for P uptake in barley for Fe-precipitated sludge due to the complexity of the hydrolysis of Al^{3+} species, which release the P at a lower rate in the limed sludge.

Manganese dioxide and bentonite-based sorbents were effective for removing K^+ in mono (**Paper IV**) and multicomponent systems as alum shale leachate. On the other hand, U^{6+} sorption followed the same behavior with a bentonite-based sorbent (**Paper V**) from the latter substrate. Both sorbents function with a cation exchange mechanism and the sorption of both K^+ and U^{6+} occurred at pH values over 7.5. The case of U^{6+}, this was particular due to the U species in the leachate, which had a drastic impact on the sorption capacity of the bentonite-based sorbent. The sorption capacity was around 100 times higher at pH = 7.5 than at pH = 4.0.

These results showed that the system is suitable for upscaling and further recovery of nutrients and metals. However, the cation exchange mechanism and the *Q* played an important role in the performance of the liquid-solid separation. In other words, the *Q* has to be optimal (*Q* around 0.5 L min^{-1}) along with the pH inside of the column (pH > 7.5) when using a cation exchanger as the bentonite-based sorbent. The pilot scale results were the first step for understanding the sorption of K^+ and U^{6+} for the design of the on-site treatment unit.

9 Further research

The optimization study in **Paper I** along with the model of **Paper II** could be used for understanding the flocculation of ADR or wastewater in the inlet of the dewatering unit. Dewatering, sorption of nutrients and the study of rheological properties of the cake are certainly of interest for the wastewater industry and hence, research requires to be conducted in that direction. The resulting cakes or biofertilizers could be tested for P uptake (as in **Paper III**).

Liming as a physical conditioner for WWT requires to be investigated in order to determine the optimal dose for P plant uptake (**Paper III**). Moreover, liming (with both $Ca(OH)_2$ and CaO forms) of sludge or ADR could be potentially tested for dewatering performance with chemical conditioners as cationic polyacrylamide. Thereby, the effluents after dewatering could be treated for K^+ recovery by sorption as in **Paper IV** and **V**. In this case, tests for P and K plant uptake could be performed in the future.

Theoretically, the column tested with DB-12P-HP in the pilot test would be able to remove 370 mg of U^{6+} or an equivalent of approximately 13 m^3 of alum shale landfill water from the site of interest for this study, although such estimation is based on the results from the laboratory scale column. However, saturation of the column must be achieved in the bigger scale as a further step for the design of an "in-situ" treatment unit of the leachate. Moreover, desorption or regeneration of the column in such scale must be investigated in order to assess the feasibility of the separation technology.

10 References

Achat D.L., Pousse N., Nicolas M., Brédoire F. and Augusto L. 2016 Soil properties controlling inorganic phosphorus availability: general results from a national forest network and a global compilation of the literature. *Biogeochemistry*, **127,** pp. 255–272. Available at: http://link.springer.com/10.1007/s10533-015-0178-0.

Alexandratos S.D. 2010 Uranium Separation – Challenges and Opportunities: Recovery of Uranium from Seawater with Solid Sorbents. *Presentation*, p.46. Available at: http://info.ornl.gov/sites/nfrw/Shared Documents/Plenary Talks-Wednesday AM- Oct 13/Alexandratos_UO2SeaWrksp2.pptx [Accessed March 30, 2016].

Al Seadi, T., Rutz D., Prassl H., Köttner M., Finsterwalder T., Volk S., Reviewers R.J., Sioulas K. and Kulisic B. 2008 *Biogas Handbook*, Available at: http://www.sdu.dk.

Alvarenga E., Hayrapetyan S., Govasmark E., Hayrapetyan L. and Salbu B. 2015 Study of the flocculation of anaerobically digested residue and filtration properties of bentonite based mineral conditioners. *Journal of Environmental Chemical Engineering*, **3**, pp.1399–1407. Available at: http://linkinghub.elsevier.com/retrieve/pii/S2213343715000172.

Alvarenga E. and Salas-Bringas C. 2014 Separation Process and Test Conditions for Digestate using a Rotational Rheometer and Computational Fluid Dynamics. In *IWA Specialist Conference on advances in particle science and separation: from mm to nm scale and beyond*. pp. 446–448.

Alvarenga E., Schüller R.B. and Salas-Bringas C. 2015 Calibration of a Jar-Tester Replicated in a Rotational Rheometer. *Annual Transactions of the Nordic Rheology Society*, **23**, pp.199–205.

Anzalone A., Betwra J.K. and Ali H.I. 2006 Physical and Chemical Treatment of Wastewaters. In Pfafflin J.R. and Ziegler E.N., eds. *Encyclopedia of Environmental Science and Engineering*. Taylor and Francis Group LLC, p. 975.

APHA 2012. *Standard Methods for the Examination of Water and Wastewater* 22nd ed. E. W. Rice et al., eds., American Water Works Association, Clearway Logistics.

Avfall Norge 2014. Deponering og forurenset grunn. Available at: http://www.avfallnorge.no/deponering1.cfm [Accessed January 5, 2016].

Bachmaf S., Planer-Friedrich B. and Merkel B.J. 2008 Effect of sulfate, carbonate, and phosphate on the uranium(VI) sorption behavior onto bentonite. *Radiochimica Acta*, **96(6)**, pp. 359–366.

Bewtra J.K. and Biswas N. 2006 Biological treatment of wastewater. In Pfafflin J.R. & Ziegler E.N., eds. *Encyclopedia of Environmental Science and Engineering*. Taylor and Francis Group LLC, p. 146.

Black A.P., Birkner F.B. and Morgan J.J. 1965 Destabilization of dilute clay suspensions with labelled polymers. *J. AWWA*, **57**, pp.1547–1560.

Black A.P. and Chen C. 1967 Electrokinetic behaviour of aluminium species in dilute dispersed kaolinite systems. *J. AWWA*, **59**, pp. 1173–1183.

Boger D. V. 2009 Rheology and the resource industries. *Chemical Engineering Science*, **64(22)**, pp.4525–4536. Available at: http://dx.doi.org/10.1016/j.ces.2009.03.007.

Boyle G. 2004 Bioenergy. In S. Larkin, ed. *Renewable Energy Power for a Sustainable Future*. New York: Oxford University Press, p. 128.

Bratby J. 2006a Coagulants. In Bratby J., ed. *Coagulation and Flocculation in Water and Wastewater Treatment*. IWA Publishing, London, UK., pp. 57–58.

Bratby J. 2006b Colloids and interfaces. In Bratby J., ed. *Coagulation and Flocculation in Water and Wastewater Treatment*. IWA Publishing, London, UK., p. 18.

Bratby J. 2006c Colloids and interfaces. In Bratby J., ed. *Coagulation and Flocculation in Water and Wastewater Treatment*. IWA Publishing, London, UK., pp. 14–17.

Bratby J. 2006d Introduction. In Bratby J., ed. *Coagulation and Flocculation in Water and Wastewater Treatment*. IWA Publishing, London, UK., pp. 3–5.

Bratby J. 2006e Treatment with metal coagulants. In Bratby J., ed. *Coagulation and Flocculation in Water and Wastewater Treatment*. IWA Publishing, London, UK., p. 149.

Bratby J. 2006f Treatment with metal coagulants. In Bratby J., ed. *Coagulation and Flocculation in Water and Wastewater Treatment*. IWA Publishing, London, UK., pp. 78–79.

Bratby J. 2006g Treatment with metal coagulants. In Bratby J., ed. *Coagulation and Flocculation in Water and Wastewater Treatment*. pp. 120–124.

Brunauer S., Emmett P.H. and Teller E. 1938 Adsorption of gases in multimolecular layers. *J. Amer. Chem. Soc.*, **60**, p.309.

Cheng T., Barnett M.O., Roden E.E., and Zhuang J. 2004 Effects of phosphate on uranium(VI) adsorption to goethite-coated sand. *Environmental Science and Technology*, **38(22)**, pp. 6059–6065.

Choppin G., Liljenzin J.-O., Rydberg J. and Ekberg C. 2013 Behavior of Radionuclides in the Environment. In -, ed. *Radiochemistry and Nuclear Chemistry*. Elsevier Inc., pp. 765–770.

Cordell D. and Neset T.S.S. 2014 Phosphorus vulnerability: A qualitative framework for assessing the vulnerability of national and regional food systems to the multi-dimensional stressors of phosphorus scarcity. *Global Environmental Change*, **24(1)**, pp.108–122. Available at: http://dx.doi.org/10.1016/j.gloenvcha.2013.11.005.

Dahlstrom D.A., Bennett R.C., Emmet R.G., Harriott P., Laros T., Leung W., Miller S.A., Morey B., Oldshue J.Y., Priday G., Silverblat C.E., Slottee J.S., and Smith J.C. 1999 Liquid–Solid Operations and Equipment. In Perry R.H. and Green D.W., eds. *Perry's Chemical Engineer's Handbook*. McGraw-Hill Companies, Inc., p. 75.

Deneux-Mustin S., Lartiges B.S., Villemin G., Thomas F., Yvon J., Bersillon J.L. and Snidaro D. 2001 Ferric chloride and lime conditioning of activated sludges: An electron microscopic study on resin-embedded samples. *Water Research*, **35(12)**, pp. 3018–3024.

Egan T. 2015 What is the meaning of "ionic layer compression in flocculation"? *QUORA*. Available at: https://www.quora.com/What-is-the-meaning-of-ionic-layer-compression-in-flocculation [Accessed January 27, 2016].

Egnér H., Riehm H. and Domingo W.R. 1960. Untersuchungen über die chemische Bodenanalyse als Grundlage für die Beurteilung des Nährstoffzustandes der Böden. II. Chemische Extraktionsmethoden zur Phosphor- und Kaliumbestimmung. *Kungliga*

Lantbrukshögskolans annaler, **26**, pp. 199–215.

Eisenhour D. and Reisch F. 2006 Industrial minerals and rocks: commodities, markets, and uses. In: Kogel J.E., Trivedi N.C., Barker J.M., Krukowski S.T., ed. *Bentonite.* 7th ed., Society for Mining, Metallurgy and Exploration Inc., Littleton, Colorado, pp. 357–368.

Estevez M.M., Sapci Z., Linjordet R., Schnürer A. and Morken J. 2014 Semi-continuous anaerobic co-digestion of cow manure and steam-exploded Salix with recirculation of liquid digestate. *Journal of Environmental Management*, **136**, pp. 9–15. Available at: http://dx.doi.org/10.1016/j.jenvman.2014.01.028.

EUR-Lex 1993 Access to European Union law, Council Directive 1999/31/EC of 26 April 1999 on the landfill of waste. Available at: http://eur-lex.europa.eu/legal-content/EN/ALL/?uri=celex%3A31999L0031 [Accessed January 5, 2016].

European Commission (EC) 2016 European Comission Environment. *Biodegradable Waste*. Available at: http://ec.europa.eu/environment/waste/compost/index.htm [Accessed February 23, 2016].

European Environment Agency (EEA) 2001 Urban Waste Water Treatment Regulations. Available at: http://www.irishstatutebook.ie/2001/en/si/0254.html [Accessed October 22, 2015].

Fisher D.T., Clayton S.A., Boger D.V. and Scales P.J. 2007 The bucket rheometer for shear stress-shear rate measurement of industrial suspensions. *Journal of Rheology*, **51**, pp. 821–831. Available at: http://scitation.aip.org/content/sor/journal/jor2/51/5/10.1122/1.2750657.

Galindo C., Del Nero M., Barillon R., Halter E. and Made B. 2010 Mechanisms of uranyl and phosphate (co)sorption: Complexation and precipitation at α-Al2O3 surfaces. *Journal of Colloid and Interface Science*, **347(2)**, pp. 282–289. Available at: http://linkinghub.elsevier.com/retrieve/pii/S002197971000336X.

Gavrilescu M., Pavel L.V. and Cretescu I. 2009 Characterization and remediation of soils contaminated with uranium. *Journal of Hazardous Materials*, 1**63(2-3)**, pp. 475–510.

Government.no 2015 Norway's climate target for 2030. Available at: https://www.regjeringen.no/en/aktuelt/innsending-av-norges-klimamal-til-fn/id2403782/ [Accessed January 5, 2016].

Guo Z., Li Y. and Wu W. 2009 Sorption of U(VI) on goethite: Effects of pH, ionic strength, phosphate, carbonate and fulvic acid. *Applied Radiation and Isotopes*, **67(6)**, pp. 996–1000.

van Halem D., van der Laan H., Heijman S.G.J., van Dijk J.C. and Amy G.L. 2009 Assessing the sustainability of the silver-impregnated ceramic pot filter for low-cost household drinking water treatment. *Physics and Chemistry of the Earth*, **34(1-2)**, pp. 36–42. Available at: http://dx.doi.org/10.1016/j.pce.2008.01.005.

Hamilton H.A., Brod E., Hanserud O.S., Gracey E.O., Vestrum M.I., Bøen A., Steinhoff H.F., Müller D.B. and Brattebø H. 2015 Investigating Cross-Sectoral Synergies through Integrated Aquaculture, Fisheries and Agriculture Phosphorus Assessments. *Journal of Industrial Ecology*, pp. 1–15.

Haynes R.J. 1982 Effects of liming on phosphate availability in acid soils - A critical review. *Plant and Soil*, **68(3)**, pp. 289–308.

Hayrapetyan S.S., Alvarenga E., Hayrapetyan L.S., Gevorgyan S.A., Pirumyan G.P and Salbu B. 2015 Manganese Dioxide (MnO_2) - Containing Composite Sorbents. In *International Conference on Advance Materials and Technologies Proceedings*. pp. 249–253.

Hedley M.J., Stewart J.W.B. and Chauhan B.S. 1982 Changes in Inorganic and Organic Soil Phosphorus Fractions Induced by Cultivation Practices and by Laboratory Incubations. *Soil Science Society of America Journal*, 46, pp. 970–976.

Henze M. and Ødegaard H. 1994 An analysis of wastewater treatment strategies for Eastern and Central Europe. *Wat. Sci. Tech.*, **30(5)**, pp. 25–40.

Intergovernmental Panel in Climate Change (IPCC) 2007 *Synthesis report. Summary for policy makers. Technical report. Intergovernmental panel on climate change*,

Jeng A.S. 1991 Weathering of Some Norwegian Alum Shales I. Laboratory Simulations to Study Acid Generation and the Release of Sulphate and Metal Cations (Ca, Mg & K). *Acta Agric. Scand.*, **41**, pp. 13–35.

Kahiluoto H., Kuisma M., Ketoja E., Salo T. and Heikkinen J. 2015 Phosphorus in Manure and Sewage Sludge More Recyclable than in Soluble Inorganic Fertilizer. *Environmental Science & Technology*, **49**, pp.2115–2122. Available at: http://pubs.acs.org/doi/abs/10.1021/es503387y.

Khalili F.I., Salameh N.H. and Shaybe M.M. 2013 Sorption of Uranium (VI) and Thorium (IV) by Jordanian Bentonite, 2013.

Kizito S., Wu S., Kipkemoi Kirui W., Lei M., Lu Q., Bah H. and Dong R. 2015 Evaluation of slow pyrolyzed wood and rice husks biochar for adsorption of ammonium nitrogen from piggery manure anaerobic digestate slurry. *Science of The Total Environment*, **505**, pp. 102–112. Available at: http://linkinghub.elsevier.com/retrieve/pii/S0048969714014181.

Krogstad T., Sogn T.A., Asdal Å. and Sæbø A. 2005. Influence of chemically and biologically stabilized sewage sludge on plant-available phosphorous in soil. *Ecological Engineering*, **25(1)**, pp. 51–60. Available at: http://linkinghub.elsevier.com/retrieve/pii/S092585740500073X.

Lee C.S., Robinson J. and Chong M.F 2014 A review on application of flocculants in wastewater treatment. *Process Safety and Environmental Protection*, **92(6)**, pp. 489–508.

LeVan M.D., Carta G. and Yon C.M. 1999 16-Adsorption and Ion Exchange. In R. H. Peery, D. W. Green, & J. O. Maloney, eds. *Perry's Chemical Engineers' Handbook*. McGraw-Hill Companies, Inc., p. 4.

Li Z. 2014 Modeling precipitate-dominant clogging for landfill leachate with NICA-Donnan theory. *Journal of Hazardous Materials*, **274**, pp. 413–419. Available at: http://dx.doi.org/10.1016/j.jhazmat.2014.04.009.

Lindsay W. L. 1979 *Chemical equilibria in soils*, New York: John Wiley & Sons.

Lindum Slam. n.d. Available at: http://lindum.no/vi-tilbyr/behandling-av-avfall/slam/ [Accessed February 24, 2016].

Lovdata 1981 Forskrift om begrensning av forurensning (forurensningsforskriften), Legislation of pollutants thresholds. Available at: https://lovdata.no/dokument/SF/forskrift/2004-06-01-931/KAPITTEL_4#KAPITTEL_4 [Accessed January 6, 2015].

Lü F., Zhou Q., Wu D., Wang T., Shao L. and He P. 2015 Dewaterability of anaerobic

digestate from food waste: Relationship with extracellular polymeric substances. *Chemical Engineering Journal*, **262**, pp. 932–938. Available at: http://www.sciencedirect.com/science/article/pii/S1385894714013837.

Massé D.I., Talbot G. and Gilbert Y. 2011 On farm biogas production: A method to reduce GHG emissions and develop more sustainable livestock operations. *Animal Feed Science and Technology*, **166-167**, pp. 436–445.

Mewis J. and Wagner N.J. 2012 Colloidal attractions and flocculated dispersions. In -, ed. *Colloidal Suspension Rheology*. Cambridge University Press, pp. 180–181.

Morken J. and Sapci Z. 2013 Evaluating biogas in Norway - bioenergy and greenhouse gas reduction potentials. *Agricultural Engineering International: CIGR Journal*, **15(2)**, pp.148–160. Available at: http://www.scopus.com/inward/record.url?eid=2-s2.0-84879733111&partnerID=40&md5=527f04cb5a45fa482b73f37b2b3be26b.

Møberg P. and Petersen L. 1982 Øvelsesvejledning til geologi og jordbundslære. Part 2 (in Danish). *Den Kongelige Veterinær-og Landbohøyskole, København*, p.136.

Napper D.H. 1983 Polymeric Stabilization of Colloidal Dispersions. *Academic Press, London*.

Norsk Vann 2010 Behandlingsmetoder som er i bruk i Norge, for å stabilisere og hygienisere slam, p. 18. Available at: www.va-norm.no/content/download/34579/354407.

Novak J.T., Goodman G.L., Pariroo A., Huang J.C. 1988 The blinding of sludges during filtration. *J. Water Pollut. Control Fed.*, **60 (2)**, pp. 206–214.

Ott C. and Rechberger H. 2012 The European phosphorus balance. *Resources, Conservation and Recycling*, **60**, pp. 159–172. Available at: http://dx.doi.org/10.1016/j.resconrec.2011.12.007.

Pettersen O.P., Steineger H. & Reve T. 2014. *BioVerdi*, Available at: http://www.oslotech.no/bioverdi/.

Report C., 1971. State of the art of coagulation. *J. AWWA*, **63**, pp. 99–108.

Rittmann B.E., Mayer B., Westerhoff P. and Edwards M. 2011 Capturing the lost phosphorus. *Chemosphere*, **84(6)**, pp. 846–853. Available at: http://linkinghub.elsevier.com/retrieve/pii/S0045653511001196.

Salas-Bringas C., Jeksrud W.K., Lekang O.-I. and Schüller R.B. 2006 A Calibration Method for a New Type of Rheometer. *Annual Transactions of the Nordic Rheology Society*, **14**.

Salas-Bringas C. 2011 *Development and Verification of Methods for the Rheological Characterization of Materials for the Process Industry*. Norwegian University of Life Sciences.

Salbu B. 2009 Fractionation of radionuclide species in the environment. *Journal of Environmental Radioactivity*, **100(4)**, pp. 283–289. Available at: http://dx.doi.org/10.1016/j.jenvrad.2008.12.013.

Salbu B., Lind O.C. and Skipperud L. 2004 Radionuclide speciation and its relevance in environmental impact assessments. *Journal of Environmental Radioactivity*, **74(1-3)**, pp. 233–242.

Schüller R.B., Tande M. and Amundsen L. 2010 Experimental determination of time dependent yield properties. *Annual Transactions of the Nordic Rheology Society*, **18**.

Sharpley A. and Moyer B. 2000 Phosphorus Forms in Manure and Compost and Their

Release during Simulated Rainfall. *Journal of Environmental Quality*, **29(5)**, pp. 1462–1469.

Singh A., Ulrich K.-U. & Giammar D.E. 2010 Impact of phosphate on U(VI) immobilization in the presence of goethite. *Geochimica et Cosmochimica Acta*, **74(22)**, pp. 6324–6343. Available at: http://www.sciencedirect.com/science/article/pii/S0016703710004801.

Singh B.R., Krogstad T., Shivay Y.S., Shivakumar B.G. and Bakkegard M. 2005 Phosphorus fractionation and sorption in P-enriched soils of Norway. *Nutrient Cycling in Agroecosystems*, **73(2-3)**, pp. 245–256.

Sinnott R.K. 2013 *Coulson & Richardson's Chemical Engineering* 4th ed., Butterworth-Heinemann.

Skipperud L., Alvarenga E., Lind O.C., Teien H.-C., Salbu B. and Wærsted F.M. 2016 *Effekter og Miljørisiko Knyttet til Inngrep i Områder med Sulfidrike Mineraler*, NMBU, Ås.

Steffe J.F. 1996a Introduction ro Rheology. In -, ed. *Rheological Methods in Food Process Engineering*. Freeman Press USA, pp. 19–22.

Steffe J.F. 1996b Introduction to Rheology. In -, ed. *Rheological Methods in Food Process Engineering*. Freeman Press USA, pp. 1–3.

Steffe J.F. 1996c Introduction to Rheology. In -, ed. *Rheological Methods in Food Process Engineering*. Freeman Press USA, pp. 33–34.

Stumm W. and Morgan J.J. 1962 Chemical aspects of coagulation. *J. AWWA*, **54(8)**, pp. 971–991.

Stumm W. and O'Melia C.R. 1968 Stoichiometry of coagulation. *J. AWWA*, May, pp. 514–539.

Svarovsky L. 2000 1-Introduction to solid-liquid separation. In L. Svarovsky, ed. *Solid-Liquid Separation*. Butterworth-Heinemann, p. 1.

Teefy S., Farmerie J. and Pyles E. 2011 Jar Testing. In -, ed. *M37 Operational Control of Coagulation and Filtration Processes*. AWWA, pp. 17–18.

Thapa K.B., Qi Y., Clayton S.A. and Hoadley A.F. 2009. Lignite aided dewatering of digested sewage sludge. *Water Research*, **43(3)**, pp. 623–634. Available at: http://dx.doi.org/10.1016/j.watres.2008.11.005.

Thapa K.B., Qi Y. and Hoadley A.F. 2009 Interaction of polyelectrolyte with digested sewage sludge and lignite in sludge dewatering. *Colloids and Surfaces A: Physicochemical and Engineering Aspects*, **334(1-3)**, pp. 66–73. Available at: http://linkinghub.elsevier.com/retrieve/pii/S092777570800681X.

Theodore L., Buonicore A.J., McKenna J.D., Kugelman I.J., Jeris J.S., Santoleri J.J. and McGowan T.F. 1999a 25-Waste Management: Industrial Wastewater Management. In Peery R.H., Green D. W. and Maloney J.O., eds. *Perry's Chemical Engineers' Handbook*. McGraw-Hill Companies, Inc., p. 63.

Theodore L., Buonicore A.J., McKenna J.D., Kugelman I.J., Jeris J.S., Santoleri J.J. and McGowan T.F. 1999b 25-Waste Management: Industrial Wastewater Management. In Perry R.H., Green D.W. and Maloney J.O., eds. *Perry's Chemical Engineers' Handbook*. McGraw-Hill Companies, Inc., pp. 76–77.

Theodore L., Buonicore A.J., McKenna J.D., Kugelman I.J., Jeris J.S., Santoleri J.J. and McGowan T.F. 1999c. 25-Waste Management: Industrial Wastewater Management. In Perry R.H., Green D.W. and Maloney J.O., eds. *Perry's Chemical Engineers' Handbook*. McGraw-Hill Companies, Inc., pp. 78–79.

Wakeman R.J. 2011 LIquid-Solid Separation. *Thermopedia A-to-Z Guide to Thermodynamics, Heat and Mass Transfer, and Fluids Engineering*. Available at: http://www.thermopedia.com/content/928/ [Accessed January 19, 2016].

Ward A.J. and Løes A.-K. 2011 The potential of fish and fish oil waste for bioenergy generation: Norway and beyond. *Biofuels*, **2(4)**, pp. 375–387. Available at: http://www.scopus.com/inward/record.url?eid=2-s2.0-79961080478&partnerID=tZOtx3y1.

World Health Organization (WHO) 2001 Radon. *Air Quality Guidelines*, **222(1)**, pp. 1–14.

Yenigün O. and Demirel B. 2013 Ammonia inhibition in anaerobic digestion: A review. *Process Biochemistry*, **48(5-6)**, pp. 901–911. Available at: http://dx.doi.org/10.1016/j.procbio.2013.04.012.

Zhang J., Xu S. and Li W. 2012 High Shear Mixers: A Review of Typical Applications and Studies on Power Draw, Flow Pattern, Energy Dissipation and Transfer Properties. *J. Chem. Eng. and Proc.*, **57-58**, pp. 25–41.

Ødegaard H., Simonsen P., Nerland J. and Rosendahl A. 1973 *Kjemisk Felling i Eksisterende Anlegg Åmot Renseanlegg Sluttrapport*, Available at: http://brage.bibsys.no/xmlui/handle/11250/200767.

Ødegaard H., Paulsrud B. and Karlsson I. 2002 Wastewater sludge as a resource: Sludge disposal strategies and corresponding treatment technologies aimed at sustainable handling of wastewater sludge. *Water Science and Technology*, **46(10)**, pp. 295–303.

Øgaard A.F. and Brod E. 2016 Efficient phosphorus cycling in food production – predicting the phosphorus fertilization effect of sludge from chemical wastewater treatment, **64(24)**, pp.4821–4829.

Örmeci B. 2007 Optimization of a full-scale dewatering operation based on the rheological characteristics of wastewater sludge. *Water research*, **41(6)**, pp. 1243–52. Available at: http://www.ncbi.nlm.nih.gov/pubmed/17303208.

11 Papers

Paper I focused on the optimization of the dosage of both mineral and chemical conditioners in the flocculation process of the ADR prior to its dewatering by vacuum filtration in a laboratory scale. The mineral conditioner was a powder of a DB based material that was treated with quick lime (CaO) in order to fixate Ca to the surface of the bentonite as a functional group. Thereby, an interaction with the ADR particles was enhanced and therefore, it was possible to decrease the dose of the chemical conditioner, a commercial cationic polyacrylamide (ZETAG 9014®). Moreover, the DB provided a porous structure for the cake in the filtration process. Therefore, an optimal dose along with a favorable filterability of the ADR was obtained for both conditioners.

An empirical mathematical model was developed in **Paper II** in a calibration procedure in which it was possible to determine the location of the average shear rate ($\dot{\gamma}_{avg}$) for the estimation of the viscosity (η) of a Newtonian fluid. The measurement system was a replicated JT adapted to a rotational rheometer (RR). Such calibration procedure aims to describe how the η varies throughout flocculation of wastewater over flow regime. The model provided information about how the shear stress was affected with a nonlinear response of Torque (M) of the RR. The linearity of M was achieved by defining and adding a turbulence component to the model over the temperature range considered for the calibration.

Paper III aimed to test how the P-availability in sludge produced from Fe- and Al-precipitation of wastewater was influenced by post-treatments such as AD and liming. The AD was performed in thermophilic (55 and 60°C) CSTR systems in a semi-pilot scale. Moreover, there was an interest to verify if the effect of liming with both CaO and hydrated lime ($Ca(OH)_2$) alone or in combination with AD was comparable to the same extent for Fe- and Al-precipitated sludge. For that purpose, sequential extractions and a plant uptake experiment with the different treated sludges were carried out to investigate the remobilization of P in the treated sludges.

The objective of **Paper IV** was to prepare a MnO_2–containing sorbent (silica and diatomite based) for the removal of K^+ in a synthetic solution. The silica and the diatomaceous earth as porosity carrier, provided selective sorption properties for K^+ in a dynamic configuration; and these materials were considered for the preparation and further treatment of a sorbent for removal of radionuclides (**Paper V**) in laboratory scale.

Paper V focused on the removal of U^{6+} with the DB sorbent. Both materials were treated chemically and thermally to improve their sorption properties in dynamic mode for two different pH levels of an alum shale landfill leachate. Upscaling of the sorption process became of interest for possible treatment of the effluent on site.

Paper I

Alvarenga E., Hayrapetyan S., Govasmark E., Hayrapetyan L. and Salbu B. 2015 Study of the flocculation of anaerobically digested residue and filtration properties of bentonite based mineral conditioners. *Journal of Environmental Chemical Engineering*, 3, pp. 1399–1407

Journal of Environmental Chemical Engineering 3 (2015) 1399–1407

Contents lists available at ScienceDirect

Journal of Environmental Chemical Engineering

journal homepage: www.elsevier.com/locate/jece

Study of the flocculation of anaerobically digested residue and filtration properties of bentonite based mineral conditioners

Emilio Alvarenga [a,*], Sergey Hayrapetyan [b,1], Espen Govasmark [c,2], Lusine Hayrapetyan [b,1], Brit Salbu [d,3]

[a] Norwegian Institute for Agricultural and Environmental Research, Bioforsk, Soil and Env. Div., Frederik A. Dahl vei 20, NO-1430 Ås, Norway
[b] Yerevan State University, A. Manoogyan St. 1, 0025 Yerevan, Armenia
[c] Energy Recovery Agency of Oslo County, PO-BOX 54 Mortensrud, NO-1215 Oslo, Norway
[d] Norwegian University of Life Sciences (NMBU), Dept. of Env. Sci., PO-BOX 5003, NO-1432 Ås, Norway

ARTICLE INFO

Article history:
Received 19 September 2014
Accepted 30 January 2015
Available online 3 February 2015

Keywords:
Mineral conditioner
Bentonite
Flocculation
Dewatering
Water retention capacity

ABSTRACT

The turbidimetric and capillary suction time (CST) methods were used for the assessment of some properties (e.g., filtration process, water uptake etc.) of diatomite–bentonite based conditioners for dewatering of effluents from digestate of a biogas plant. These physical conditioners were prepared based on natural porous highly dispersible systems such as bentonite and diatomaceous earth. A characterization of the materials was performed by scanning electron microscopy (SEM) and fluorescence of X-rays spectrometry (XRF). A cationic polyacrylamide polymer (ZETAG® 9014) was added prior to the dewatering process of the anaerobic digestion residue and an optimal dose of the mineral conditioner and the polymer was determined. It was suggested the formula, by means of which the amount of separated water was identified as water retention capacity (WRC). A favorable filterability region was determined with WRC between 1.5 and 4.4 (high level of WRC) and 1.5 and 2.9 (low level of WRC) in terms of the percentage of polymer in the dry cake.

Introduction

Anaerobic digestion produces a methane-rich biogas, as well as a digested effluent also known as anaerobic digestion residue (ADR) or digestate, which contains significant amounts of various nutrients, including nitrogen, potassium and phosphorus among other plant nutrients. Currently, one of the most feasible options for the correct management of digestate is its direct application to agricultural fields. The relative cost of transportation of the ADR can be high due to the low concentration of both nutrients and dry matter. Conversely, stockpiling of digestate may occur as a result, meaning that nutrients contained therein may pose potential environmental risks to the surrounding water bodies if improperly managed. Consequently, a more effective separation from liquid to solid phase in the digestate would favor an increased sale ability of these products and their derivatives, with less environmental associated risks. Moreover, significant amounts of water can be recycled and returned to the inlet stream of the bio-gas process in order to process new batches of bio-degradable waste. On the other hand, wastewater treatment processes (WWTPs) produce large amounts of sludge commonly containing over 90% of water with similar transportation and handling problems as for the ADR.

Colloidal systems which are present in undewatered sludge and the ADR form a stable suspension in water and enhances difficulties (commonly encountered) in the mechanical dewatering process such as vacuum and pressurized filtration. The addition of chemical conditioners such as coagulants and flocculants is frequently necessary to help the sludge or ADR particles to agglomerate into larger aggregates which precede the solid–water separation. However, due to the highly compressible nature of the sludge solids, the sludge dewatering rate is often hindered by the blinding of the filtration media and the filter cake [1,11–13]. Novak et al. [14] suggested that the clogging or blinding of pores in the filter cake is primarily responsible for the deterioration of the filtration rather than the blinding of the filtering media. Furthermore, when high molecular weight organic polymers are used for flocculation, sludge dewatering rate can be increased to a

* Corresponding author. Tel.: +47 92 01 04 92; fax: +47 63 00 94 10.
E-mail address: Emilio.Alvarenga@bioforsk.no (E. Alvarenga).
[1] Tel.: +374 10 45 41 66.
[2] Tel.: +47 40 48 02 33.
[3] Tel.: +47 6496 5541.

http://dx.doi.org/10.1016/j.jece.2015.01.015
2213-3437/

certain extent by decreasing the sludge specific resistance. In this stage and under a certain pressure, no further water can be removed [15]. Such long compression times equate to extremely slow rates of dewatering.

There are two widely accepted flocculation mechanisms: particle–particle bridging and surface charge neutralization [16–18]. With the particle bridging mechanism, the polyelectrolyte chains adsorb on the solid surface forming loops, trains and tail configurations. When two particles come together, the loops and tails of one particle attach themselves to bare patches on the approaching particle to form bridges [19]. In general, the effectiveness of bridging flocculation is directly related to the molecular weight (MW) or chain length of the polyelectrolyte [20].

Physical conditioners, commonly known as skeleton builders or filter aids improve the mechanical strength and permeability of the sludge cake during compression. These materials can form a permeable and more rigid lattice structure which can remain porous under high pressure during mechanical dewatering [2]. A wide range of carbon-based materials have been used as physical conditioners, including char [3], coal fines [3,4] and bio-waste such as wood chips and wheat dregs [5] and bagasse [6]. Minerals including fly ash [2,6,7], cement kiln dust [6] and gypsum [8,9] have also been used for such approach. A physical conditioner can be used individually to enhance sludge dewatering such as in the investigation carried out by Jing et al. [10].

The requirements of the physical mineral conditioners for filtration of sludge are that they should be inert and should avoid filter blinding [1]. However and as investigated from [2], the surface of these systems could have a charge. Therefore, it means that during the dewatering by means of the addition of mineral conditioners, there is not a "pure" filtration achieved, due to the interactive surfaces of such systems involved in the flocculation process. The degree of such interaction is dependent on:

- Surface area of filter-aids powder;
- Surface charges;
- Porosity (pore volume, mean diameter of pore);
- Types of functional groups on the surface.

The analysis of literature points out that the selection of such materials has a random character and there is not logical strategy in the selection of these agents. On one hand, relatively inert materials are used (e.g., coal) as done previously by [3,4], and on the other hand, there are physical conditioners which have surfaces with very active groups (cement, lime, char etc.) [6,9]. Thirdly, there are materials inert but without any porosity etc.

The main material of the mineral conditioner used in this study is a bentonite (from the Republic of Armenia). Typically, the measured specific surface area by use of nitrogen gas gives results in the range of 20–100 m^2/g of clay regardless of the preparation technique and montmorillonite content. Comparison with the total theoretical surface area of montmorillonite of around 750 m^2/g indicates that montmorillonite layers in close contact dominate the dry material, and that the interlayers are inaccessible for the nitrogen gas [22]. The second important component in the mineral conditioner is the silica containing material (diatomite earth). The use of the silica-containing component provides the structure for making porosity and rigidity of the mineral conditioner. These properties provide good filterability of the aforementioned materials in order to avoid blinding of the cake during the filtration as investigated by Novak et al. [14]. In addition, the bentonite and diatomite system contains Ca which influences the mechanism of clogging [23] and the flocculation of colloidal suspensions [24,25].

Commonly, the physical conditioner addition is followed by coagulation or flocculation with a chemical conditioner. When physical conditioners are used in conjunction with chemical conditioners, sludge dewaterability can achieve its optimum. Without chemical conditioners, which are used to manage sludge colloids, physical conditioners alone do not usually function as filter aids to the same extent or at all.

It has also been found that the application of physical conditioners can reduce the use of chemical conditioners and, thus, the cost of the treatment process, while still achieving the same level of dewatering performance [11].

The goal of this study was to optimize the dose of the polyelectrolyte (ZETAG® 9014) in the dewatering of digestate by vacuum filtration. For that purpose, natural high dispersible porosity materials as mineral conditioners were prepared as a bentonite and diatomite combined system. The latter was added to the digestate prior to the addition of ZETAG® 9014 for improving the dewatering process [10,11]. Moreover, a favorable filterability region in terms of the concentration of ZETAG® 9014 in the dry cake and WRC in a high and low level, was determined in order to avoid the filter cloth clogging [12,13].

Materials and methods

ADR substrate

The ADR substrate that was used in all the experiments was sampled from the rejected stream after the decanter from the bio-gas plant of Lindum AS (Norway). The physicochemical parameters of the ADR substrate are shown in Table 1 and were analyzed in accordance to the standard methods for the examination of water and wastewater [21].

Mineral conditioner DB-12Ca

The code of the mineral conditioner "12" refers to the ratio of diatomite to bentonite mixed. This filter material was treated with a slurry of CaO in order to increase its Ca content up to 5% and the mixture was washed several times with deionized water for removal of the excess of CaO. The material was afterwards dried at 105 °C in an air oven until constant weight.

Cationic polymer (ZETAG® 9014)

A suspension of the cationic polyacrylamide polymer (ZETAG® 9014) produced by BAFS SE (Germany), was used as the chemical conditioner. The dried matter content of the polymer was 50% (w/v) and was determined by a gravimetric method by drying it at 105 °C until constant weight in an air oven. This step was carried out to express the results in the next section as $mg_{polymer}/g\ TS_{ADR}$. The polymer was added to the ADR as a suspension in the dewatering experiments.

Table 1
Physicochemical parameters of the ADR.

Parameter	Value or concentration
pH[a]	8.3 ± 0.2
TS	0.8 ± 0.1%
SS	0.4 ± 0.07%
VS	99.90 ± 0.01%
Conductivity	7.65 ± 0.02 mS/cm
Turbidity	4700 ± 50 FTU
P_{total}	83 ± 5 mg/L
orto-P	2.5 ± 0.2 mg/L
K	350 ± 20 mg/L
NH_4	50 ± 3 mg/L
COD	2500 ± 70 mg/L

[a] Measured at 25 °C.

Dewatering experiments method

The batch volume of the ADR that was treated with physical and chemical conditioner was 1 L. The same volume of ADR was used for the measurements of turbidity and CST. The dewatering of the ADR was performed for different doses of the physical conditioner and the polymer. The amounts or doses of the filter powder were 0.8, 1.6, 3.1 and 4.7 g/g of TS in the digestate. The polymer dose addition was 19, 38, 75 and 150 mg/g of TS for each of the physical conditioner doses. The design of the dewatering experiments can be seen from Table 2.

A Kemira Jar-test Flocculator 2000 unit was utilized with a rapid mixing of the physical conditioner DB-12Ca at 300 rpm for 300 s [26]. The polymer was added at $t = 300$ s and it was dispersed at 300 rpm for 180 s for each of the doses of DB-12Ca.

The flocculation phase (slow mixing) lasted 600 s with a speed of 30 rpm. The flocculated ADR was immediately decanted to a laboratory scale vacuum filtration assembly [27] at −750 mm bar equipped with an open Buchner funnel and a filter cloth OptiFiber PA2-13®. When the separation process of the cake and the supernatant was finalized with no further water flow, the filter cake (FC) was removed from the filter cloth. The FC or wet cake was afterwards weighted on a scale with a 0.01 g resolution. The FC was finally dried at 105 °C until constant weight and the final dry sludge weight was measured.

A Hanna turbidimeter model HI 93703 was utilized for the turbidity measurement of the separated filtrates of the 16 experiments by means vacuum filtration. During the flocculation process, three replicates of 5 mL aliquots were taken at 0, 30, 180, 360 and 480 s after the addition of 0.8 g of DB-12Ca per g of TS of digestate (to 1 L) in the rapid mixing phase. The polymer was added at $t = 300$ s. These were dispensed in a conical cylinder for its filtration in a Whatman filter paper #17 for the determination of the CST. The CST value for each of the aliquots was determined in a Stephany Abwassertechnik equipment only for the experiment #1.

Analytic methods

Each of the experiments from Table 2 provided insight (wet cake weight, dry cake weight and turbidity) of the dewatering process of the ADR by vacuum filtration for the further discussions of the separation (liquid to solid) in the following section.

The pH of the ADR substrate was measured in a Thermo Orion pH-meter model Dual Star and the conductivity was determined in a Mettler Toledo instrument model Seven Multi with an electrode Inlab 730. The total solids (TS), suspended solids (SS) and volatile solids (VS) were determined by a gravimetric method at 105 °C until constant weight. The total phosphorus (P_{total}) and the potassium (K) concentrations were measured by inductively coupled plasma mass spectrometry (ICP-MS-MS). The orto-P was measured by a UV-spectrophotometry. The ammonia concentration was determined by the ion selective electrode (ISE) method by a Thermo Scientific, Orion electrode model 9512HPBNWP connected to the Thermo Orion device model Dual Star.

Table 2
Design for the dewatering batch experiments and doses for 1L of ADR.

Experiment	Dose of DB-12Ca (g/g of TS)	Dose of ZETAG® 9014 (mg/g of TS)
1	0.8	19
2	0.8	38
3	0.8	75
4	0.8	150
5	1.6	19
6	1.6	38
7	1.6	75
8	1.6	150
9	3.1	19
10	3.1	38
11	3.1	75
12	3.1	150
13	4.7	19
14	4.7	38
15	4.7	75
16	4.7	150

The amount of separated water was quantified as water retention capacity (WRC) in the dewatered sludge and it was defined as the difference in weight after the drying process divided by the weight of the dry sludge as seen in Eq. (1).

$$\mathrm{WRC} = \frac{[\text{Weight of wet sludge (g)} - \text{Weight of dry sludge (g)}]}{\text{Weight of dry sludge (g)}} \quad (1)$$

The parameters which were considered for the assessment of the flocculation process and the sludge dewaterability were respectively the turbidity (FTU) of the filtrate and the capillary suction time (CST).

Statistic method

The discussions of the next section are based on the trends with the inclusion of correlation coefficients as statistical assurance and the introduction of the term WRC as a dewatering performance parameter.

Results and discussion

Mineral conditioner (DB-12Ca)

Bentonite is responsible for the variation of different types of functional groups on the surface of the previously mentioned materials. It can be observed from Fig. 1 and Table 3, the composition and homogeneity of the material by scanning electron microscopy (SEM) and fluorescence X-ray spectrometry (XRF) with a high content of Si and Al as the functional groups of the surface.

Filtered sludge cake relationships

Fig. 2 presents the relationship between the amount of sludge cake with the amount of filter powder and polymer. It follows from Fig. 2, that the influence of the polymer to the increase of the wet

Table 3
XRF data of the mineral conditioner (results in weight %).

Spectrum	Elements										
	O	Na	Mg	Al	Si	P	K	Ca	Ti	Fe	Total
1	63.30	0.53	0.64	2.87	22.34	3.72	0.32	4.79	0.11	1.49	100
2	65.39	0.55	0.66	2.97	23.08	3.85	0.33	4.95	0.11	1.54	100
3	68.54	0.58	0.69	3.11	24.19	4.03	0.35	5.18	0.12	1.61	100
Mean	65.74	0.55	0.66	2.9	23.20	3.87	0.33	4.97	0.11	1.55	100
STD dev.	2.64	0.02	0.03	0.12	0.93	0.10	0.01	0.20	0.004	0.06	–

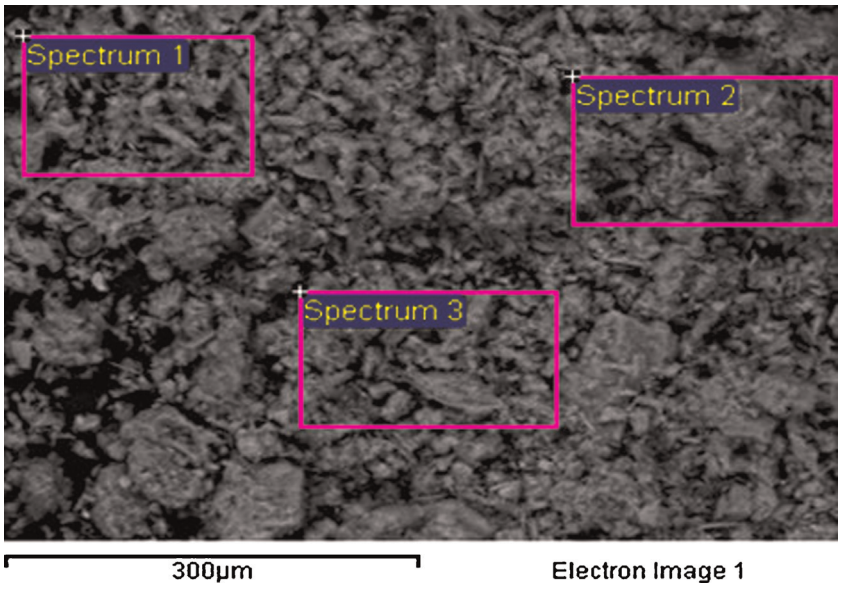

Fig. 1. SEM image of the mineral conditioner, DB-12Ca.

cake amount is more significant than the one from the addition of the filter powder. By comparison of the slopes in the plots as shown in Table 4, it can be noticed that in the case of filter powder the slopes are 19.15, 19.40, 22.84 and 29.91 and they do not change drastically for the concentrations or doses of polymer from 19 to 75 mg/g TS as seen in Fig. 2(a). The dose of polymer of 150 mg/g TS is the one with the highest slope and the latter is 1.6 times higher than the one for the first polymer dose. Conversely, in the case of

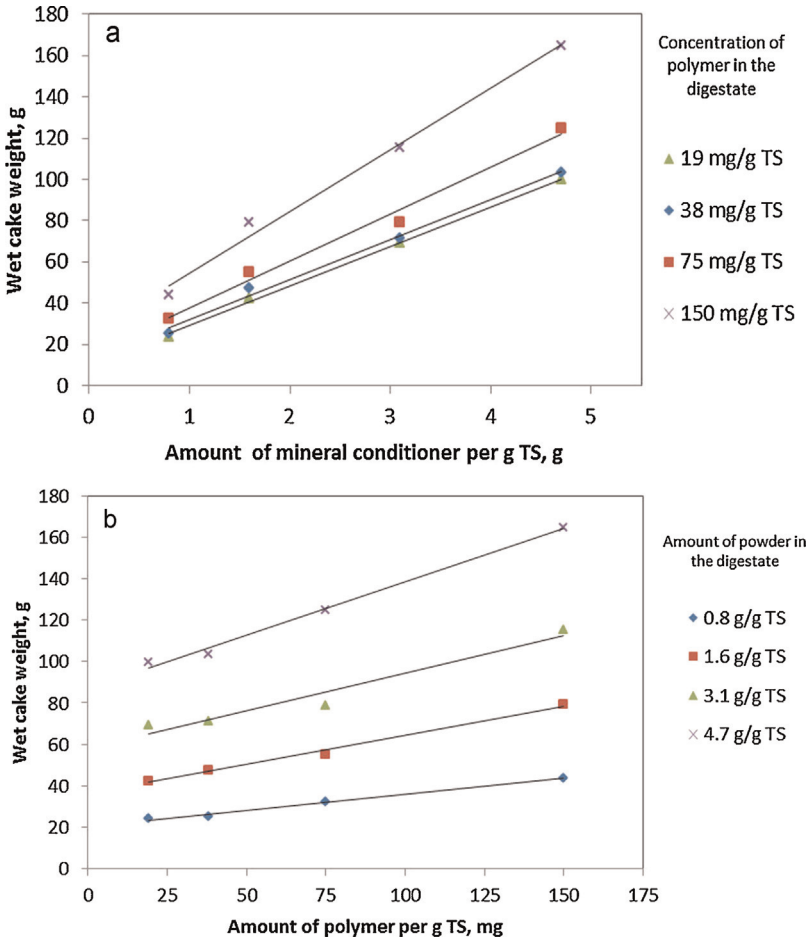

Fig. 2. Weight of the wet filtered cake: dependence on the amounts of mineral conditioner (a) and polymer (b).

Table 4
Regression equations from Fig. 2.

Concentration of polymer in the digestate (mg/g TS)	Regression equation	R^2	Amount of powder in the digestate (g/g TS)	Regression equation	R^2
19	$y = 19.15x + 10.10$	0.9984	0.8	$y = 0.16x + 20.32$	0.9937
38	$y = 19.40x + 12.43$	0.9925	1.6	$y = 0.28x + 36.27$	0.9912
75	$y = 22.84x + 14.53$	0.9862	3.1	$y = 0.36x + 58.32$	0.9513
150	$y = 29.91x + 24.52$	0.9908	4.7	$y = 0.51x + 86.98$	0.9929

the polymer, the highest slope is 3.2 times higher than the one for the first amount of powder in the digestate. These differences in the slope increase are related to the fact that the cake obtaining process is more intense in the case of increasing the amount of polymer rather than the amount of powder as investigated by Thapa et al. [15] with dewatering rates slower for flocculated sludge with polymer than for conditioned sludge with lignite. The solids content of the cake was reduced after the separation for the conditioned sludge with lignite. This result can be compared to the one obtained in this study for the dose of 1 $g_{DB\text{-}12Ca}$/g TS from Fig. 2(a) where there is no a significant increase of the wet cake weight over the dose range of polymer from 19 to 150 mg/g TS. However, an increase of the solids content increases the wet cake weight over the same dose range of the polymer due to the retention of the water. Hence, the solid fraction decreases as well. This phenomenon has to be pointed out when using the polymer as a flocculant agent. Moreover, Thapa et al. [16] have found that doses of polymer over 10 mg/g TS of sludge would not achieve a water removal over 85% for flocculated sludge. Hence, the use of an excess of polymer will cause gelation, dewatering would require further pressure and energy in order to release the water from the cake.

The mineral conditioner has a content of 5% of Ca that interacts by ion exchange with the dissolved organic content of the ADR as investigated by Li [23] for the mechanism of clogging by the formation $CaCO_3$ in landfill leachates. However, the polymer influences the most the dewatering performance of this study although flocculation can be enhanced to certain extent with the mineral conditioner as seen from Fig. 2(a). The flocculation behavior of the ADR could significantly be improved in order to achieve favorable permeability in the dewatering processes by modifying the surface charge of the ADR by means of the polymer [24]. Thereby, particle–particle bridging occurs for the ADR when adding the polymer.

Water retention capacity relationships

An interesting fact is observed in Fig. 3. The WRC is increased linearly by increasing the amount of polymer as shown in Fig. 3(b) and Table 5. However, in the case of increasing the amounts of mineral conditioner, an opposite trend is observed. It means that the mineral conditioner has a tendency to weaken the water retention properties of the polymer [16–18]. This phenomenon is very relevant for understanding and for designing the type of filtration and dewatering processes, in order to find the optimal amounts of polymer and mineral conditioner. This will allow achieving efficient filtration performance of the wet cake and in addition, to obtain a wet cake without a gel structure.

Table 5
Regression equations from Fig. 3(b).

Amount of powder in digestate (g/g TS)	Regression equation	R^2
0.80	$y = 0.0098x + 1.31$	0.9957
1.60	$y = 0.0119x + 1.28$	0.9787
3.10	$y = 0.0128x + 1.77$	0.9944
4.70	$y = -1E-06x^3 + 0.0005x^2 - 0.02x + 2.28$	1

Filterability region

It is followed from Fig. 4 that a relatively low amount of polymer can drastically increase the WRC. This fact is important for understanding the mechanism of water retention in the wet cake [19]. The role of the polymer in this case is more significant [20] than the role of mineral conditioner as previously mentioned.

The data from Fig. 4 was obtained from all the dewatering experiments from Table 6. Two levels (high and low) of WRC are plotted and the maximum and minimum % of polymer in the dried cakes of the two levels was obtained as follows,

High level WRC (minimum) per L of ADR:

Wet cake weight = 96.5 g

Dry cake weight = 38.0 g

$$\text{WRC} = \frac{96.5 - 38.0}{38.0} = 1.5$$

$$\%\ \text{polymer in dry cake} = \left[\frac{g_{\text{polymer}}}{g_{\text{dry cake}}}\right] \times 100 \quad (2)$$

$$\%\ \text{polymer in dry cake} = \left[\frac{0.15\ g_{\text{polymer}}}{38\ g_{\text{dry cake}}}\right] \times 100 = 0.4$$

In Eq. (2), 0.15 g of polymer were added to 1 L of ADR and it corresponds to the dose of 19 mg/g TS.

High level WRC (maximum) per L of ADR:

Wet cake weight = 43.2 g

Table 6
WRC vs. % polymer in the dry cake for all the dewatering experiments with two levels (high and low).

% of polymer in the dry cake	High level of WRC	Low level of WRC
0.4	1.5	–
0.6	1.6	–
0.8	1.6	–
1.2	1.7	–
1.5	2.0	1.5
2.0	2.1	–
2.1	2.2	–
2.4	–	2.1
3.0	2.8	–
3.9	–	2.2
4.3	2.7	–
4.8	3.1	–
6.4	3.7	–
7.6	–	2.9
15.1	4.4	–

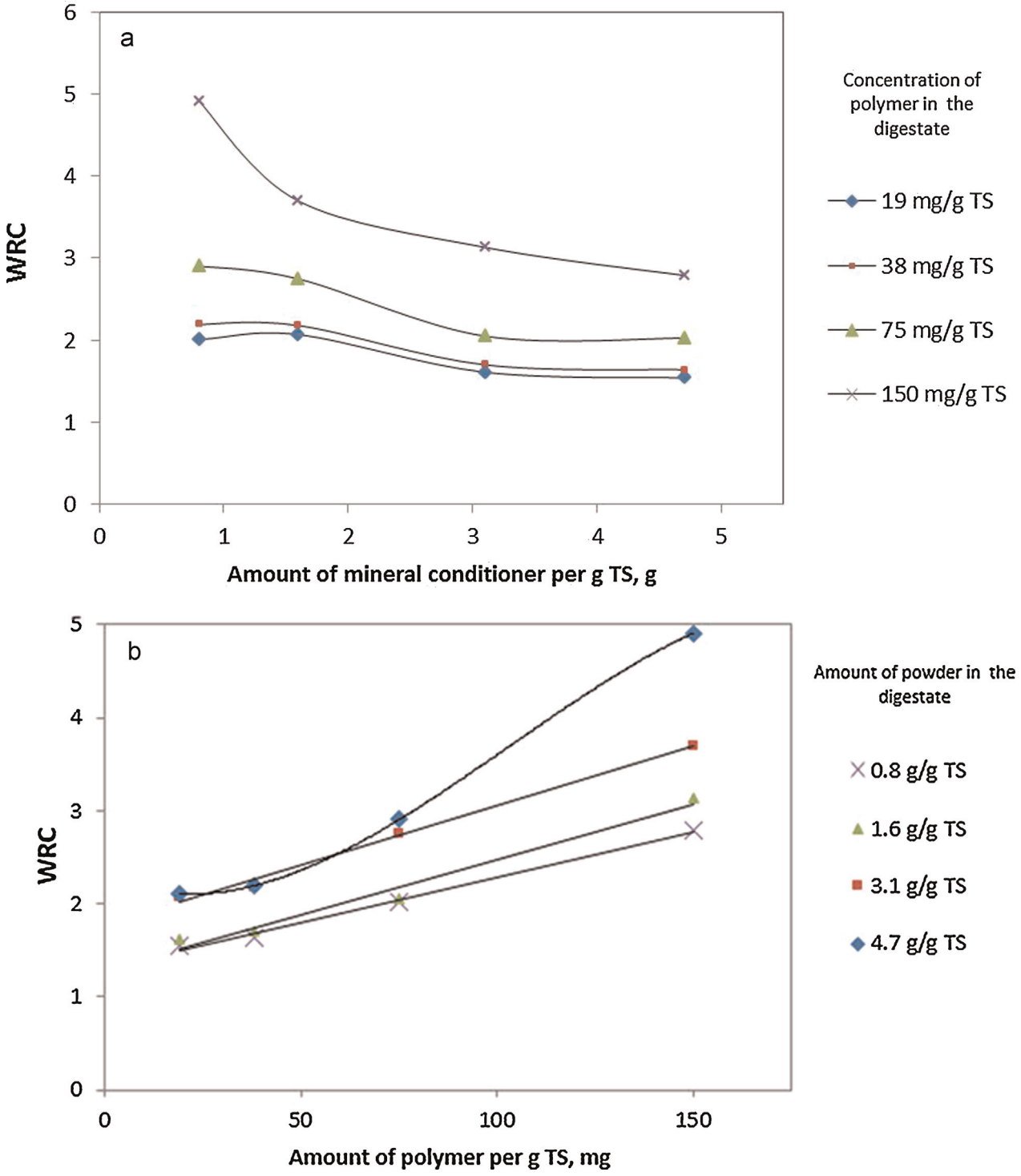

Fig. 3. Influence in the WRC with filter powder (a) and polymer addition (b).

Dry cake weight = 8.0 g

$$WRC = \frac{43.2 - 8.0}{8.0} = 4.4$$

$$\%\ \text{polymer in dry cake} = \left[\frac{1.2\ g_{polymer}}{8.0\ g_{dry\ cake}}\right] \times 100 = 15.0$$

In Eq. (2), 1.2 g of polymer were added to 1 L of ADR and it corresponds to the dose of 150 mg/g TS.

Low level WRC (minimum) per L of ADR:

Wet cake weight = 18.6 g

Dry cake weight = 7.4 g

$$WRC = \frac{18.6 - 7.4}{7.4} = 1.5$$

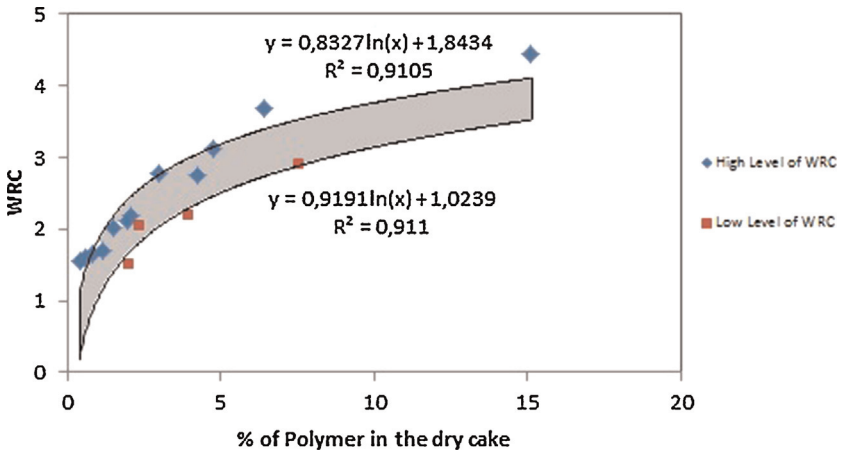

Fig. 4. The influence of polymer content on the water retention capacity.

$$\%\ \text{polymer in dry cake} = \left[\frac{0.15\ g_{\text{polymer}}}{7.4\ g_{\text{dry cake}}}\right] \times 100 = 2.0$$

Low level WRC (maximum) per L of ADR:

Wet cake weight = 61.6 g

Dry cake weight = 15.8 g

$$\text{WRC} = \frac{61.6 - 15.8}{15.8} = 2.9$$

$$\%\ \text{polymer in dry cake} = \left[\frac{1.2\ g_{\text{polymer}}}{15.8\ g_{\text{dry cake}}}\right] \times 100 = 7.6$$

It is possible to determine by means of Fig. 4 the optimal dose for the polymer and the physical conditioner. The left bottom point represents in fact the most mineralized form in which the contribution of the polymer to the flocculation is not substantial. Moreover, this point is critical due to the fact than lower doses of both the filter agent and polymer would lead to clogging problems in the filtration process. Conversely, the top right point defines the boundary of the range gray area in which efficient filterability is achieved between a high level and a low level of WRC. Over this point, there is gelation of the system which would require pressing for improving water recovery in the process. Furthermore, this WRC point corresponding to 16% of polymer in the dry cake is slightly different that the one from 4 to 5% which is in the range of good filterability. This is certainly an indication that there could be an overdose of the polymer that is not required to improve the performance in the filtration process which would undoubtedly lead to a gelation of the system.

The behavior and further treatment of the wet cake is highly dependent on the amounts of both conditioners in the dewatered solid. Relatively high doses of polymer would lead to a gel consistency in opposite to the mineralized solid structure when increasing the powder amount. This is more critical as mentioned before when increasing the polymer concentration in the wet cake compared to the contribution of the mineral conditioner. It is therefore important to select the correct weight ratio of polymer and mineral conditioner not only for research purposes but for a step towards up-scaling in a pilot and/or industrial scale as well.

Turbidity and capillary suction time measurements

The flocculation and filtration properties of bentonite based mineral conditioners and polymeric flocculant ZETAG® 9014 were evaluated by turbidimetric and CST methods. In Fig. 5, it is presented the influence of amount of mineral conditioner and concentration of polymer on the turbidity of effluent samples. The initial turbidity of the ADR was 4700 FTU. The system has a

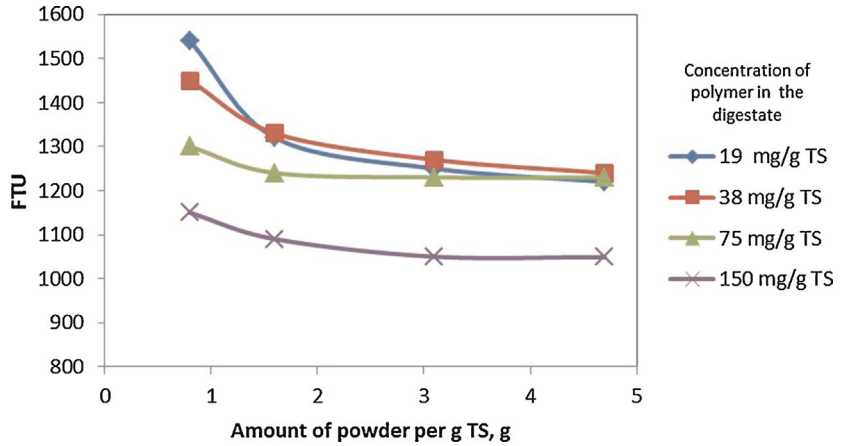

Fig. 5. Turbidity of the anaerobic digestion residue treated by mineral conditioner and polymer.

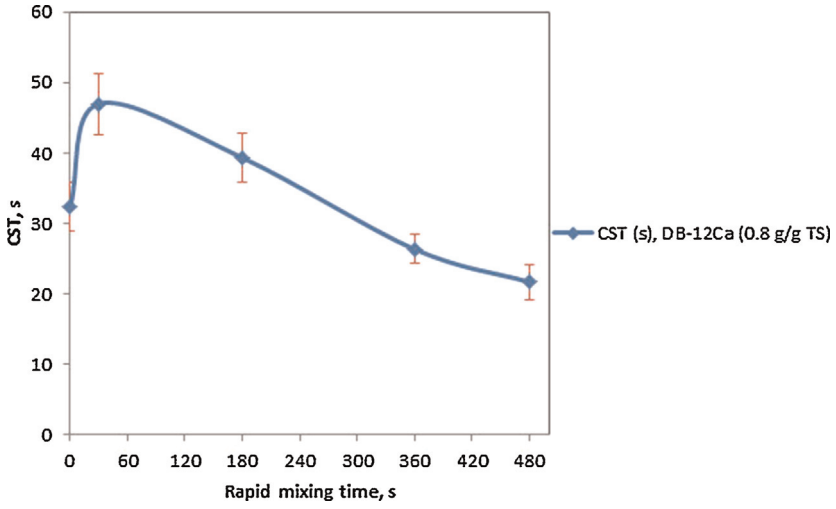

Fig. 6. Capillary suction time (s) of the flocculated ADR during the rapid mixing of the flocculation process at 0, 30, 180, 360 and 480 s after the addition to the ADR of DB-12Ca (0.8 g/g TS) at $t = 0$ s and ZETAG® 9014 (19 mg/g TS) at $t = 300$ s.

tendency to reach a constant level of turbidity when increasing the mineral conditioner dose as shown in Fig. 5. Thus, there is a contribution to the dry matter (DM) content of the system however, no further interaction is achieved in terms of turbidity removal.

The influence of the mixing conditions could be described in terms of the CST during the rapid mix phase (300 rpm). It follows from Fig. 6 that the CST increases drastically within the first 30 s of rapid mixing. A maximum CST is achieved most likely due to the fact that the mineral conditioner was starting to interact with the organic matter and aggregation was therefore enhanced after 30 s of rapid mixing. Moreover, a decreasing trend of the CST can be observed from Fig. 6, due to the aggregation of the organic matter in the ADR. It can be seen from Fig. 6 that the flocculation was occurring firstly, because of the mineral conditioner from 30 to 300 s and secondly, due to the addition of the polymer ZETAG® 9014. The polymer dose can thus be decreased as low as 19 mg/g TS for a concentration of mineral conditioner of 0.8 g/g TS due to the trend of the CST over time. Moreover, the CST is not sharply decreased after the addition of the polymer at $t = 300$ s and onwards. This is due to a sufficient contact time between the mineral conditioner and the ADR. Furthermore, Li et al. [25] have investigated the tendency of kaolin to be flocculated in water suspensions with Ca content for pH values over the isoelectric point ($pH_{IEP} = 7.2$), which is in accordance to the trend of the CST in Fig. 6 for the case of the DB-12Ca system. The pH of the ADR was stable during the dewatering treatment at 8.3.

Hence, the mixing conditions as well as the Ca content of DB-12Ca had a direct impact in the further dewaterability of the ADR prior to the polymer addition.

Conclusions

1 The range of optimal amounts of mineral conditioner bentonite based and polymeric flocculant ZETAG® 9014 were determined. In this case, the optimal content of polymer is about 19–25 mg of polymer and 0.8–1.6 g mineral conditioner per g of TS of digestate. These contents allow achieving good filterability after 30 s of rapid mixing without gelation of the wet cake.

2 The term for the characterization of water retention by the mineral conditioner and the polymer – water retention capacity – WRC is suggested for such optimal dose studies. A concentration over 5% of the polymer in the dry cake represents an excess of the chemical conditioner that would not improve the dewatering performance of the ADR by vacuum filtration.

3 This study represents a basis for the study of optimal doses in the inlet stream of a decanter due to the fact that the suspended colloidal content is substantially higher than in the rejected stream. It is in fact a starting point for the inlet stream dewatering process by use of combined physical and chemical conditioners.

Acknowledgments

The authors of this work are thankful with the Norwegian research council and the Norwegian industrial partners, Lyse Neo AS, IVAR IKS, Cambi AS, HØST Verdien i avfall, Lindum AS and Agroplas AS for the funding of this work through the Fixation of Nutrient Elements in Digestate project (grant # ES 459248/0).

References

[1] J.R. Williams, Dewatering system for sludge removal, US Patent 5156749 (1992) USA.
[2] Y. Qi, K.B. Thapa, F.A. Hoadley, Application of filtration aids for improving sludge dewatering properties – a review, Chem. Eng. J. 171 (2) (2011) 373–384, doi:http://dx.doi.org/10.1016/j.cej.2011.04.060.
[3] O.E. Albertson, M. Kopper, Fine-coal-aided centrifugal dewatering of waste activated sludge, J. Water Pollut. Control Fed. 55 (2) (1983) 145–156.
[4] B. Sander, H. Lauer, M. Neuwirth, Process for producing combustible sewage sludge filter cakes in filter presses, US Patent 534681 (1989) 7.
[5] Y.F. Lin, S.R. Jing, D.Y. Lee, Recycling of wood chips and wheat dregs for sludge processing, Bioresour. Technol. 76 (2) (2001) 161–163, doi:http://dx.doi.org/10.1016/S0960-8524(00)00098-5. 11131800.
[6] J. Benítez, A. Rodríguez, A. Suárez, Optimization technique for sewage sludge conditioning with polymer and skeleton builders, Water Res. 28 (10) (1994) 2067–2073, doi:http://dx.doi.org/10.1016/0043-1354(94)90016-7.
[7] C. Chen, P. Zhang, G. Zeng, J. Deng, Y. Zhou, H. Lu, Sewage sludge conditioning with coal fly ash modified by sulfuric acid, Chem. Eng. J. 158 (3) (2010) 616–622, doi:http://dx.doi.org/10.1016/j.cej.2010.02.021.
[8] Y.Q. Zhao, Involvement of gypsum ($CaSO_4 \cdot 2H_2O$) in water treatment sludge dewatering: a potential benefit in disposal and reuse, Sep. Sci. Technol. 41 (12) (2006) 2785–2794, doi:http://dx.doi.org/10.1080/01496390600785558.
[9] Y.Q. Zhao, Enhancement of alum sludge dewatering capacity by using gypsum as skeleton builder, Colloids Surf. A: Physicochem. Eng. Aspects 211 (2–3) (2002) 205–212, doi:http://dx.doi.org/10.1016/S0927-7757(02)00277-7.
[10] S.R. Jing, Y.F. Lin, Y.M. Lin, C.S. Hsu, C.S. Huang, D.Y. Lee, Evaluation of effective conditioners for enhancing sludge dewatering and subsequent detachment from filter cloth, J. Environ. Sci. Health A 34 (7) (1999) 1517–1531, doi:http://dx.doi.org/10.1080/10934529909376909.
[11] F.F. Notebaert, D.A. Wilms, A.A. Van Haute, A new deduction with a larger application of the specific resistance to filtration of sludges, Water Res. 9 (7) (1975) 667–673, doi:http://dx.doi.org/10.1016/0043-1354(75)90175-X.

[12] W. Leu, F.M. Tiller, Experimental study of the mechanism of constant pressure cake filtration: clogging of filter media, Sep. Sci. Technol. 18 (12–13) (1983) 1351–1369, doi:http://dx.doi.org/10.1080/01496398308059930.
[13] M.J.D. White, R.C. Baskerville, Solution to a problem of filter cloth blinding, Effluent Water Treat. J. 14 (1974) 503–505.
[14] J.T. Novak, G.L. Goodman, A. Pariroo, J.C. Huang, The blinding of sludges during filtration, J. Water Pollut. Control Fed. 60 (2) (1988) 206–214.
[15] K.B. Thapa, Y. Qi, S.A. Clayton, A.F. Hoadley, Lignite aided dewatering of digested sewage sludge, Water Res. 43 (3) (2009) 623–634, doi:http://dx.doi.org/10.1016/j.watres.2008.11.005. 19058831.
[16] K.B. Thapa, Y. Qi, A.F.A. Hoadley, Interaction of polyelectrolyte with digested sewage sludge and lignite in sludge dewatering, Colloids Surf. A: Physicochem. Eng. Aspects 334 (1–3) (2009) 66–73, doi:http://dx.doi.org/10.1016/j.colsurfa.2008.10.007.
[17] N. Böhm, W.-M. Kulicke, Optimization of the use of polyelectrolytes for dewatering industrial sludges of various origins, Colloid Polym. Sci. 275 (1) (1997) 73–81, doi:http://dx.doi.org/10.1007/s003960050054.
[18] J. Gregory, Polymer adsorption and flocculation in sheared suspensions, Colloids Surf. 31 (1988) 231–253, doi:http://dx.doi.org/10.1016/0166-6622(88)80196-3.
[19] D.H. Napper, Polymeric Stabilization of Colloidal Dispersion, Academic Press, London, 1983.
[20] J.A. Caskey, R.J. Primus, The effect of anionic polyacrylamide molecular conformation and configuration on flocculation effectiveness, Environ. Prog. 5 (2) (1986) 98–103, doi:http://dx.doi.org/10.1002/ep.670050210.
[21] American Public Health Association (APHA), Water environment federation, in: E.W. Rice, R.D. Baird, A.D. Eaton, L.S. Clesceri (Eds.), Standard Methods for the Examination of Water and Wastewater, 22nd ed., American Water Works Association, Clearway Logistics, 2012, ISBN-13: 978-0875530130.
[22] D. Eisenhour, F. Reisch, Industrial minerals and rocks: commodities, markets, and uses, in: J.E. Kogel, N.C. Trivedi, J.M. Barker, S.T. Krukowski (Eds.), Bentonite, seventh ed., Society for Mining, Metallurgy and Exploration Inc., Littleton, Colorado, 2006, pp. 357–368, ISBN-13: 978-0873352338.
[23] Z. Li, Modeling precipitate-dominant clogging for landfill leachate with NICA-Donnan theory, J. Hazard. Mater. 274 (2014) 413–419, doi:http://dx.doi.org/10.1016/j.jhazmat.2014.04.009. 24806870.
[24] Z. Li, T. Katsumi, T. Inui, Modeling cake filtration under coupled hydraulic, electric and osmotic effects, J. Membr. Sci. 378 (1–2) (2011) 485–494, doi:http://dx.doi.org/10.1016/j.memsci.2011.05.038.
[25] Z. Li, T. Katsumi, T. Inui, A. Takai, Fabric effect on hydraulic conductivity of kaolin under different chemical and biochemical conditions, Soils Found. 53 (5) (2013) 680–691, doi:http://dx.doi.org/10.1016/j.sandf.2013.08.006.
[26] J. Dosta, J. Rovira, A. Galí, S. Macé, J. Mata-Álvarez, Integration of a coagulation/flocculation step in a biological sequencing batch reactor for COD and nitrogen removal of supernatant of anaerobically digested piggery wastewater, Bioresour. Technol. 99 (13) (2008) 5722–5730, doi:http://dx.doi.org/10.1016/j.biortech.2007.10.021. 18068357.
[27] D.A. Dahlstrom, R.C. Bennett, R.G. Emmet, P. Harriott, T. Laros, W. Leung, S.A. Miller, B. Morey, J.Y. Oldshue, G. Priday, C.E. Silverblatt, J.S. Slottee, J.C. Smith, Liquid–solid operations and equipment, in: R.H. Perry, D.W. Green (Eds.), Perry's Chemical Engineer's Handbook, seventh ed., McGraw-Hill, United States of America, 1999, pp. 75 ISBN 0-07-049841-5.

Paper II

Alvarenga E., Schüller R.B. and Salas-Bringas C. 2015 Calibration of a Jar-tester replicated in a rotational rheometer. *Annual Transactions of the Nordic Rheology Society*, 23, pp. 199–205

Calibration of a Jar-Tester Replicated in a Rotational Rheometer

Emilio Alvarenga [1], Reidar Barfod Schüller [2] and Carlos Salas-Bringas [3]

[1]Dep. Of Environmental Sciences, Norwegian University of Life Sciences, P.O. Box 5003, N-1432 Ås, Norway.

[2]Dep. Of Chemistry, Biotechnology and Food Science, Norwegian University of Life Sciences, P.O. Box 5003, N-1432 Ås, Norway.

[3]Dep. Of Mathematical Sciences and Technology, Norwegian University of Life Sciences, P.O. Box 5003, N-1432 Ås, Norway.

ABSTRACT

A prediction method to determine viscosity in laminar and turbulent regimes was investigated in this article for a replicated Jar-tester adapted to a rotational rheometer. The calibration enables the prediction of an average torque and rotational speed by means of a model for both flow regimes.

INTRODUCTION

Coagulants and flocculants optimal dosage is commonly determined in the wastewater treatment plants (WWTPs) by the Jar-test (JT) device. This instrument resembles a paddle mixer in a cylindrical cup.

In addition, corrective measures can be implemented in the WWTPs for the removal of particles when overflow conditions (e.g. rain water) occur along with re-adjustments for other physicochemical water parameters to keep an efficient separation process that complies with environmental regulations. This fact is firstly attributable to the geometry of the stirrers. Secondly, there are controlled mixing conditions over time in the rapid mixing (coagulation phase) and slow mixing (flocculation phase)[1]. Thereby, these type of tests are expected to have a similar flow behavior as in the full plant scale.

Albeit, operators in the plants must consider a theoretical and empirical baseline of the process in order to get close to the real process conditions. Moreover, this particular feature is inherent to every treatment process and thus, iterative calculations are required for matching the baseline conditions and for the achievement of a correct adjustment. Such procedure leads to a time consuming correction in the process[1].

An understanding of the flow behavior is needed due to the changes in viscosity that occur when adding physical or chemical conditioners to the wastewater in a turbulent regime (rapid mixing). Effects associated to turbulence in addition to the viscosity contribution could influence the location of the average shear rate[2]. Conversely, in the laminar regime (slow mixing) the average shear rate could be determined by means of an analogue radius[3]. The estimation of these average shear rates and average viscosity in both flow regimes would bring additional information about the optimization of coagulants and flocculants when performing standard JT experiments in the WWTPs. Moreover, such approach could provide insight for replicating shear conditions with different geometries for paddles when upscaling similar shear rates in industrial equipment as investigated by Örmeci[4].

A calibration procedure is required in order to determine the constants for the determination of the average shear rate and average shear stress like previously studied by Salas-Bringas et al.[5].

The aim of this study is to determine an average shear rate ($\dot{\gamma}_{avg}$) and its location from rotational speed and an average shear stress (τ_{avg}) from torque for a Newtonian fluid in a replicated Jar-Tester. Both laminar and turbulent regime calibrations are assessed with a mathematical model and experimental data from a rotational rheometer.

MATERIALS AND METHODS

Part 1: Experimental Calibration Procedure

All the measurements for the calibration procedure were carried out with rotational rheometers. The standard fluid utilized was a Newtonian silicon oil labelled as 1000 cP at 25°C (Brookfield Engineering Laboratories, Inc., USA).

The actual viscosity (A_η) of the silicon oil was measured by means of a cone-plate geometry (50 mm diameter, 1°, 50 µm gap) at constant shear rate ($5s^{-1}$) in an Anton Paar rheometer MCR-301. The temperature range from 20 to 60°C with 10°C ramping steps was taken into consideration for the calibration procedure.

A Jar-tester mixer from a Kemira Flocculator 2000 was replicated in a CAD program, SolidWorks, as seen in Fig. 1 (a) and (b) and printed in an ABS 3D printer (Mojo). The replicated JT was connected to a Paar Physica UDS 200 rheometer as shown in the experimental assembly of Fig. 2. The experimental conditions (speed and temperature) were controlled in order to obtain accurate measurements of the Torque (M) and rotational speed (N). The range from 10 to 50 rpm is used for the slow mixing and from 100 to 500 rpm for the rapid mixing. The temperature range considered for the experiment was from 20 to 60°C with 10°C ramping steps.

The fluid volume was 725 mL and the flow curves (M vs. N) were determined for each temperature in the range of interest in order to calculate two constants K_1 and K_2. K_1 is used to convert M into an τ_{avg} and K_2 to convert N into an $\dot{\gamma}_{avg}$.

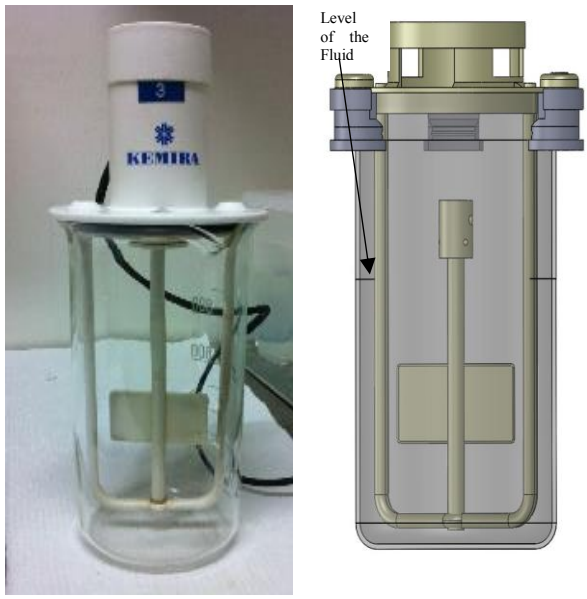

(a) (b)

Figure 1: (a) the standard JT (b) 3D drawing of the JT system and its lid and shaft coupled to a Paar Physica UDS200 rheometer

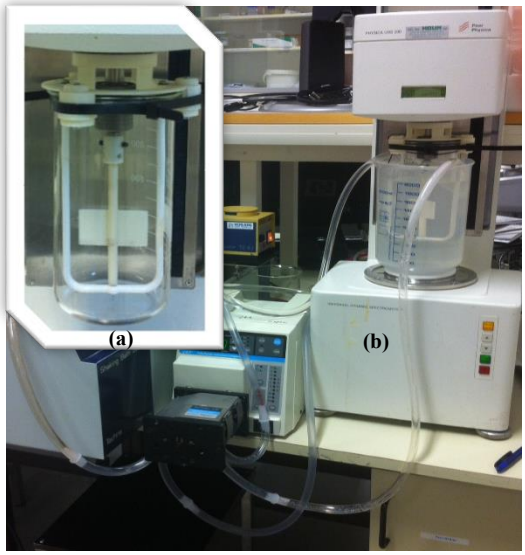

Figure 2: Experimental assembly. The figure shows: (a) a replicate of the JT system assembled in an Anton Paar UDS200 rheometer and (b) the replicated system inside a cylindrical container surrounded with water pumped by a peristaltic pump for the control of the temperature

Part 2: Analytical determination of the average shear stress and mean shear rate for the slow mixing phase

In an analogue cylinder geometry, the τ_{avg} and the $\dot{\gamma}_{avg}$ are given by Eq. 1 and 2 as follows[3],

$$\tau = \frac{M}{2\pi r^2 h} \quad (1)$$

$$\dot{\gamma} = \frac{2\pi r N}{60\delta} \quad (2)$$

In these equations, r (m) represents the radius of the analogue cylinder whereas h (m) is its height and δ (m) is the gap between the stationary wall of the flask and the analogue cylinder. It is thus possible to determine an expression for K_1 and K_2 to obtain η_{avg}. This is shown in Eq. 3, 4 and 5.

$$\eta = \frac{M}{2\pi r^2 h} \Big/ \frac{2\pi r N}{60\delta} \quad (3)$$

$$K_1 = \frac{1}{2\pi r^2 h} \quad (4)$$

$$K_2 = \frac{2\pi r}{60\delta} \quad (5)$$

The unit for K_1 is m^{-3} whereas K_2 is a dimensionless number. Eq. 3 can be simplified in order to express the viscosity in terms of a *slope a* that is the ratio between M and N (Nm/rpm) as seen in Eq. 6. Furthermore, δ can be replaced by "$r_{cyl} - r$" for the iterative calculation of the analogue radius r (m) where r_{cyl} represents the internal radius of the cylindrical container (Fig. 2 (a)). In the JT system, the internal radius r_{cyl} is 0.0445 m and h is 0.0303 m (paddle section).

$$\eta = \frac{15(r_{cyl} - r)}{\pi^2 r^3 h} \cdot slope\ a \quad (6)$$

A relative error (E) from the experimental work was calculated in order to determine the accuracy of the experimental measurements of the Newtonian fluid in the calibration procedure, with the coaxial analogue cylinder. The latter predicted viscosity (P_η) obtained by means of the UDS200 rheometer was compared with the actual viscosity (A_η) derived from the MCR-301 device. Eq. 7 includes the previously mentioned terms,

$$E = (P_\eta - A_\eta)/A_\eta \quad (7)$$

Part 3: Analytical determination of the average shear stress and mean shear rate for the rapid mixing phase

The approach of the linear curve fit was not suitable between M and N for the rapid mixing. In this range of rotational speeds (from 100 to 500 rpm), a turbulent regime was generated and a non-linear trend was hence obtained. It was thus assumed that the τ_{avg} is a function of the η_{avg} and $\dot{\gamma}_{avg}$ as shown in Eq. 8 (in terms of M and N),

$$M = A \cdot N^B \cdot \eta + C \cdot N^D \quad (8)$$

In Eq. 8 η is the A_η. It was expressed in terms of the temperature (T, in Kelvin) from the Arrhenius relationship[6], and it is given by,

$$\eta = e^{(-5.77 + \frac{1722.2}{T})} \quad (9)$$

M is given as µNm and N as rpm. In order to determine the values of the constants (A and C) and the coefficients (B and D) in Eq. 8, a script was written in MATLAB using the function *fminsearch*[7] for the optimal minimal value of the function J expressed as,

$$J = \frac{1}{F}\sum(z - \hat{z})^2 \quad (10)$$

Where F represents the total set of data points (25) in the space (x, y) and the predicted value, $\hat{z}$, is given by the Eq. 8 as M. Thereby, the function *fminsearch* minimizes the prediction error function J[7]. A relative error distribution for P_η was determined from Eq. 7.

RESULTS AND DISCUSSIONS

Part 1: Determination of the average viscosity in the slow mixing phase

The A_η data over the whole temperature range is shown in Table 1.

Table 1: Actual viscosity of the silicon oil measured with a cone plate at $\dot{\gamma} = 5s^{-1}$ in an Anton Paar MCR301 rheometer.

T (°C)	Viscosity (Pa·s)
20	1.110
30	0.913
40	0.759
50	0.641
60	0.549

As previously mentioned, there was a good prediction of the η_{avg} obtained through a linear fit between the *M* and the *N*. Fig. 3 shows the variation of the *slope a* from Eq. 6. Such shear rate generated a laminar condition as expected for a Newtonian fluid. Effects associated with viscous shear were considered by *slope a*.

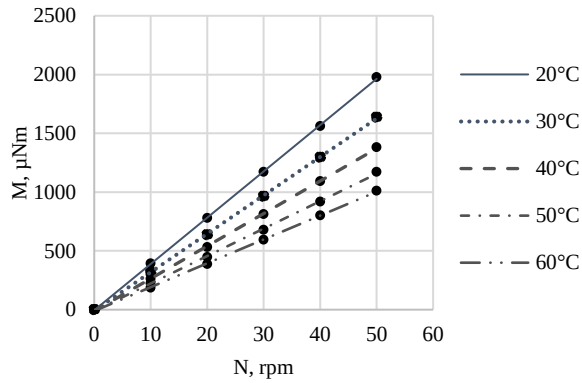

Figure 3: Linear relations between average Torque, *M* (Nm) and rotational speed, *N* (rpm) over the whole temperature range. The measurements were performed in a Paar Physica UDS200 rheometer.

Slope a is included in Table 2 along with, P_η (calculated from Eq. 6) and the relative error. The analogue radius (r = 0.03056 m) was calculated by iterations in Eq. 6 with the function Goal Seek in Excel. The constants K_1 and K_2 obtained were 5902.7 m^{-3} and 0.213 accordingly.

Table 2: Variation of *slope a* with temperature range and the inclusion of the predicted viscosity and the relative error.

T (°C)	Slope (Nm/rpm)	Predicted Viscosity (Pa.s)	*E*
20	0.000039241	1.088	0.020
30	0.000032465	0.9	0.014
40	0.000027326	0.757	0.002
50	0.000023043	0.639	0.004
60	0.000019978	0.554	0.009

Part 2: Determination of the average viscosity in the fast mixing phase

The Reynolds number (Re) was calculated from Eq. 11 with a density of 1090 kg/m^3 (ρ at 20°C for the silicon oil) for some of the *N* values as shown in Table 3. The regime of the fluid was considered fully turbulent[8] for values of Re above 10 000.

$$Re = \frac{\rho \cdot v \cdot D_{mixer}}{\eta_{avg}} \quad (11)$$

In Eq. 11, *v* (m/s) is the mean velocity derived from *N* and D_{mixer} (m) is the diameter of the stirrer (0.044 m) of the JT system.

Table 3: Reynolds number of the silicon oil for several rotational speeds (*N*) in the JT system at 20°C.

Rotational Speed (rpm)	Reynolds Number (Re)
40	3982
50	4977
100	9954
200	19 909
300	29 863

It can be seen from Table 3 that the transition from laminar to turbulent regime occurs between 100 and 200 rpm at 20°C.

In the N range from 100 to 500 rpm, a non-linear trend between M and N was obtained as seen from Fig. 4.

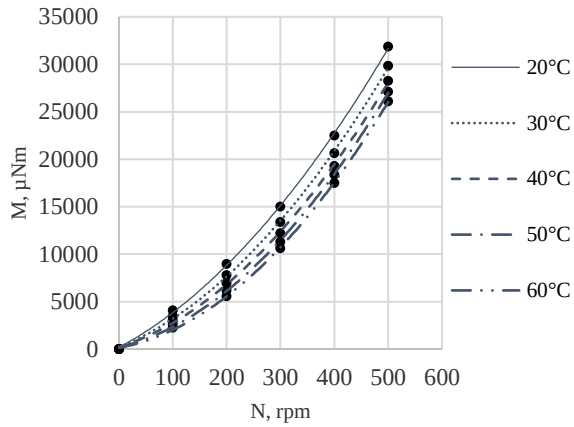

Figure 4: Non-linear relations between average Torque, M (µNm) and rotational speed, N (rpm) over the whole temperature range. The measurements were performed in a Paar Physica UDS200 rheometer.

The torque M measured represents the term z in Eq. 10. The prediction error J was minimized and the constants and the coefficients calculated in MATLAB for the proposed model in Eq. 8, were A = 100.9, B = 0.75, C = 0.032 and D = 2.15. Eq. 12 shows the predicted M (or $\hat{z}$ in Eq. 10) with the obtained constants and coefficients. It is hence possible to predict the average viscosity (P_η) from Eq. 12 with the model.

$$\hat{z} = 100.9 \cdot N^{0.75} \cdot \eta + 0.032 \cdot N^{2.15} \qquad (12)$$

The experimental M (z) versus the predicted M ($\hat{z}$) can be seen in Fig. 5. There is a good prediction of the M and it can be seen from the model (Eq. 12) that there is viscous contribution to the dynamic of the fluid along with a turbulent effect. The latter is reflected in the second term of the Eq. 12 with a coefficient D = 2.15 and the non-linear trend from Fig. 4 can hence be attributed to the fact that D is positive and higher than 2. Moreover, the second term of Eq. 12 shows that the location of the $\dot{\gamma}_{avg}$ is dependent on N when the turbulent regime is generated.

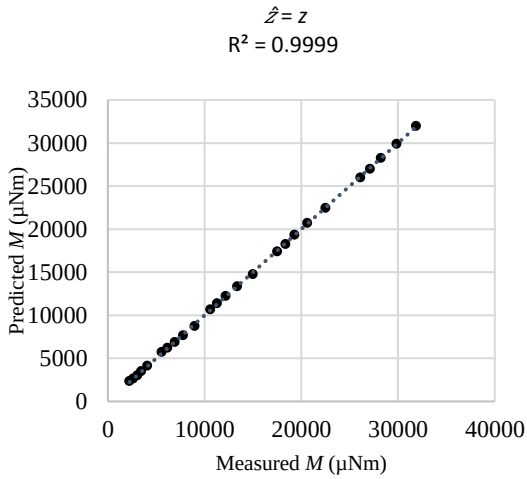

Figure 5: Linear relationship between the experimental and the predicted torque for all the rotational speeds (100-500 rpm) over the whole temperature range (20-60°C)

Although Eq. 12 was obtained from the experimental data in the rapid mixing (100-500 rpm), it expresses the contribution to the M_{avg} from both laminar and turbulent effects at all the speeds (10-500 rpm). There are most likely laminar effects in the layer close to the mixer surface (with fluid velocities close to zero) whereas larger scale turbulent effects may prevail in other sections of the container[2]. Hence, both contributions differ in magnitude over the whole speed range (10-500 rpm).

The P_η was calculated from Eq. 12 for all the measured M (25). The E distribution (calculated from Eq. 7) of the P_η is shown in Fig. 6.

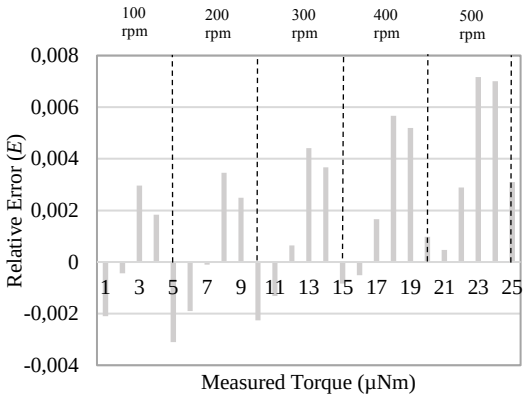

Figure 6: Relative error distribution of the predicted viscosity for all the experimental measurements for average torque (25) over the whole temperature range (20-60^{0}C) for each rotational speed (100-500 rpm). Measurements 1-5 correspond to 100 rpm, 6-10 to 200 rpm, 11-15 to 300 rpm, 16-20 to 400 rpm and 21-25 to 500 rpm.

It can be seen from Fig. 6 that the *E* has an even variation for *N* between 100 and 200 rpm whereas from 300 rpm onwards, there is a slight increase of it. Therefore, the model is suitable for the prediction of the η_{avg} of a Newtonian fluid in such temperature range in the turbulent regimes from 100 to 500 rpm.

It is suggested as a further step of this research, to test an $\dot{\gamma}_{avg}$ in a flocculation of wastewater in the replicated Jar-Tester system. Secondly, the same $\dot{\gamma}_{avg}$ of this calibration procedure for a water-based fluid (e.g. wastewater) could be replicated in a larger scale (e.g. pilot or industrial) in order to compare the separation efficiency in a flocculation process between the Jar-Tester and a larger scale mixing equipment[4]. Such separation efficiency could be expressed for instance, in terms of changes in M_{avg} in the laminar and turbulent regimes in the flocculation of wastewater.

CONCLUSIONS

A prediction model of the viscosity can be obtained from the replicated JT system for both laminar and turbulent regimes from a standard with known viscosity. However, the calibration procedure of this investigation showed that the location of the average shear rate in turbulent regime was dependent on rotational speed.

The model provides information about the turbulent regime with a component that affects the average shear stress with a non-linear response from the rotational rheometer.

This investigation is a first step for the understanding of the changes in average viscosity in the laminar and turbulent regime when performing a JT for the flocculation of wastewater.

ACKNOWLEDGMENTS

The authors of this work are thankful with the Norwegian research council as well as with the Norwegian industrial partners, Lyse Neo AS, IVAR IKS, Cambi AS, HØST Verdien i avfall, Lindum AS and Agroplas AS for the funding of this work through the Fixation of Nutrient Elements in Digestate project (grant # ES 459248/0).

REFERENCES

1. Teefy, S., Farmerie, J. and Pyles, E. (2010), "Operational Control of Coagulation and Filtration Processes", 3rd Ed., **2**, pp. 17-18, ISBN 978-1-58321-801-3.

2. Zhang, J., Xu, S. and Li, W. (2012), "High Shear Mixers: A Review of Typical Applications and Studies on Power Draw, Flow Pattern, Energy Dissipation and Transfer Properties", *J. Chem. Eng. and Proc.*, **57-58**, 25-41.

3. Steffe J.F., (1996), "Rheological methods in food process engineering", Freeman Press, East Lansing, Mich., pp. 213-214.

4. Ömerci, B., (2007), "Optimization of a Full-Scale Dewatering Operation Based on the Rheological Characteristics of Wastewater Sludge", *J. Water Research*, **41**, 1243-1252.

5. Salas-Bringas, C., Jeksrud, W.K., Lekang, O.-I. and Schüller, R.B. (2006), "A Calibration Method for a New Type of Rheometer", *Annual Transactions of the Nordic Rheology Society*, **14**, 197-201.

6. Steffe J.F., (1996), "Rheological methods in food process engineering" Freeman Press, East Lansing, Mich., pp. 33-34.

7. Schüller, R.B., Tande, M. and Amundsen, L. (2010), "Experimental determination of time dependent yield properties", *Annual Transactions of the Nordic Rheology Society*, **18**, 25-30.

8. Sinnott, R. K. (2013), "Coulson & Richardson's Chemical Engineering", 4th Ed., **6**, Butterworth-Heinemann, p. 73. ISBN 0-7506-6538-6.

Paper III

Alvarenga E., Øgaard A.F. and Vråle L. 2016 Effect of anaerobic digestion and liming on plant availability of phosphorus in iron– and aluminium–precipitated sewage sludge from primary wastewater treatment plants. *Manuscript*

Effect of anaerobic digestion and liming on plant availability of phosphorus in iron- and aluminium-precipitated sewage sludge from primary wastewater treatment plants

Emilio Alvarenga[a*], Anne Falk Øgaard[b], Lasse Vråle[c]

[a,b]Norwegian Institute of Bioeconomy Research, NIBIO, Frederik A. Dahls vei 20, NO-1430 Ås, Norway

[c]Siv. Ing. Lasse Vråle AS, Steinspranget 20 Drammen, Norway, Tel: (+47) 90 82 16 62

[*]Corresponding author: Tel: (+47) 92 01 04 92; Fax: (+47) 63 00 94 10; e-mail address: Emilio.Alvarenga@nibio.no

Abstract

More efficient plant utilisation of the P in sewage sludge is required because rock phosphate is a limited resource. To meet environmental legislation thresholds for phosphorus (P) removal from wastewater (WW), primary treatment with iron (Fe) or aluminium (Al) coagulants is effective. There is also a growing trend for WW treatment plants to be coupled to a biogas process, in order to co-generate energy. The sludge produced, when stabilised, is used as a soil amendment in many countries. This study examined the effects of anaerobic digestion (AD), with or without liming as a post-treatment, on P release from Fe- and Al-precipitated sludges originating from primary WW treatment plants. Plant uptake of P from Fe- and Al-precipitated sludge after lime treatment but without AD was also compared. Chemical characterisation with sequential extraction of P and a greenhouse experiment with barley (*Hordeum vulgare*) were performed to assess the treatment

effects on plant-available P. Liming increased the P-labile fraction in all cases. Plant P uptake increased from 18.5 mg pot^{-1} to 53 mg P pot^{-1} with liming of Fe-precipitated sludge and to 35 mg P pot^{-1} with liming of the digestate, while it increased from 18.7 mg pot^{-1} to 39 and 29 mg P pot^{-1} for the Al-precipitated substrate and digestate, respectively. Thus, liming of untreated Fe-precipitated sludge and its digestate resulted in higher P uptake than liming its Al-precipitated counterparts. Anaerobic digestion alone had a negative impact on P mobility for both sludges.

Keywords: Phosphorus recycling, sludge stabilisation, anaerobic digestion, lime treatment

1. Introduction

The continuous growth in the world's population is a major concern for future food production and supply (Cordell & Neset 2014). Finite natural resources that are not renewable, such as phosphorus (P), play an important role in the food chain. Phosphorus is essential for the metabolism and functioning of plants and animals and hence there is a strong dependence on P in the agriculture sector in order to maintain or increase crop yield levels. However, agricultural practices have led to a surplus of highly soluble P from mineral fertilisers in soils that is further transported to water bodies (Huang & Shenker 2004) and then irreversibly lost to the sea, affecting the P cycle globally (Rittmann et al. 2011; März et al. 2014).

44 The fast rate of depletion of P mineral resources, which are located in only a few countries, is
45 leading to concerns about the impact of potential future scarcity of the resource on global markets
46 and food costs, so the focus is now turning to more effective use of P (Rittmann et al. 2011). This
47 change in focus is increasingly reorientating agricultural practices towards recycling P safely,
48 together with other macronutrients such as nitrogen, by managing organic residues such as manure
49 and dewatered sewage sludge. Ott and Rechberger (2012) show how critical P has become as a
50 resource, with e.g. only 1.2 kg P $year^{-1}$ per capita reaching the consumer from the 4.7 kg $year^{-1}$ per
51 capita imported to Europe. Management of this resource is of great relevance for the future food
52 supply and therefore recovering and recycling P would contribute to closing the P balance
53 regionally in Europe and worldwide, reducing the dependence on P mineral reserves (Schoumans
54 et al. 2015).

55 The collection and use of P-rich wastes is a suitable alternative for recycling P through the
56 agriculture sector. A large amount of P is collected in sewage sludge, since on average 98% of P
57 in the human diet is discharged to the sewage system as urine and faeces (Smil 2000). In a European
58 context, sewage sludge is widely reused for agricultural purposes. For example, in Norway 60% of
59 sewage sludge is used in agriculture (Hamilton et al. 2015). However, a precondition for efficient
60 replacement of mineral P fertiliser with P-rich wastes is high plant availability of the P in the
61 wastes. Different types of wastes have specific fertilisation effects associated with their chemical
62 properties (Bøen & Knapp 2013; Brod et al. 2015). In particular, sewage sludge produced by

63 chemical precipitation of P in sewage with aluminium (Al) and/or iron (Fe) salts often results in
64 sludge with a low P fertilisation effect and therefore most of the P it contains is stored in the soil
65 when applied (Frossard et al. 1996; Maguire et al. 2001; O'Connor et al. 2004; Krogstad et al.
66 2005; Plaza et al. 2007). The expansion of the biogas industry had broadened the options for
67 effective management of the P resource in biodegradable waste and sewage sludge, providing the
68 possibility to produce methane as an energy carrier and digestate for nutrient recycling. The biogas
69 process also stabilises the sewage sludge (odour reduction and hygienisation) and reduces its
70 volume. The processing of sludge can be continued after anaerobic digestion (AD) by post-
71 treatment of the anaerobic digestion residue (ADR) with slaked lime ($Ca(OH)_2$) to further stabilise
72 the substrate and facilitate further dewatering. Quicklime (CaO) can also be used, with the aim of
73 hygienisation in addition to stabilisation.

74 Sludge stabilisation treatments may influence the plant availability of P in Fe- and/or Al-
75 precipitated sludge. Therefore, exploring the effects of these post-treatments on P availability is of
76 great interest. Aerobic digestion studies have shown conclusively that the plant availability of P is
77 considerably influenced by the metabolic processes that solubilise P (Wild et al. 1997; Bachmann
78 et al. 2014; Christel et al. 2014; Hupfauf et al. 2015). For example, Bachmann et al. (2014)
79 demonstrated that the performance of soil microorganisms in remobilising P is influenced when
80 ADR is used for maize production. However, those studies did not consider the effects of Fe and
81 Al precipitation of the sewage sludge. Studies on the behaviour of soluble P in anaerobically

digested Fe- and Al- precipitated sewage sludge are limited (Kahiluoto et al. 2015). The reduction of Fe^{3+} during AD could release adsorbed phosphates. However, simultaneous P re-precipitation (with Fe^{2+}) could decrease the solubility of the nutrient in the digestate through formation of secondary minerals (e.g. as vivianite with Fe^{2+}), as shown by Cheng et al. (2015). Similarly, Kahiluoto et al. (2015) found that AD of Fe-precipitated sludge reduced the plant availability of P. However, there is a knowledge gap concerning the role of such reduction processes in AD for Al-bound P. Any re-precipitation and/or adsorption of P during or after AD could proceed differently for Fe- and Al-precipitated sludge. For example, Fe precipitation is frequently well described by Langmuir isotherms, whereas Al precipitation follows Freundlich adsorption pathways (Bratby 2006). For that reason, post-treatments such as liming could be expected to release the P from Fe- and Al-precipitated sludge, whether anaerobically digested or not, in different ways.

Liming of sewage sludge is commonly used in the Norwegian WW industry as a treatment for stabilisation or sanitisation of the sludge. Liming the sludge also gives a porous structure, improving the separation between liquid and solid in further processing of the digestate (Deneux-Mustin et al. 2001). Such treatment can increase P plant uptake, as indicated in studies by Illmer (1995) and Schinner and Illmer et al. (1995), Krogstad et al. (2005) and Øgaard and Brod (2016). However, knowledge about the effect on P availability of liming of Fe- and Al-precipitated sludge

100 is lacking. Moreover, the effect of combined AD and Fe/Al precipitation of sludge, with liming as
101 a post-treatment step before dewatering, is unknown.

102 The aim of this study was thus to compare the effects of AD and liming, both separately and in
103 combination, on P plant availability in Fe- and Al-precipitated sludge. The stabilisation treatments
104 carried out were thermophilic AD in a semi-pilot scale digester and liming with two products (CaO
105 and $Ca(OH)_2$). The different sludges were characterised by sequential extraction of P and, in
106 addition, the plant availability of P was evaluated in a greenhouse experiment with barley
107 (*Hordeum vulgare L.*) as a crop.

108

109 2. Materials and Methods

110 2.1 Sludges

111 The substrates, which are referred to hereafter as untreated Fe- or Al-precipitated sludges or 'UT',
112 were sampled on March 2014 at two WW treatment plants (WWTPs) FREVAR KF (FRE) and
113 Ullensaker Gardermoen (ULL). The streams considered were sewage sludge chemically
114 precipitated with iron chloride ($FeCl_3$) at FRE and sewage sludge chemically precipitated with
115 aluminium sulphate ($Al_2(SO_4)_3$) at ULL. Both streams were thickened in the WWTPs to increase
116 their dry matter (DM) content prior to sampling. Both streams were sampled at the inlet of the
117 thermophilic biogas process (60°C for FRE and 55°C for ULL) coupled to the WWTP. The samples
118 were stored at 4°C until analysis of their physicochemical parameters. The UT sludges were

119 analysed using standard methods for analysis of water and WW, as shown in Table 1 (APHA 2012).

120 An overview of the subsequent post-treatments is shown in Fig. 1.

121 Table 1: Physicochemical parameters of the primary untreated sludges (UT) at the FRE and ULL
122 wastewater treatment plants

Parameter	FRE	ULL
Total dry solids (TS, %)	9.5 ± 0.06	5.9 ± 0.04
Volatile solids (VS, % of TS)	71 ± 0.65	72 ± 0.45
pH (25°C)	6.2 ± 0.2	5.9 ± 0.2
Conductivity (mS cm^{-1})	9.64 ± 0.02	4.53 ± 0.02
	g kg^{-1} TS	
Fe	115 ± 0.1	7.5 ± 0.1
Al	11 ± 0.1	60 ± 0.1
Ca	9.6 ± 0.08	5.9 ± 0.2
K	5.5 ± 0.1	3.5 ± 0.1
Na	3.8 ± 0.03	0.91 ± 0.01
Mg	1.9 ± 0.1	2 ± 0.1
P_{total}	8.8 ± 0.1	12 ± 0.1
P_{org}*	0.6 ± 0.14	1.9 ± 0.1
N	14 ± 0.1	24 ± 0.1
Cr	0.05 ± 0.002	0.022 ± 0.001
Cu	0.074 ± 0.0008	0.076 ± 0.0008
Mn	0.079 ± 0.0007	0.15 ± 0.0002
Ni	0.014 ± 0.002	0.013 ± 0.001
Cd	0.0004 ± 6e-5	0.0005 ± 6e-5
Pb	0.013 ± 0.001	0.035 ± 0.0002
Zn	0.25 ± 0.01	0.24 ± 0.01

123 *Organic P

124

125

126

127

128

129

130

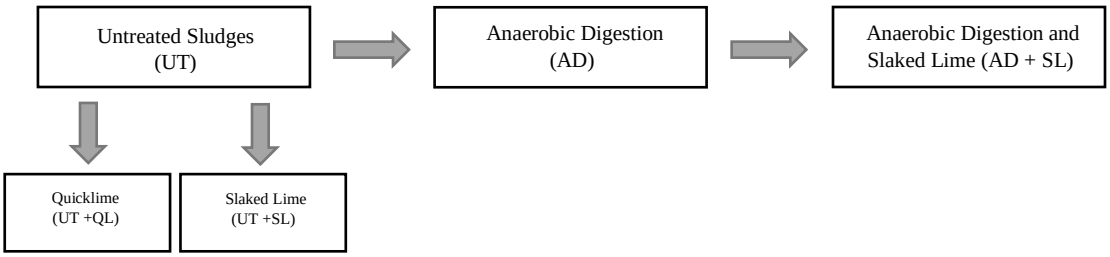

Figure 1: Sequence of treatments of the untreated metal-precipitated sludges. UT = untreated sludge, AD = anaerobic digestion, SL = slaked lime, QL = quicklime.

2.2 Anaerobic Digestion Treatment

Two 25-L continuous stirring tank reactor (CSTR) systems were used for AD of each sludge (Fe- or Al-precipitated). The inoculum used in the reactors was collected along with the samples from the FRE and ULL WWTPs and stored at 37°C for 2 days before being added to the CSTR reactors.

The start-up procedure for the AD process was as described by Estevez et al. (2014). In the start-up phase, 9 L of each inoculum were added and diluted with water to 15 L (nominal working volume) and stirred at 20 rpm. Only one hydraulic retention time (HRT) was considered for AD treatment of the UT sludges. The operating temperature for the whole AD treatment was 60°C for FRE and 55°C for ULL (the same temperature as used at the respective WWTPs). Gas chromatography was used to monitor the composition of the biogas. Some physicochemical parameters of the ADRs are presented in Table 2.

153 Table 2: Physicochemical parameters of the anaerobic digestion residues (ADR, from two reactors)
154 of sewage sludge from the FRE and ULL wastewater treatment plants after one hydraulic retention
155 time (HRT)

Parameter	FRE-1	FRE-2	ULL-1	ULL-2
Total dry solids (TS, %)	4.48 ± 0.06	4.54 ± 0.05	3.00 ± 0.04	2.90 ± 0.06
pH (25°C)	8.01 ± 0.2	7.93 ± 0.1	7.97 ± 0.2	7.89 ± 0.2
P_{total} (g kg^{-1} TS)	15.2 ± 0.05	n.d.	21.8 ± 0.88	n.d.
P_{org} (g kg^{-1} TS)	2.1 ± 0.2	n.d.	3.4 ± 0.6	n.d.
$N\text{-}NH_4^+$ (mg L^{-1})	2210	2335	2545	2455

156 n.d. = not determined

157

158 2.3 Liming Treatment

159 Liming of the UT sludges and ADRs was performed according to the schedule in Fig. 1. Solid
160 $Ca(OH)_2$ was added to a final concentration of 26% (0.35 g $Ca(OH)_2$/g TS) in the UT sludge/ADR
161 and solid CaO was added to a final concentration of 27% (0.39 g CaO/g TS) only in the UT sludge.
162 Both lime types were of industrial reagent quality and were provided by the company Miljøkalk
163 AS, Norway.

164 The lime was dispersed at 100 rpm for 10 min in 800 mL of sludge/ADR by means of a Jar-test
165 device manufactured by Phipps & Bird™. The limed products were then decanted and dried at
166 105°C to constant weight.

167

168 2.4 Pot Experiment

169 A total of 10 different sludges were obtained from the treatments described above. The relative
170 plant availability of P in the sludges compared with that in mineral P fertiliser (MinP) was studied
171 in a pot experiment with barley (*Hordeum vulgare* L. cv. Heder) as the reference crop.

This pot experiment was conducted using 3-L pots filled with 3.65 kg DM of a 'soil' consisting of a limed mixture of nutrient-deficient sand and 4 weight-% sphagnum peat. The soil had a very low content of plant-available P, 11 mg P kg^{-1} measured by the ammonium lactate-extractable P method (P-AL, (Egnér et al. 1960)) and consisted of 1% clay, 2% silt and 97% sand. Sludge dose was calculated based on total P content and amounted to 90 mg P pot^{-1}, equivalent to 60 kg P ha^{-1} (assuming 20 cm topsoil depth). The P fertilisation effect of the sludges was compared with that of a treatment providing no P fertiliser and with MinP in control treatments that received $Ca(H_2PO_4)_2$ at a rate of 45 and 90 mg P pot^{-1}, equivalent to 30 and 60 kg P ha^{-1}. All other nutrients were applied in amounts regarded as sufficient for ensuring that only P would be the limiting nutrient for plant growth. Nitrogen (N) was applied as $Ca(NO_3)_2$ (300 mg N pot^{-1}), potassium (K) as K_2SO_4 (300 mg K pot^{-1}) and magnesium (Mg) as $MgSO_4$ (37.5 mg Mg pot^{-1}). In addition, micronutrients (Fe, manganese (Mn), copper (Cu), molybdenum (Mo), boron (B) and zinc (Zn) were added in solution. The controls had two pH levels (6.5 and 6.9), to account for a possible effect of pH on P uptake, whereas the sample pots had only one initial pH level (6.5). The pH was adjusted by means of reagent-grade solid calcium carbonate ($CaCO_3$) for all pots, using 0.3 g $CaCO_3$ per kg soil mixture for the pH 6.5 pots and 0.8 g $CaCO_3$ per kg soil mixture for the pH 6.9 pots. There were three replicates per treatment.

The relative P fertilisation effect, or relative agronomic efficiency (RAE), for the treatments of the sludges was calculated as:

$$\%\ \text{Relative P fertilisation effect} = \frac{P_{uptake} - P_{uptake\ (control\ 0\ mg\ P\ per\ pot)}}{P_{\ uptake\ (control\ 90\ mg\ P\ per\ pot)} - P_{uptake\ (control\ 0\ mg\ P\ per\ pot)}} X100 \quad (1)$$

The sand and peat mixture was mixed homogeneously with the sludges, except for a top layer of approximately 2.5 cm without sludge to avoid negative effects of the sludge on germination. Holes (1 cm depth) were made in the soil and 18 seeds of barley were sown. The number of plants was adjusted to 15 after germination.

Deionised water was applied three times a week to about 60% of water-holding capacity. Light was provided by 400 W fluorescent lamps (model Osram Powerstar HQI-BT®). The photosynthetic flux in the room was 200 µmol m^{-2} s^{-1} at plant height, with a 16 h/8 h light/dark cycle. Heating was provided if the temperature dropped below 18°C during the light period and 15°C during darkness. The average air temperature oscillated between 14.5 and 22°C, with an average temperature during the whole experiment of 18°C. The plants were harvested approximately 7 weeks after sowing, when they were at start of heading. The plants were cut roughly 2.5 cm above the soil surface, stored in a paper bag per pot and dried at 60°C to constant weight.

2.5 Analytical Methods

2.5.1 Biogas treatment control

Biogas production was controlled by continuously measuring biogas composition, pH, ammonium (NH_4^+) concentration, alkalinity (total inorganic carbon (TAC) as mg L^{-1} $CaCO_3$) and volatile organic acids (FOS) as mg L^{-1} of acetic acid in the ADR. The TAC and FOS values were

210 determined by means of a TitroLine® 6000 basic titration unit with a magnetic stirrer TM 235
211 produced by SI Analytics GmbH. The titration was controlled by a pH combination electrode A
212 7780 1M-DIN-ID. The pH of the ADR was measured with a Thermo Orion pH meter model Dual
213 Star. The TS and VS concentrations were determined by a gravimetric method at 105°C and 550°C,
214 respectively, at constant weight. The NH_4^+ concentration was determined by the ion selective
215 electrode (ISE) method using a Thermo Scientific Orion electrode model 9512HPBNWP
216 connected to a Thermo Orion Dual Star device.
217
218 The four CSTRs (FRE-1, FRE-2, ULL-1, ULL-2) were connected to a gas chromatographer (GC)
219 model 8610C in order to continuously monitor the biogas composition (concentrations of methane
220 (CH_4) and carbon dioxide (CO_2)) from the start-up phase until the end of the HRT period for each
221 reactor. The GC was equipped with a thermal conductivity detector and a 2 m Haysep-D column.
222 Chromatography, data acquisition and integration were performed using the PeakSimple 3.88
223 software for Windows. The injector, detector and column were operated at 41, 153 and 81 °C,
224 respectively. Helium was used as a carrier gas, at 20 mL min^{-1}. A standard gas mixture (CH_4/CO_2)
225 at 65/35% was used for calibration of the GC.

226 2.5.2 Sludge analyses
227 All the substrates obtained from the processes illustrated in Fig. 1 were sequentially extracted
228 using a modified Hedley fractionation of P for manure and compost (Hedley et al. 1982; Sharpley

& Moyer 2000). The fractionation scheme consisted of five fractions obtained by extraction of 1 g of dried substrate with 200 mL of deionised water for 1 h, followed by 200 mL of 0.5 M $NaHCO_3$ (P-labile), 0.1 M NaOH (P-Al/Fe) and 1 M HCl (stable Ca-P), each for 16 h. Residual P was determined following digestion with ultrapure and concentrated HNO_3 and HCl in a high performance microwave reactor (HPMR) (model IV, MLS GmbH) for 4 h at 260°C and 50 bar. All the extracts except residual P were filtered through 0.45 µm membranes and the ortho-P in the filtrate was analysed by colorimetry using the molybdenum blue method in a Stasar II Gitford Instrument® spectrophotometer at 882 nm (Murphy & Riley 1962). The P_{total} concentration in the filtered extracts and in the residues of the fractionation was analysed using an inductively coupled plasma (ICP) optical emission spectrometer (OES) (Perkin-Elmer model 5300 DV). The Fe, Al, Ca and Mg concentrations in the filtrates and residues were determined by ICP-OES.

The total P (P_{total}), Fe, Al, Ca, K, Na and Mg and heavy metals Cr, Cu, Mn, Ni, Cd, Pb and Zn concentrations in all the dry sludges were determined by microwave digestion and ICP-OES as described in the previous paragraph for the residues of the fractionation. Organic P (P_{org}) was estimated by solubilising the inorganic P with 12 N H_2SO_4 in a water bath at 70°C for 10 min and subtracting the value from P_{total} (Møberg & Petersen 1982).

2.5.3 Plant and soil analyses

The dried plants from each pot were milled (Laboratory Mill 3100, Perten Instruments), mesh size 0.5 mm) and digested with ultrapure and concentrated HNO_3 at 260°C and 50 bar in the HPMR.

The P_{total} and heavy metal concentrations (Cr, Cu, Mn, Ni, Cd, Pb and Zn) were analysed by ICP mass spectrometry (MS) model Agilent Tech. 8800 Triple Squad. In addition, total N was determined by means of infrared spectroscopy in a LECO TruSpec® CHN device in the milled samples. After completion of the pot experiment, soil samples were analysed for pH (ISO 2015) and P-AL (Egnér et al. 1960). Uptake of P (mg pot^{-1}) in aboveground biomass was computed by multiplying P concentration by aboveground DM yield.

2.6 Statistical methods

In the AD treatment, two replicates per UT sludge were used in the reactors. Three replicates were used for the fertiliser, plant and soil analyses, with the inclusion of the standard deviation for quality assurance of the data. Analysis of variance (ANOVA) was performed to study the effect of the sludges on plant P uptake. To perform multiple comparisons, the Tukey's honest significant difference (HSD) multiple comparison test was used ($\alpha = 0.05$).

3. Results and Discussions

3.1 Anaerobic Digestion Treatment

From the control parameters (pH, FOS, TAC, etc.), it was possible to ensure that the biogas process was running effectively throughout the start-up phase and the HRT (Figs. 2 (a) and (b)). The HRT started on 13 April 2014 for FRE-1, FRE-2 and ULL-1. The case of ULL-2 was slightly different due to low pH values and high FOS/TAC ratio (Fig. 3). A very high content of FOS and production of volatile fatty acids in the ADR decreased the pH to 6.5 and thus the biogas process was inhibited

(Yuan & Zhu 2016). The start-up process stabilised after the 16th of April and the first feeding of the HRT was made on 24th of April. The process was considered under control for pH values in the ADR of between 7.5 and 8 (25°C) and a FOS/TAC ratio below 2 (Drosg 2013).

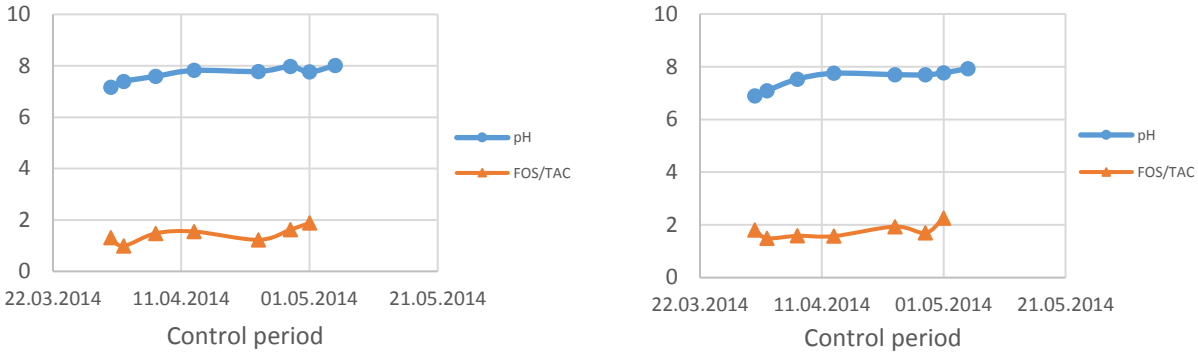

Figure 2: Measured pH and FOS/TAC ratio of the anaerobic digestion residue (ADR) for the biogas reactors (a) FRE-1 and (b) FRE-2 during the start-up and HRT periods.

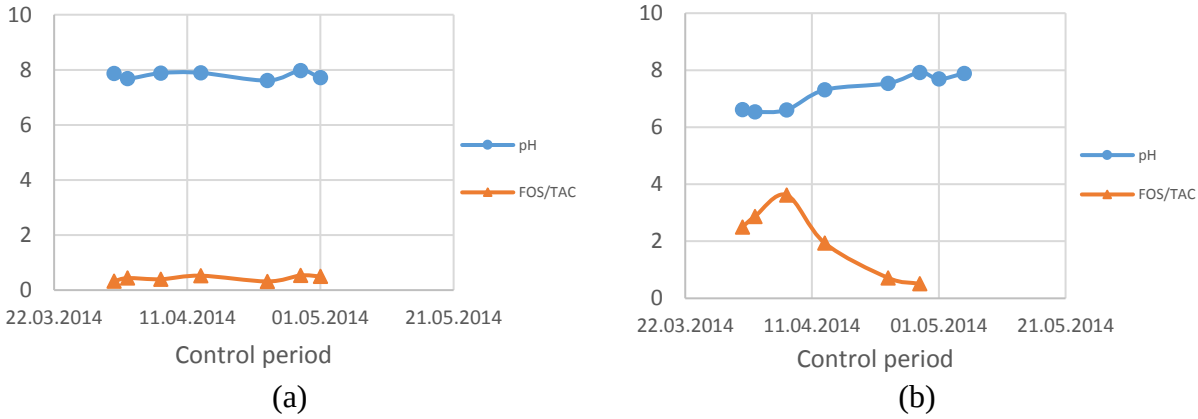

Figure 3: Measured pH and FOS/TAC ratio of the anaerobic digestion residue (ADR) for the biogas reactors (a) ULL-1 and (b) ULL-2 during the start-up and HRT periods.

The normalised biogas CH_4 concentration (% by weight) was determined daily as an additional control of the HRT for all reactors (Figs. 4 (a) and (b)). The lower CH_4 concentration for ULL

compared with FRE is most likely attributable to the degradation of organic compounds in a biological treatment step in ULL prior to the chemical precipitation, whereas FRE has no such biological step. ULL therefore had a lower VS content than FRE.

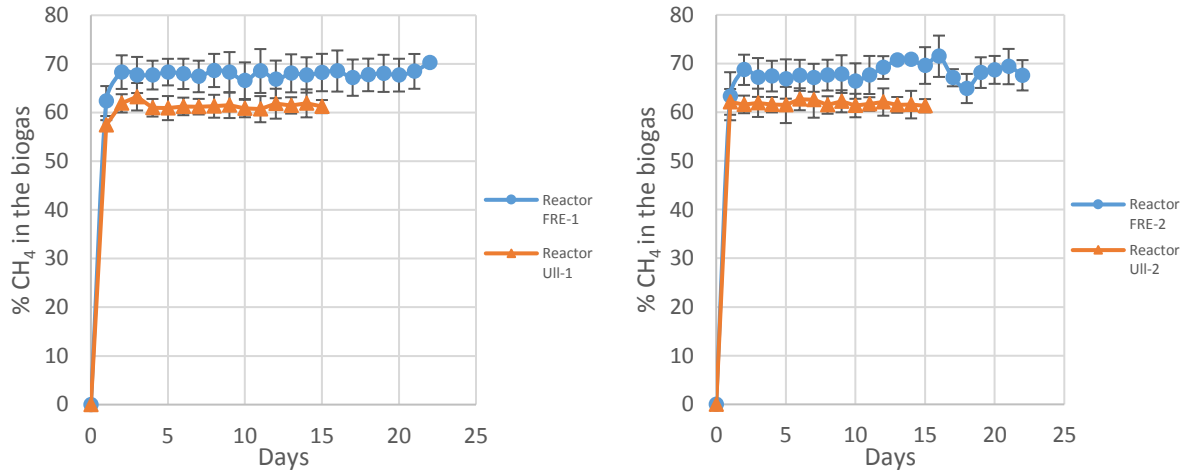

Figure 4: Daily normalised CH_4 concentration (% by weight) in the biogas from reactors (a) FRE-1 and ULL-1 and (b) FRE-2 and ULL-2. The HRT was 22 days for FRE-1 and FRE-2 and 15 days for ULL-1 and ULL-2.

3.2 Anaerobic Digestion and Lime Treatment Effect on Plant-Available P

The effect of AD and liming on plant availability of P was studied with two approaches. The first involved chemical characterisation of the different sludges (untreated and treated) with a modified scheme for sequential P extraction, while the second involved a growth experiment with barley.

3.2.1 *Sequential P extraction*

By the sequential extraction of P, the distribution of P in pools of different solubility could be studied.

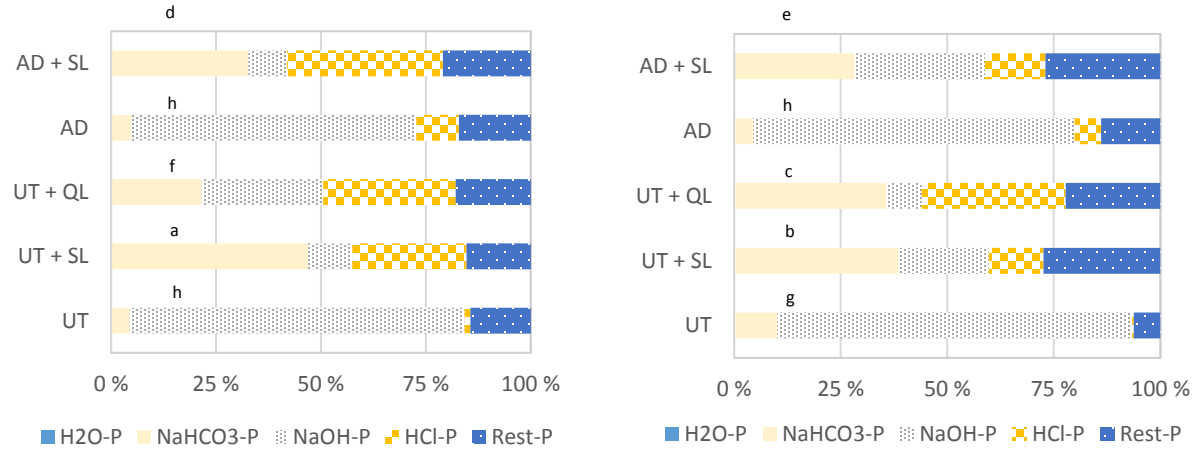

(a) (b)

297

298 Figure 5: Distribution of total P (P_{total}) into different P fractions for the (a) FRE and (b) ULL
299 untreated and treated sludges. UT – untreated raw sludge, AD = anaerobic digestion, SL = slaked
300 lime ($Ca(OH)_2$), QL = quicklime (CaO). Different lower case letters above bars indicate significant
301 differences (p<0.05) between FRE and ULL and their treatments for the $NaHCO_3$-P fraction.

302

303

304 As can be seen from Figs. 5 (a) and (b), there was a very low H_2O-P (loosely bound P) concentration

305 in all untreated and treated sludges. Both the untreated sludges and the non-limed AD sludges also

306 contained a considerable low P-labile fraction ($NaHCO_3$-P). The effect of AD treatment was not

307 significant for this P fraction. Moreover, the P-Fe/Al (NaOH-P) fraction was the highest for both

308 of these substrates.

309 The liming treatment (both slaked lime and quicklime) had a positive effect in increasing the P-

310 labile fraction significantly. However, this positive impact on P availability was significantly

311 higher for slaked lime than for quicklime. This difference was more pronounced for the FRE

312 sludges than the ULL sludges, with slaked lime increasing the P-labile fraction in FRE sludges by
313 more than twice as much as quicklime.

314 3.2.2 *Growth experiment*

315 Phosphorus uptake at the two pH levels tested in the control treatments was similar, and therefore
316 only the results for the lowest pH level (pH 6.5) are shown. The P uptake by barley in all treatments
317 is shown in Figs. 6 (a) and (b).

318

319

320

321

322

323

324

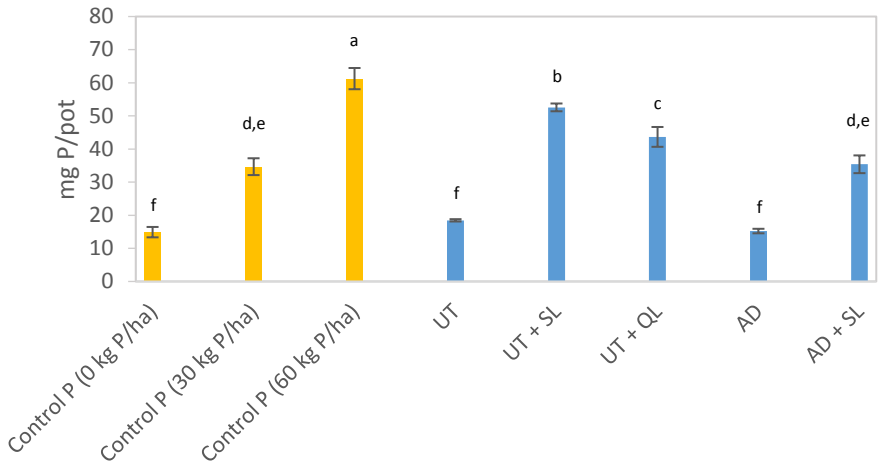

(a)

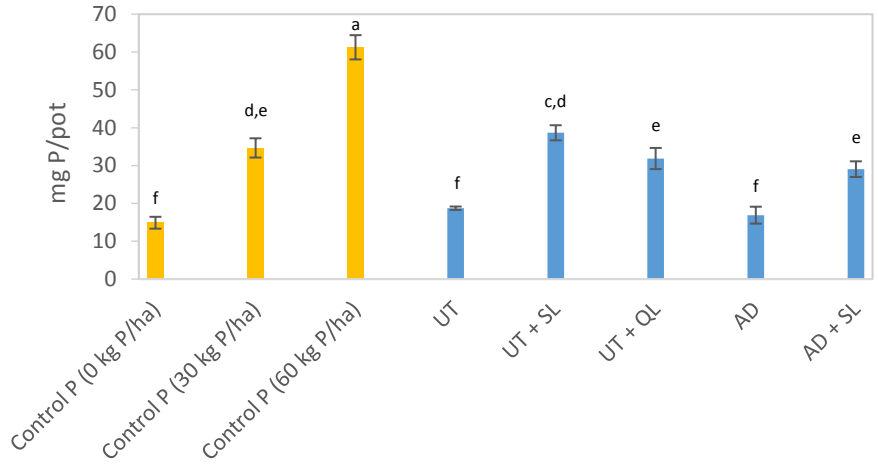

(b)

Figure 6: Average P plant uptake per pot for the (a) FRE and (b) ULL untreated and treated sludges. UT = raw sludge, AD = anaerobic digestion, SL = slaked lime ($Ca(OH)_2$), QL = quicklime (CaO). Different letters above the bars indicate significant differences (p<0.05) between FRE and ULL and their treatments.

A poor effect on P uptake was achieved from AD without liming. Plant uptake of P in that treatment was not significantly different from that in the untreated sludge and the control (receiving 0 kg P

333 ha^{-1}). The P plant uptake results confirmed the findings from the P-fractionation analysis that the

334 liming treatments gave the highest availability of P (see Fig. 6). Moreover, the $NaHCO_3$-P

335 fractionation gave similar results, with a close correlation with plant P uptake for both FRE and

336 ULL untreated and treated sludges (Figs. 7 (a) and (b)).

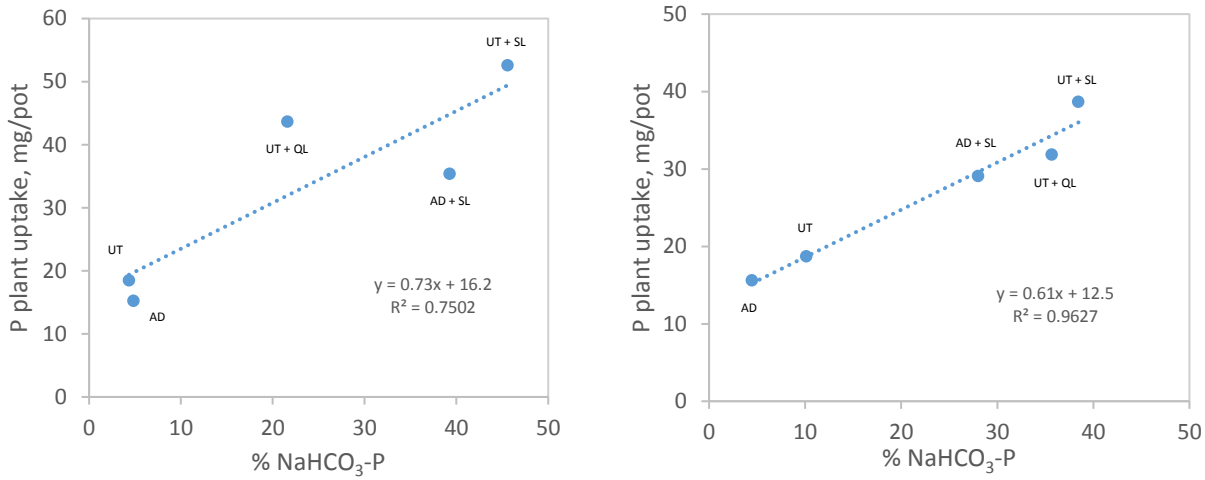

337

338 Figure 7: Correlation between plant P uptake and the $NaHCO_3$-P fraction in sequential extraction
339 for (a) FRE and (b) ULL untreated and treated sludges.

340

341 The highest P plant uptake occurred with slaked lime treatment of the UT sludges, and these values

342 were significantly higher than those obtained by slaked lime treatment of AD sludges (Fig. 6).

343 There is thus a negative effect of AD on comparing with the slaked lime treatment of UT (UT+

344 SL). Moreover, plant P uptake was significantly higher (1.2-fold) for slaked lime treatment of UT

345 than for quicklime treatment of the UT substrates from both FRE and ULL. The P fractionation of

346 the fertilisers showed a similar trend for ULL (with 1.08-fold higher P uptake for SL liming), as

347 seen from Fig. 7.

Relative agronomic efficiency, or the relative P fertilisation effect compared with MinP, was markedly low for the AD treatment, only 0.7% for FRE and 4.3% for ULL (Table 3). Therefore AD had scarcely any P fertiliser effect. In contrast, liming increased the RAE values substantially. The highest RAE (81.3 %) was obtained by Fe precipitation and liming (UT + SL).

Table 3: Relative agronomic efficiency (RAE) of P fertilisation for the primary precipitated untreated sludges (UT) from the FRE and ULL wastewater treatment plants and their treatments. UT = raw sludge, AD = anaerobic digestion, SL = slaked lime ($Ca(OH)_2$), QL = quicklime (CaO)

	RAE (%)	
Treatment	FRE	ULL
UT	7.7	8.2
UT + SL	81.3	51.3
UT + QL	62	36.6
AD	0.7	4.3
AD + SL	44.2	30.6

3.3 Effects of Liming of Fe- and Al-precipitated Sludge on Plant-available P

Liming of sludge led to increased concentrations of P-labile and Ca-P and a reduced concentration of P-Fe/Al, as shown by the sequential P fractionation. This improved the plant availability of P and plant P uptake compared with unlimed sludges, where the majority of the P was bound to Fe or Al. This can be explained by the increased pH value in limed sludge being reflected in the fertilised soil (Table 4). As a result, Fe/Al (hydr)oxides were less positively charged and the solubility of P-Fe/Al increased with increasing pH (Lindsay 1979). Simultaneously, the Ca concentration was raised by liming, resulting in a shift of Fe-/Al-bound P to Ca-bound P in the

sludges. This Ca-bound P was most likely a non-crystalline type of Ca phosphate in the sludges (Øgaard & Brod 2016). However, Al hydrolysis products have previously been reported to desorb P at a lower rate than Fe hydrolysis products as the pH increases following liming (Haynes 1982; Singh et al. 2005; Achat et al. 2016).

Table 4: Soil pH value after seven weeks of the pot experiment. UT = raw sludge, AD = anaerobic digestion, SL = slaked lime ($Ca(OH)_2$), QL = quicklime (CaO)

Fertiliser	Soil pH at the end of the pot experiment
FRE	
Raw sludge (UT)	6.1 ± 0.06
UT + SL	8.2 ± 0.05
UT + QL	8.3 ± 0.06
AD	5.8 ± 0.04
AD + SL	7.3 ± 0.03
ULL	
Raw sludge (UT)	6.1 ± 0.05
UT + SL	7.6 ± 0.06
UT + QL	8.4 ± 0.03
AD	5.8 ± 0.04
AD + SL	7.1 ± 0.02

For soils, Achat et al. (2016) have found that the concentration of phosphate ions in the soil solution had a stronger negative correlation with Al than with Fe extracted with ammonium oxalate (correlation coefficient = -0.42 and -0.17, respectively; $p<0.05$). In similar findings by Singh et al. (2005), the corresponding correlation coefficients were -0.68 ($p<0.05$) and -0.49 (non-significant) for Al and Fe, respectively. Thus from a chemical extraction point of view, the P binding is most likely stronger for Al- than for Fe-oxides. This is explained by lower solubility of Al-phosphate

than Fe-phosphate, and thus stronger and more stable binding with Al (Lindsay 1979; Øgaard & Brod 2016).

3.4 Treatment Scheme Suggestions for Sludge

Anaerobic digestion is a treatment needed in order to recycle energy and nutrients contained in the sewage sludge at WWTPs. Anaerobic digestion can mineralise organic P, but if the concentration of Fe^{3+} or Al^{3+} is high in the inlet stream of the biogas plant, P released by mineralisation will be adsorbed to Fe/Al. Further post-AD treatment, such as liming, is required for Fe-/Al-precipitated sludge in order to significantly improve P recycling. In the present study, liming increased P availability to a greater extent for Fe-precipitated sludge than for Al-precipitated sludge. This suggests that a combined treatment scheme comprising Fe precipitation of sludge, AD and liming is the optimal approach for maximising energy and P recycling.

Conclusions

- Liming with both slaked lime and quicklime increased P uptake in barley, particularly for Fe-precipitated sludge.

- Liming with slaked lime was more effective than liming with quicklime in increasing plant P uptake, for both Fe- and Al-precipitated sludges.

- Anaerobic digestion in combination with liming had a negative effect on P availability for both Fe- and Al-precipitated sludges, whereas anaerobic digestion without a liming post-treatment had no significant effect on P availability.

Acknowledgments

This work was part of the research project 'Biosolids in Food Production – Phosphorus Recycling and Food Safety', which was funded by the Research Council of Norway (Grant No. 207811) and industry partners.

415 References

416 Achat D.L., Pousse N., Nicolas M., Brédoire F., Augusto L. 2016 Soil properties controlling
417 inorganic phosphorus availability: general results from a national forest network and a
418 global compilation of the literature. *Biogeochemistry*, **127**, pp.255–272.

419 APHA 2012 *Standard Methods for the Examination of Water and Wastewater* 22nd ed. American
420 Public Health Association/American Water Works Association/Water Environment
421 Federation, Washington DC, USA.

422 Bachmann S., Gropp M. & Eichler-Löbermann B. 2014 Phosphorus availability and soil
423 microbial activity in a 3 year field experiment amended with digested dairy slurry. *Biomass*
424 *and Bioenergy*, **70**, pp.429–439.

425 Bratby J. 2006 Colloids and interfaces. In -, ed. *Coagulation and Flocculation in Water and*
426 *Wastewater Treatment*. IWA Publishing, London, UK., pp. 14–17.

427 Brod E., Øgaard A.F., Hansen E., Wragg D., Haraldsen T.K. & Krogstad T. 2015 Waste products
428 as alternative phosphorus fertilisers part I: inorganic P species affect fertilisation effects
429 depending on soil pH. *Nutrient Cycling in Agroecosystems*. Available at:
430 http://link.springer.com/10.1007/s10705-015-9734-1.

431 Bøen A. & Haraldsen T.K. 2013 Meat and bone meal and biosolids as slow-release phosphorus
432 fertilizers, *Agricultural and Food Sci.*, **22**, pp.235–246.

433 Cheng X., Chen B., Cui Y., Sun D. & Wang X. 2015 Iron(III) reduction-induced phosphate
434 precipitation during anaerobic digestion of waste activated sludge. *Separation and*
435 *Purification Technology*, **143**, pp.6–11.

436 Christel W., Bruun S., Magid J. & Jensen L.S. 2014 Phosphorus availability from the solid
437 fraction of pig slurry is altered by composting or thermal treatment. *Bioresource technology*,
438 **169**, pp.543–51.

439 Cordell D. & Neset T.S.S. 2014 Phosphorus vulnerability: A qualitative framework for assessing
440 the vulnerability of national and regional food systems to the multi-dimensional stressors of
441 phosphorus scarcity. *Global Environmental Change*, **24**(1), pp.108–122.

442 Deneux-Mustin S., Lartiges B.S., Villemin G., Thomas F., Yvon J., Bersillon J.L. & Snidaro D.
443 2001 Ferric chloride and lime conditioning of activated sludges: An electron microscopic
444 study on resin-embedded samples. *Water Research*, **35**(12), pp.3018–3024.

445 Drosg B. 2013 *Process monitoring in biogas plants*, Available at: http://www.iea-
446 biogas.net/files/daten-redaktion/download/Technical Brochures/Technical Brochure
447 process_montoring.pdf.

448 Egnér H., Riehm H. & Domingo W.R. 1960 Untersuchungen über die chemische Bodenanalyse
449 als Grundlage für die Beurteilung des Nährstoffzustandes der Böden. II. Chemische
450 Extraktionsmethoden zur Phosphor- und Kaliumbestimmung. *Kungliga*
451 *Lantbrukshögskolans annaler*, **26**, pp.199–215.

452 Estevez M.M., Sapci Z., Linjordet R., Schnürer A. & Morken J. 2014 Semi-continuous anaerobic
453 co-digestion of cow manure and steam-exploded Salix with recirculation of liquid digestate.
454 *Journal of Environmental Management*, **136**, pp.9–15.

Frossard E., Sinaj S., Zhang L.-M., & Morel J.L. 1996 The Fate of Sludge Phosphorus in Soil-Plant Systems. *Soil Science Society of America Journal*, **60**(4), p.1248.

Hamilton H.A., Brod E., Hanserud O.S., Gracey E.O., Vestrum M.I., Bøen A., Steinhoff F.S., Müller D.B., Brattebø H. 2015 Investigating Cross-Sectoral Synergies through Integrated Aquaculture, Fisheries and Agriculture Phosphorus Assessments. *Journal of Industrial Ecology*.

Haynes R.J. 1982 Effects of liming on phosphate availability in acid soils - A critical review. *Plant and Soil*, **68**(3), pp.289–308.

Hedley M.J., Stewart J.W.B. & Chauhan B.S. 1982 Changes in Inorganic and Organic Soil Phosphorus Fractions Induced by Cultivation Practices and by Laboratory Incubations. *Soil Science Society of America Journal*, **46**, pp.970–976.

Huang X.-L. & Shenker M. 2004 Water-soluble and solid-state speciation of phosphorus in stabilized sewage sludge. *Journal of environmental quality*, **33**(5), pp.1895–1903.

Hupfauf S., Bachmann S., Fernández-Delgado Juárez M., Insam H. & Eichler-Löbermann B. 2015 Biogas digestates affect crop P uptake and soil microbial community composition. *Science of The Total Environment*, **542**(B), pp.1144–1154.

Illmer P., Barbato A. & Schinner F. 1995 Solubilization of hardly-soluble AlPO4 with P-solubilizing microorganisms. *Soil Biology and Biochemistry*, **27**(3), pp.265–270.

Illmer P. & Schinner F. 1995 Solubilization of inorganic calcium phosphates - Solubilization mechanisms. *Soil Biology and Biochemistry*, **27**(3), pp.257–263.

International Organization for Standardization, 2015. ISO 10390:2005 Soil quality -- Determination of pH. Available at: http://www.iso.org/iso/catalogue_detail.htm?csnumber=40879.

Kahiluoto H., Kuisma M., Ketoja E., Salo T. & Heikkinen J. 2015 Phosphorus in Manure and Sewage Sludge More Recyclable than in Soluble Inorganic Fertilizer. *Environmental Science & Technology*, **49**, 2115−2122.

Krogstad T., Sogn, T., Asdal Å.& Sæbø A. 2005 Influence of chemically and biologically stabilized sewage sludge on plant-available phosphorous in soil. *Ecological Engineering*, **25**(1), pp.51–60.

Lindsay W.L. 1979 *Chemical equilibria in soils*, New York: John Wiley & Sons.

Maguire R.O., Sims J.T., Dentel S.K., Coale F.J.& Mah J.T. 2001 Relationships between biosolids treatment process and soil phosphorus availability. *Journal of environmental quality*, **30**(3), pp.1023–1033.

Murphy J. & Riley J.P. 1962 A Single Solution Method for the Determination of Phosphate in in Natural Waters. *Analytica Chimica Acta*, **27**, pp.31–36.

März, C., Poulton S.W., Wagner T., Schnetger B., & Brumsack H.-J. et al., 2014 Phosphorus burial and diagenesis in the central Bering Sea (Bowers Ridge, IODP Site U1341): Perspectives on the marine P cycle. *Chemical Geology*, **363**, pp.270–282.

Møberg, P. & Petersen L. 1982 Øvelsesvejledning til geologi og jordbundslære. Part 2 (in

494 Danish). *Den Kongelige Veterinær-og Landbohøyskole, København*, p.136.

495 O'Connor G., Sarkar D., Brinton S.R., Elliott H.A. & Martin F.G. 2004 Phytoavailability of
496 biosolids phosphorus. *Journal of environmental quality*, **33**(2), pp.703–712.

497 Ott C. & Rechberger H. 2012 The European phosphorus balance. *Resources, Conservation and*
498 *Recycling*, **60**, pp.159–172. Available at: http://dx.doi.org/10.1016/j.resconrec.2011.12.007.

499 Plaza C., Sanz R., Clemente C., Fernández J.M., González R., Polo A. & Colmenarejo M.F. 2007
500 Greenhouse evaluation of struvite and sludges from municipal wastewater treatment works
501 as phosphorus sources for plants. *Journal of Agricultural and Food Chemistry*, **55**(20),
502 pp.8206–8212.

503 Rittmann B.E., Mayer B., Westerhoff P. & Edwards M. 2011 Capturing the lost phosphorus.
504 *Chemosphere*, **84**(6), pp.846–853.

505 Schoumans O.F., Bouraoui F., Kabbe C., Oenema O. & van Dijk K.C. 2015 Phosphorus
506 management in Europe in a changing world. *Ambio*, **44**(S2), pp.180–192.

507 Sharpley A. & Moyer B. 2000 Phosphorus Forms in Manure and Compost and Their Release
508 during Simulated Rainfall. *Journal of Environmental Quality*, **29**(5), pp.1462–1469.

509 Singh B.R., Krogstad T., Shivay Y.S., Shivakumar B.G., Bakkegard M. 2005 Phosphorus
510 fractionation and sorption in P-enriched soils of Norway. *Nutrient Cycling in*
511 *Agroecosystems*, **73**(2-3), pp.245–256.

512 Smil V. 2000 PHOSPHORUS IN THE ENVIRONMENT : Natural Flows and Human
513 Interferences. *Annu. Rev. Energy Environ.*, **25**, pp.53–88.

514 Wild D., Kisliakova A. & Siegrist H. 1997 Prediction of recycle phosphorus loads from
515 anaerobic digestion. *Water Research*, **31**(9), pp.2300–2308.

516 Yuan H. & Zhu N. 2016 Progress in inhibition mechanisms and process control of intermediates
517 and by-products in sewage sludge anaerobic digestion. *Renewable and Sustainable Energy*
518 *Reviews*, **58**, pp.429–438.

519 Øgaard A.F. & Brod E. 2016. Efficient phosphorus cycling in food production – predicting the
520 phosphorus fertilization effect of sludge from chemical wastewater treatment. , **64**(24),
521 pp.4821–4829.

522

523

524

525

Paper IV

Hayrapetyan S., Alvarenga E., Hayrapetyan L., Gevorgyan S.A., Pirumyan G.P. and Salbu B. 2015 Manganese dioxide (MnO_2) – containing composite sorbents. *International Conference on Advanced Materials and Technologies–Proceedings*, pp. 249–253

MANGANESE DIOXIDE (MnO_2) - CONTAINING COMPOSITE SORBENTS

S.S. Hayrapetyan[1], E. Alvarenga[2], L.S. Hayrapetyan[1], S.A. Gevorgyan[1], G.P. Pirumyan[1] and B. Salbu[3]

[1]Yerevan State University, A. Manoukyan 1, 0025, Yerevan, Armenia
[2] NIBIO, Norwegian Institute of Bioeconomy Research,
Pb 115, N-1431, Ås, Norway
[3]Norwegian University of Life Sciences, Dep. of Environmental Sciences, P.O. Box 5003, N-1432 Ås, Norway
E-mail: [1]Scirec@mail.ru, [2]Emilio.Alvarenga@nibio.no and [3]Brit.Salbu@nmbu.no

ABSTRACT

The scanning electron microscopy (SEM), x-ray fluorescence spectrometry (XRF) and inductively coupled plasma mass spectrometry (ICP-MS) methods were used for investigation of manganese dioxide (MnO_2)–containing composite sorbents and their sorption properties were evaluated as well. A characterization of the sorbents was performed by SEM and XRF. Diatomite and silicagel were used as the porous carrier for the MnO_2 (which provides the functionality of the sorbents). The silica component was prepared by co-precipitation of water glass with manganese dioxide. Potassium permanganate was used as a source of manganese dioxide. Deposition of MnO_2 was carried on the pore surfaces of porous materials (silica, diatomite) by means of hydrogen peroxide and formaldehyde. The sorbent prepared under the previously described procedure was tested for compounds containing potassium (K^+).

Keywords: Sorbents, manganese dioxide, silica, diatomaceous earth.

INTRODUCTION

At the beginning MnO_2 were used for analytical purposes of sorption of alkali, alkaline earth, actinides and other metals and for nuclear waste systems treatment [1]. Basic research on the sorption of metal ions on manganese dioxide and selectivity, were published in the seventies of the last century [2]. Furthermore, such publications have been used and appeared later in the nineties of last century [3,4]. These studies have shown that the mixed $xMnO_2 \cdot ySiO_2$ oxide sorbents actively adsorb such cations in synthetic solutions at pH 4 and have an increased sorption capacity for strontium (Sr). The urgent need for the use of MnO_2–containing sorbents has not lose its relevance and the research continues for the application of such systems for the adsorption of radionuclides. Composites of manganese - titanium dioxide (MnO_2–TiO_2) show a high affinity for Sr and uranium (U) at pH 7.0 [5]. A α-MnO_2–containing sorbent is prepared with selective adsorption properties for K by thermal treatment of the mixture of Mn carbonate with the potassium (K) formate and/or

Mn carbonate with the K butoxide. This is the most acceptable commercial sorbent for separating K^+ [6] from water.

Hydrated MnO_2 is obtained by precipitation of permanganate by means of H_2O_2. The reaction is conducted in the presence of silica (SiO_2)–containing systems, for example, sodium silicate. Afterward, the precipitate was washed deionized water, dewatered by filtration and dried [3] .

MATERIALS AND METHODS

Liquid glass - $KMnO_4$ - H_2O_2 system

This reagent was prepared with 200 ml of water glass (390 g/l SiO_2, silicate modulus M = 3.0) and 35g $KMnO_4$. The mixture was diluted to 1200 ml with water and 350 ml H_2O_2 were added. Afterwards, the pH of the system was adjusted to pH 9.0 by means of phosphoric acid (H_3PO_4). The aging of the gel is carried out at room temperature for 40 hours, after which the resulting mixture is dried at 105 ^oC for 2-3 hours, after drying the dried gel is washed with water and dried again. Calcination was carried out at 500 °C for 1 hour. After that, the material was washed with a nitric acid solution (5-6%) and dried at 150 °C until constant weight. After grinding and sieving, the final product obtained is a sorbent.

Liquid glass - $KMnO_4$ – formaldehyde

The liquid glass is prepared from 2 solutions: 1st sol., 200 ml water glass (390 g/l, M = 3.0) was diluted with distilled water to 800 ml; 2nd sol., 50 g $KMnO_4$ were added to 48 ml of sulfuric acid (conc.) and the crystals were dissolved in the water. The final volume was adjusted to 500 ml with water. A colloidal system is obtained because of the mixing of the two solutions (the 1st sol. is added while stirring to the 2nd one). A further gelation of the system occurs when NaOH is added. Further post-treatment of the gel is carried out in accordance with the above-described scheme in sub-section 2.1.

The system SiO_2 -MnO_2 – diatomite system

The sorption process was carried out in dynamic mode configuration in columns with dimensions of 200x1.0mm at room temperature (20 ^0C). The substrates taken into account for this study were the following solutions: 1. KOH solution (concentration – 2 g/l); 2. KCl (concentration 2 g/l, pH 12,5 increased by means of KOH) and 3. CH_3COOK (concentration 1 g/l and 2 g/l, pH 11.5 increased by means of KOH).

RESULTS AND DISCUSSION

On the Figures 1, 3 and 5 and in the Tables 1, 2 and 3 are presented the SEM images and the XRF data of the obtained sorbents.

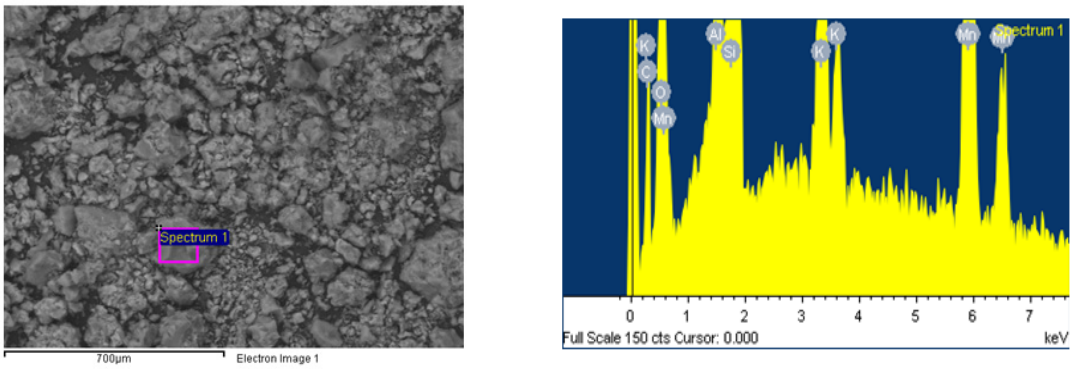

(a) (b)

Figure 1. (a) SEM image and (b) XRF spectrum of the sorbent $SiMnO_4$.

From these figures and tables, it follows that the resulting sorbents have a uniform structure and these materials contain MnO_2 in an amount of 3.34–7.40 wt.% of Mn. This amount of MnO_2 in the composition of the sorbent allows this system to be an effective sorbent (See below).

Table 1.XRF data of the sorbent $SiMnO_4$.

Element	Weight%	Atomic%	Weight%	Atomic%	Weight%	Atomic%	Average value Weight%
	Spectrum 1		Spectrum 2		Spectrum 3		
C	15.88	22.98	8.34	12.85	8.35	12.87	10.86
O	56.23	61.08	57.02	66.00	57.67	66.72	56.97
Al	1.29	0.83	4.89	3.35	5.34	3.66	3.84
Si	21.90	13.55	23.10	15.23	21.11	13.91	22.04
K	0.50	0.22	2.30	1.09	2.19	1.04	1.47
Mn	4.19	1.33	4.36	1.47	5.33	1.80	4.63
Totals	100.00		100.00		100.00		

Figure 2 shows the sorption curves of K^+ sorbent prepared in accordance with the scheme described in the previous section. From Figure 2, it follows that the resulting sorbent has a sorption capacity for K^+. In addition, the sorption capacity increases significantly after his regeneration. Regeneration was performed with 10 % nitric acid. The curves in Fig. 2 and in subsequent figures were built on the basis of data obtained by ICP-MS.

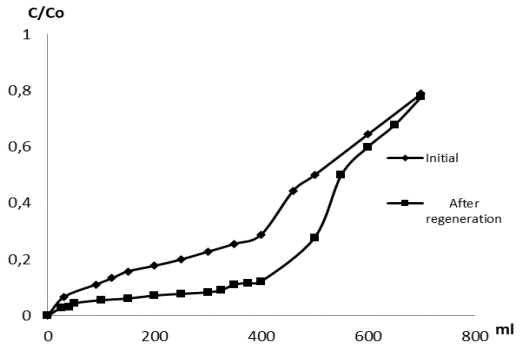

Figure 2. Sorption of K^+ on sorbents $SiMnO_4$: 1- Initial, 2- after regeneration. KOH concentration – 2g / l.

The second type of MnO_2–containing sorbent was prepared using formaldehyde (HCOH) instead of hydrogen peroxide (see. Experimental part). Thus, the MnO_2 content in the sorbent is 3.34 wt.% expressed as Mn (See. Table 2). Figure 3 shows the potassium sorption properties of the sorbent prepared according to the scheme described in the previous section.

From Figure 4 it follows that the sorbent prepared at relatively low pH values of 9.0 has more sorption capacity than the sorbent prepared at a relatively high pH 11.0.

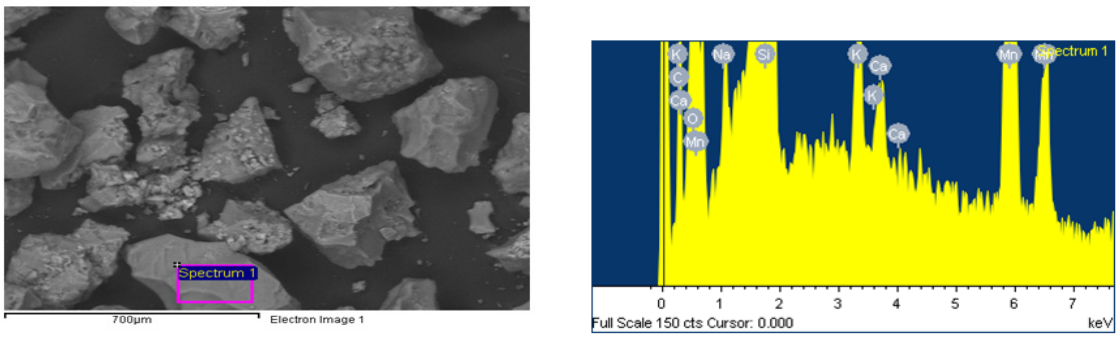

(a) (b)

Figure 3. (a) SEM image and (b) XRF spectrum of sorbent $SiMnO_4$–HCOH.

Table 2.XRF data of the sorbent $MnSiO_4$–HCOH.

Element	Atomic%	Weight%	Atomic%	Weight%	Atomic%	Weight%	Average value Weight%
	Spectrum 1		Spectrum 2		Spectrum 3		
C	15.41	11.55	17.27	12.60	18.67	10.83	17.12
O	65.63	56.52	63.42	56.50	62.84	57.16	62.96
Na	0.28	0.42	0.33	0.33	0.25	0.41	0.29
Al	0.08	0.07	0.05	0.14	0.09	0.17	0.07
Si	17.21	27.56	17.61	26.65	16.88	27.53	17.23
K	0.16	0.30	0.14	0.23	0.11	0.33	0.14
Ca	0.05	0.16	0.07	0.09	0.04	0.10	1.1
Mn	1.16	3.23	1.06	3.29	1.07	3.30	3.34
Fe	0.03	0.19	0.06	0.17	0.05	0.18	0.05
Totals		100.00		100.00		100.00	

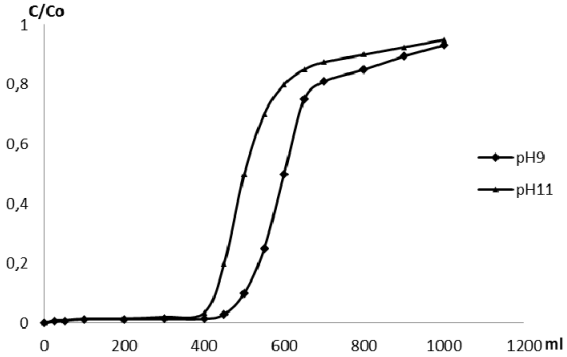

Figure 4. Sorption of K^+ on sorbents $SiMnO_4$–HCOH. KOH concentration - 2 g/l.

In the preparation of the sorbent at higher pH values, it appears that partial gelation occurs. Presumably, at higher pH values structuring of silica gel and manganese dioxide fixation on the surface of the silica matrix does not occur. It is known that at high pH in the silica-water system has a silicate character and the solubility of this system is relatively high, than in lower pH values. Hence, the conditions to form a porous structure in a labile state are difficult to control. Gelling of the system does not occur in the preparation of the sorbent in accordance with the known method [3] in which the residue is obtained from water glass and manganese dioxide after the addition of hydrogen peroxide. However, this procedure does not allow adjusting the porous characteristics of the obtained adsorbents. Therefore, the silica-gel component (in this case water glass) becomes important for the preparation of sorbents. The gelling allows fixing MnO_2 in the structure of silica gel. Furthermore, the use of silica-containing material improves the characteristics of the porous structure of the sorbents. It is assumed that if the gelling is carried out in the presence of $KMnO_4$, i.e. $KMnO_4$ fixed completely in intermicellar spaces, leaching of MnO_2 is minimized during the acid treatment (e.g. during the regeneration of the sorbent).

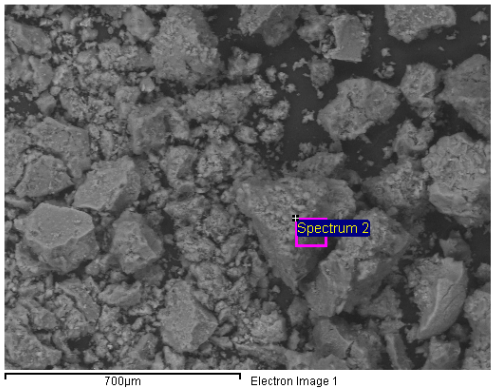

(a)

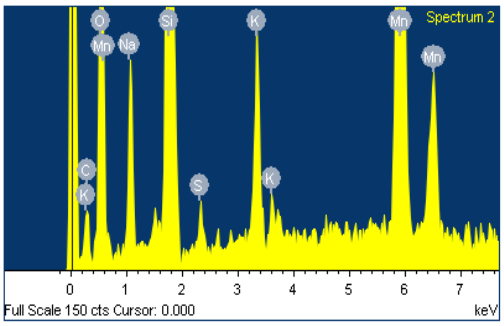

(b)

Figure 5. (a) SEM image and (b) XRF spectrum of sorbent SiO_2–MnO_2–Diatomite

Table 3. XRF data of the sorbent SiO_2–MnO_2–Diatomite.

Element	Weight%	Atomic%	Weight%	Atomic%	Weight%	Atomic%	Average value Weight%
	Spectrum 1		Spectrum 2		Spectrum 3		
C	4.52	7.41	7.91	12.96	9.33	14.75	
O	52.93	65.16	55.56	68.40	51.96	61.69	53.48
Na	4.54	3.89	5.06	4.33	3.74	3.09	4.45
Al	0.18	0.13	0.14	0.10	0.19	0.14	0.17
Si	27.50	19.29	22.88	16.05	24.27	16.41	24.88
S	0.54	0.33	0.32	0.19	0.18	0.11	0.35
K	1.90	0.96	1.47	0.74	1.55	0.75	1.64
Ca	0.10	0.05	0.11	0.05	0.22	0.10	0.14
Mn	7.47	2.68	6.39	2.29	8.35	2.89	7.40
Fe	0.31	0.11	0.16	0.05	0.21	0.07	0.23
Totals	100.00		100		100.00		

The third type of MnO_2– containing sorbent contains diatomite (Dt) as large porous carrier with the silicagel (see. Experimental part) and it showed peculiar results. Figure 6 shows the curves of sorption of K^+ on the surface of such sorbent (SiO_2–MnO_2–Dt).

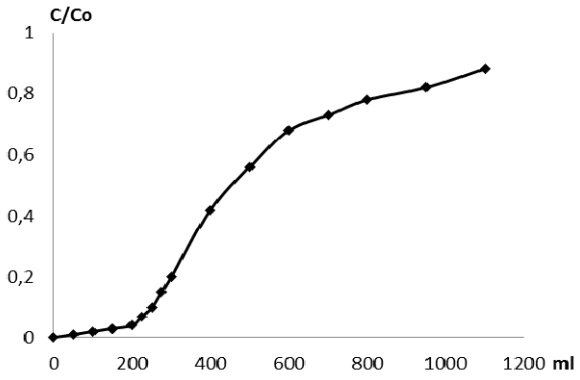

Figure 6. Sorption of K^+ on the sorbent SiO_2– MnO_2–Dt. Concentration ref. KOH – 2 g/l.

The content of MnO_2 on the surface of the sorbent is most likely the most important factor for the sorption process. However, a uniform distribution on the surface of the porous system has relevance as well due to the availability of functional groups that would influence the sorption capacity of the system. Thus, in the case of SiO_2–MnO_2–Dt the average content of MnO_2 is 7.4 wt. % is expressed as Mn as shown in Table. 3. However, the adsorbent has the lowest adsorption capacity (see. Fig. 7).

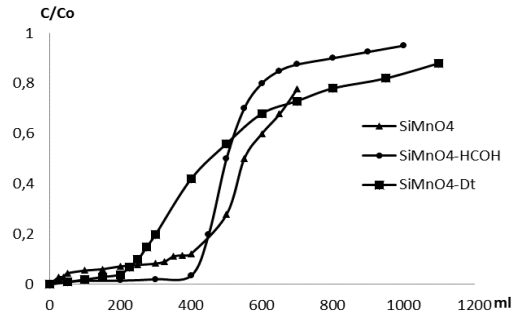

Figure 7. Sorption of K^+ to MnO_2–containing sorbents. Concentration ref. KOH – 2 g/l.

The mechanism of adsorption: To understand the mechanism of sorption of MnO_2 containing sorbents, a solution of K^+ was passed through a column filled with the above-mentioned sorbents. Figure 8 shows the change in pH of the KOH solution (concentration 2.0 g/l, pH 12.58, 20 ^{0}C), passed through a column packed with the sorbent $MnSiO_4$. From Fig. 8 it follows that after passing the potassium hydroxide solution through the column, it appears a sharp decreasing of pH (to pH 3.0, 20 ^{0}C). In the range of 200–600 ml of solution pH does not change and is about pH 6, then with an increase of volume passed through the column solution to 900 ml, the pH increases to 9.0 and finally, in the range of 900–1800 ml to pH 10.

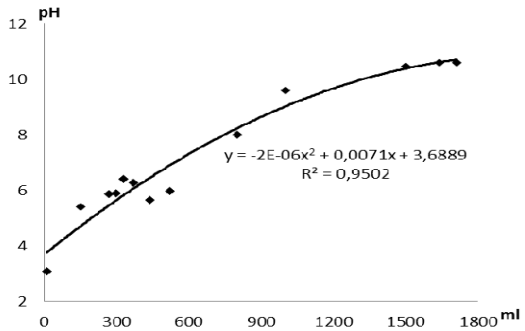

Figure 8. Changing the pH of the KOH solution – 2.0 g/l (pH 12.58 at 20 °C) after passing it through a column packed with the sorbent $SiMnO_4$.

Similar results were obtained in the case of using CH_3COOK solutions (Fig. 9) and KCl solution (Fig. 10). In the latter case, the sorbent used was $SiMnO_4$–HCOH.

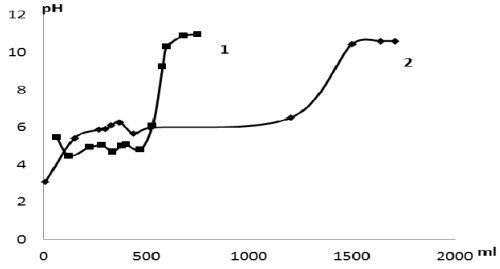

Figure 9. Changing the solution pH CH_3COOK (pH 11.5 with KOH at 20 ^{0}C) after passing it through a column packed with sorbent $SiMnO_4$. 1–1.5 g /l and 2–1 g /l.

From Fig. 9 it follows, as expected, that saturation of the sorbent is faster (2.5 times) by increasing of concentrations of the CH_3COOK. If the concentration of potassium acetate solution is 1 g/l, the sorbent saturation (pH of solution passed through the column until the pH reaches the starting solution) occurs when using 1500 ml. Conversely, in the case of a concentration of CH_3COOK of 1.5g /l the saturation occurs only after passing through the column 600 ml of the solution.

The similar behaviour appears in the case of using KCl solution on the sorbent $MnSiO_4$– HCOH as shown in Fig. 10. Such behaviour of the sorbents indicates that the sorption mechanism has ion-exchange character.

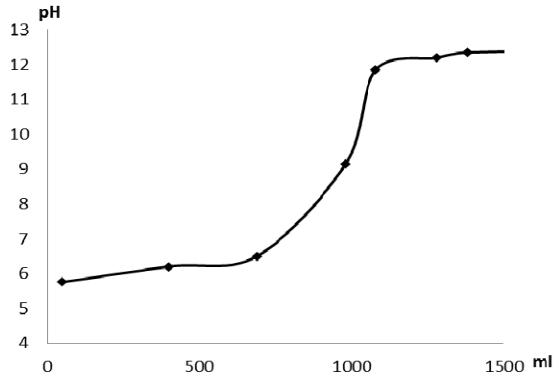

Figure 10. Changing the pH of the solution KCl (pH 12,5 at 20 ^{0}C increased by KOH) after passing it through a column packed with sorbent $MnSiO_4$–HCOH.

CONCLUSIONS

1. The gelling of silica-containing component in the preparation of the system SiO_2 - MnO_2 and controlling the pH of precipitation of MnO_2 on the surface of the silica gel is decisive in the production of composite sorbents.

2. The mechanism of adsorption on MnO_2 - containing sorbents has ion exchange character.

3. The distribution of the MnO_2 on the surface of the sorbent influences the sorption capacity regardless of the MnO_2 content of the sorbent.

ACKNOWLEDGEMENTS

The financial support of the Norwegian Research Council Grant # ES 459248/0 is gratefully acknowledged.

REFERENCES

1. B. Amphlett Inorganic ion exchangers, Elsevier 1964, 136p.

2. M. J. Gray, M. A. Malati Adsorption from aqueous solution by δ-manganese dioxide II. Adsorption of some heavy metal cations Issue Journal of Chemical Technology and Biotechnology v. 29, p. 135–144, 1979.

3. D. A. White, R. Labayru Synthesis of a manganese dioxide-silica hydrous composite and its properties as a sorption material for strontium. Ind. Eng. Chem. Res., 1991, 30 (1), pp 207–210.

4. J. Serrano G., O.C. Garcia D. – Ce^{3+} adsorption on hydrated MnO_2. J. of Radioanalytical and Nuclear Chemistry V.230, No1-2 (1998) p.33-37.

5. O.I. Pendelyuk, T.V. Lisnycha, V.V. Strelco, S.A. Kirilov – Amorphous MnO_2- TiO_2 Composites as Sorbents for Sr2+ and UO_2^{2+}. Adsorption 11 p. 2005, 799-804.

6. Y. Tanaka, M. Tsuji New synthetic method of producing α-manganese oxide for potassium selective adsorbent. Materials research bulletin ISSN 0025-5408 CODEN MRBUAC 1994, vol. 29, No11, pp. 1183-1191.

Paper V

Alvarenga E., Hayrapetyan S., Skipperud L., Hayrapetyan L., Linjordet M. and Salbu B. 2016 Sorption properties of a bentonite based material for removal of uranium from alum shale leachate. Accepted for publication in the *Journal of Chemistry and Chemical Engineering*

Sorption Properties of a Bentonite Based Material for Removal of Uranium from Alum Shale Leachate

Emilio Alvarenga[a*], Sergey Hayrapetyan[b], Lindis Skipperud[c], Lusine Hayrapetyan[d], Marte Linjordet[e], Brit Salbu[f]

[a]: Norwegian Institute of Bioeconomy Research, NIBIO, Frederik A. Dahls vei 20, NO-1430 Ås, Norway

[*]: Corresponding author: Emilio Alvarenga, MSc. (Tech.), Environmental Chemistry (Wastewater Treatment), Tel: (+47) 92 01 04 92, Fax: (+47) 63 00 94 10, e-mail address: Emilio.Alvarenga@nibio.no

[b,d]: Yerevan State University, A. Manoogyan St. 1, 0025, Yerevan, Armenia, Tel: (+374) 10 45 41 66

[c,f]: Norwegian University of Life Sciences (NMBU), Dept. of Env. Sci., PO-BOX 5003, NO-1432, Ås, Norway, Tel: (+47) 64 96 55 41

[e]: Norwegian University of Life Sciences (NMBU), Dept. of Chem., Biotech. and Food Sci., PO-BOX 5003, NO-1432, Ås, Norway, Tel: (+47) 93 40 15 59

Abstract

A dynamic sorption experiment was performed for removal of uranium (VI or 6+) from a leachate from an alum shale landfill with a diatomite-bentonite based sorbent in a laboratory scale. Such material was grounded and treated chemically with phosphoric acid (H_3PO_4) and thermally for improving its porosity and resistance to water flow. A specific surface area of 209 m^2 g^{-1} was

determined by the BET method. A sorption capacity of 30 μg g^{-1} and 0.6 μg g^{-1} were obtained at a pH of 7.5 and 4 respectively by means of Langmuir and Freundlich isotherm models. The flow rate 3 mL min^{-1} was effective for controlling the pH inside of the column. The sorption mechanism was investigated along with desorption of the element of interest for further process design considerations for a treatment unit on the landfill site.

Keywords: Clay based sorbents, Sorption of uranium, Langmuir and Freundlich adsorption models, adsorption capacity.

1. Introduction

Exploitation and/or disturbance of natural reserves of Uranium (U) in Norway, as shale deposits from the Cambrian era could release significant amounts of radionuclides to the environment during and after closing of such operations as mining or all kinds of man-made disturbances. Alum shale rocks are unevenly distributed in the country and are particularly abundant in Oslo region [1]. Usually, U is present in the environment in hexavalent form as UO_2^{2+} and it threatens aquatic life and human health due to its mobilization along with other radionuclides (^{222}Rn, ^{218}Po and ^{214}Po), heavy metals (Fe, Cu, Zn, Ni, Cd, Pb and Mn), trace elements and salts of Na and K [2-7]. On the other hand, urbanization and the development of highway infrastructures as railways, roads, bridges and tunnels can contribute further to such environmental impact. An environmental impact assessment during and after the completion of mining or construction projects is hence required.

47 Uncontrolled deposits of alum shale material with a high pyrite (FeS_2) content undergo weathering
48 where sulfides are oxidized to sulfate[2]. A further hydrolysis of the sulphates dissolves a large
49 number of heavy metals, radionuclides and trace elements. In other words, these contaminants are
50 being leached from the solid phases in different weather conditions and rainfall and these become
51 very mobile. Under very acidic conditions (pH < 3) metal content (heavy metals, radionuclides or
52 trace elements) is greatly increased in the acid streams or leachate. The leachate, which also
53 releases metals, increases thereby their content in aqueous systems. In addition, trace elements may
54 be present in various forms, from molecular dissolved state to colloidal sizes and micron-sized
55 particles. Among these inorganic pollutants, U and its decay products could have high
56 concentrations in the mineral due to its heterogeneity and these could potentially be mobilized to
57 ground- and surface water bodies. Furthermore, other inorganic pollutants could be present in
58 leachates in trace levels or higher concentrations.

59

60 Liming or natural calcium carbonate in the ores, delays the hydrolysis of S^{2-} and further solubility
61 of cations [3]. However, the environmental issue is temporarily solved due to possible
62 remobilization of the ionic pollutants under oxic conditions. Separation processes from liquid to
63 solid are therefore getting relevance for the treatment of leachates from landfills or mining tails as
64 significant amounts of water can be treated in order to reach legislation thresholds for discharges.
65 Some of the water contaminants are Ca, Mg, K, Fe, Cu, Zn, Ni, Cd, Pb and Mn [1;4] and

66 radionuclides U-238 and daughters like Ra-226, Po-210, Pb-210 . There are many alternatives for
67 the treatment of such wastewater streams. The primary methods for heavy metals removal are
68 1.reagent, 2.membrane, 3.electrochemical, 4.biochemical and 5.sorption methods. Several
69 alternatives have already been investigated for U^{6+}, among them co-precipitation, membrane
70 filtration and sorption [9-11].

71 Other methods as ion exchange and electrochemical ones have several disadvantages. Among
72 them, large amounts of heavy metal solutions are formed during the ion exchange by removing
73 pollutants of interest but releasing simultaneously other heavy metals to the water phase.
74 Electrochemical methods along with membrane filtration are energy intensive on the other hand.

75

76 The most common and effective method is sorption. The advantage of this method is that is
77 possible to purify wastewater, which contain large amounts of impurities (e.g. either organic or
78 inorganic). Effectiveness of water treated by this method may rise up to 80-95 %, depending on
79 the chemical nature of the sorbents, their structure and size of the adsorption surface. In recent
80 years, attention has been given to natural sorbents or sorbents obtained based on materials of natural
81 origin for water treatment. The most interesting are fibrous filled sorbents, ferrocyanides of
82 transition metals and titanium compounds. They have been successfully used for radionuclide
83 separation [5-9]. Furthermore, it is possible to combine a pretreatment of the effluent either by a

84 process sequence with pH adjustment, chemical precipitation, coagulation/flocculation and
85 sorption of dissolved pollutants as a last step to increase the separation efficiency.
86 Sorption processes represent a feasible alternative as well due to multiple regenerations of the
87 sorbents with strong acids and use of natural abundant materials as apatites, clays and other silica-
88 containing systems which have porosity and functional groups for physical/chemical binding of
89 pollutants in solution [10-12] . In order to increase the efficiency of separation, it is necessary to
90 create new types of sorbents, which have a maximum selectivity towards specific elements.
91 There are porous materials available from which it is possible to produce effective sorbents. Many
92 natural minerals (e.g. zeolites, clay, clinoptilollite, mordenite, tuffs) have such advantage and for
93 this reason, they have widely been studied [13-16]. However, these materials require chemical
94 and/or physical treatments to become effective sorbents. Moreover, selectivity is among the
95 greatest challenges in these naturals minerals. Among these, the most widely used methods are acid
96 and alkali treatment, hydrothermal and thermal treatment, mechanical activation and pillaring.
97 However, there is a knowledge gap for improving selectivity and removal capacity for U species
98 in water. There are not natural sorbents with a high efficacy that could become an alternative to the
99 expensive titanium dioxide sorbents. The sorption of U^{6+} has been investigated in clays as
100 montmorillonites and smectites [17] and other types of materials as zeolites [18] and granites [19]
101 have been studied as well. In addition, olivines have -OH functional groups that complexate UO_2^{2+}
102 in the surface as shown by El Aamrani et al. [20]. In the last few years, it has been suggested to

103 impregnate chemically the carrier or surface of the sorbent, which shows selectivity for the ion, or
104 ions, of interest. The carrier might be an ion-exchange resin, cellulose, active carbon, natural
105 minerals. The application of this method resulted hence, in the development of several new sorbents
106 [21;22].

107 Challenges are encountered additionally in sorption processes concerning the affinity to remove
108 U^{6+} in multiphase systems. The latter are commonly found in the environment. Competition for
109 sorption sites is thus enhanced and does have an impact in the U^{6+} removal capacity. Such effects
110 could be attributed to anions (carbonates and phosphates) [23-26], cations (e.g. Ba^{2+}, Ca^{2+} and K^{+})
111 [27;28] and humic substances [29;30]. Moreover, high concentrations of both anions and cations
112 could either increase or decrease the sorption of U^{6+} by forming stable species of U as calcium-
113 uranyl-carbonate-complex or anion-cation-surface ternary complexes. Therefore, there are
114 expected changes in both the surface and the species of U in solution where pH in the solution
115 plays an important role concerning the speciation. Furthermore, organic complexation over the
116 surface of the sorbent could have or not an effect on the separation as investigated by Logue et al.
117 [29] and Křepelová et al. [30]. The former investigation revealed that the U^{6+} removal was reduced
118 by 50% by means of an iron sand system when citrate was present in solution. The latter study
119 showed how U^{6+} "preferred" to sorb to kaolinite and not to humic acid that was directly bound to
120 a clay surface [30].

121 The upscaling of the removal of U^{6+} by sorption, can be investigated in static or dynamic mode
122 [10]. In the latter, binders are required to avoid permeability problems associated to flow rate (Q)
123 in the columns. The flow resistance of a granulated sorbent is a challenge for up-scaling.

124 The aim of this work is to study the sorption of U^{6+} (naturally present in alum shale) in dynamic
125 mode with a bentonite based material in a laboratory scale. The wastewater effluent was a leachate
126 sampled from an alum shale landfill. Treatment of the natural materials was carried out for binding
127 or granulating the sorbents to enhance mass transfer through their porous structure as well as for
128 avoiding permeability problems in the columns.

129 **2. Materials and Methods**

130 *2.1 Leachate*

131 The leachate was sampled in the spring 2015 from a superficial water of an open alum shale landfill.
132 The latter was constructed under the Norwegian Public Road Administration (Statens Vegvesen
133 Vegdirektoratet) standards. It was located by the construction site of a road (RV4) and a tunnel in
134 Gran County, Norway. The physicochemical parameters of the leachate were analyzed in
135 accordance to the standard methods for examination of water and wastewater and can be seen from
136 Table 1 [31]. The sample was stored at 4°C prior to the start of the sorption experiments.

137

138 **Table 1**: Physicochemical parameters of the leachate.

Parameter	Unit	Value or concentration
pH (25°C)	-	7.5
TOC*	mg/L	1.2
Alkalinity (pH = 8.3)	mmol/L	<0.15
Turbidity	FNU	26.4
Suspended solids	mg/L	26.1
S	mg/L	116
SO_4^{2-}	mg/L	309
N_{total}	mg/L	27.5
P_{total}	mg/L	0.03
Cl^-	mg/L	25.4
Ca	mg/L	110
Fe	µg/L	327
K	mg/L	12.2
Mg	mg/L	14
Na	mg/L	110
Al	µg/L	213
As	µg/L	5.35
Ba	µg/L	140
Cd	µg/L	0.50
Co	µg/L	0.33
Cr	µg/L	0.23
Cs	µg/L	0.71
Cu	µg/L	0.56
Hg	µg/L	<0.002
Mn	µg/L	48.4
Mo	µg/L	800
Ni	µg/L	10
Pb	µg/L	0.70
Si	mg/L	7.10
Sr	µg/L	1900
Zn	µg/L	33
V	µg/L	10.2
B	µg/L	85.5
Th	µg/L	<0.04
U	µg/L	150

139 *: Total organic carbon

140 *2.2 Sorbents Preparation and Characterization*

141 *2.2.1 Diatomite-bentonite sorbent*

142 The sorbent coded as DB-12P-HP was prepared in the same way for the laboratory and pilot scale.
143 Its chemical composition of the base materials was determined by fluorescence x-ray spectrometry
144 (XRF) from scanning electron microscopy and it can be seen from Table 2. The base materials are
145 a bentonite produced by the Ijevan Bentonite Company and a diatomite elaborated by the Diatomite
146 Company, both from the Republic of Armenia. The code "DB" refers to the diatomite-bentonite
147 combined system. A 1 L bentonite slurry of 200 g L^{-1} was prepared and mixed with 100 ml of a 10
148 $\%_{v/v}$ solution of phosphoric acid (H_3PO_4). The volume ratio of bentonite to H_3PO_4 was 10:1. The
149 mixture was left in contact and undisturbed overnight. Afterward, a 0.5 L slurry of diatomite of
150 200 g L^{-1} was added to the aforementioned mixture. The code "12P" refers to the DB weight ratio
151 of Bentonite:Diatomite = 2:1. The system was then filtered and the resulting cake was dried at
152 room temperature; followed by a drying at 105°C. The system was grounded in order to obtain a
153 homogeneous powder consistency. The term "HP" refers to a further treatment with H_3PO_4.

154 **Table 2**: XRF data of the DB-12P-HP sorbents.

Sorbent	Element									
	O	Na	Mg	Al	Si	P	K	Ca	Ti	Fe
DB-12P-HP	63.5	0.50	0.70	2.60	21.60	9.00	0.30	0.40	0.20	1.20

155

156 A 5%$_{v/v}$ H_3PO_4 solution was used for the granulation of the powdered DB-12P-HP. The granulation
157 process was performed manually by adding gradually the H_3PO_4 solution (approximately 50 mL)
158 to a container with DB-12P-HP system as powder with an amount lower than 50 g. Granules where
159 obtained by shaking the mixture with circular movements until the system was aggregated. The
160 wet granules were sieved in a 3 to 4 mm mesh and the process was repeated until obtaining a
161 particle size between 3 to 4 mm. It was possible to granulate 400-500 g of DB-12P-HP per batch
162 with approximately 50 mL of the H_3PO_4 solution. These batches were dried at room temperature
163 followed by a heat treatment of 500°C for 4 h for improving its porosity and further resistance to
164 water flow.

165 *2.2.2 Sorption properties*

166 The specific surface area as m^2/g was measured for DB-12P-HP with the BET method [32] by
167 means of a Gemini VI® instrument manufactured by Micromeritics USA Ltd. The value obtained
168 was 209 m^2 g^{-1} for DB-12P-HP.

169 *2.3 Dynamic mode sorption assembly*

170 The DB-12P-HP granules were placed inside of a column of 1.5 cm diameter and 50 mL capacity.
171 The amount of sorbent was 24 g for the column and the bulk density was 0.54 g mL^{-1} for DB-12P-
172 HP. An initial regeneration with 0.1 L of a 7.5 %$_{v/v}$ HCl solution was performed prior to the first
173 sorption experiment. The column was then washed with deionized water for removal of the

174 remaining acid. Afterward, the sample was introduced without any pH adjustment (pH 7.5), from
175 the top of the column at a Q of 3 mL min^{-1} by gravity. The temperature was 10 °C over the whole
176 sorption experiment. Volume samples were collected from the bottom of the columns. In addition,
177 aliquots of 5 mL were taken for each of the volumes sampled for quantifying the concentration of
178 U^{6+} after contact with the sorbent.

179 After reaching saturation of the sorbent at pH 7.5, a second regeneration was carried out with the
180 7.5 %v/v HCl solution. Samples were taken during the regeneration in order to determine the
181 amount of acid required for "cleaning" the sorbent. After regeneration and washing with deionized
182 water, the pH of the sample was adjusted to 4.0 with concentrated HCl and then a second sorption
183 experiment was performed at the same temperature and Q as the previous one.

184 *2.4 Analytic methods*

185 The analytic methods were performed in accordance to the standard methods for examination of
186 water and wastewater [31]. The pH of the volumes sampled from the outlet of the columns was
187 measured in a Thermo Orion pH-meter model Dual Star. All the aliquots taken from the volumes
188 samples (for both scales) were preserved by adding ultrapure HNO_3 to a final concentration of
189 $5\%_{v/v}$ in the samples diluted with milli-Q water. Thereafter, all the samples were analyzed by
190 inductively coupled plasma (ICP) mass spectrometry (MS) model Agilent Tech. 8800 Triple Squad
191 for the data evaluation and determination of adsorption isotherms (Langmuir and Freundlich). A

192 set of three blanks was analyzed simultaneously with the samples for the estimation of the detection
193 and quantification limits of ^{238}U.

194 *2.5 Data Evaluation*

195 The amount of the element adsorbed at equilibrium was calculated with Equation 1 as follows [33],

196 $$q = \frac{(c_0 - c) \cdot V}{m} \quad \text{(Eq. 1)}$$

197 Where: q is the amount of the metal ion adsorbed per unit of mass of the sorbent (mg g^{-1}) at
198 saturation; c_0 is the initial concentration (mg L^{-1}) of the analyte in solution; c is the residual
199 concentration (mg L^{-1}) of the analyte after contact with the sorbent; V is the volume sampled (L)
200 and m is the mass of dry sorbent (g).

201 Two models were utilized in order to assess the experimental sorption isotherms: Langmuir and
202 Freundlich models [34]. The Langmuir approach was selected for the estimation of the maximum
203 adsorption capacity corresponding to the surface of the sorbents as seen from Equation 2 [33].
204 Whereas, the Freundlich model was chosen to estimate the adsorption intensity of the metal ion
205 towards the sorbent as shown in Equation 3 [33].

206 $$\frac{1}{q} = \frac{1}{c q_0 \cdot K_L} + \frac{1}{q_0} \quad \text{(Eq. 2)}$$

Where: K_L is a constant derived from the adsorption/desorption energy (L mg^{-1}), and q_0 is the maximum adsorption upon equilibrium or saturation of the sorbent's surfaces (mg g^{-1}) [33]. The plot $1/q$ versus $1/c$ allows determining these constants.

$$\log(q) = \log(K_F) + \frac{1}{n}\log(c) \quad \text{(Eq. 3)}$$

Where: K_F is known as the Freundlich constant and a measure of the sorption capacity; n is a constant that describes the affinity of the metal towards the surface of the sorbent [33]. The constant K_F and n can be calculated from the slope and the intercept of the linear plot of log (q) versus log (c) [33].

3. Results and Discussions

3.1 Sorption Experiment

The effect of the pH was investigated in order to determine the saturation volume of DB-12P-HP at a Q of 3 mL min^{-1}. As seen from Fig. 1, the sorption capacity was significantly decreased by adjusting the pH of the sample (leachate) to 4. The sorbent was saturated with approximately 50% of the volume passed through the column as for pH 7.5.

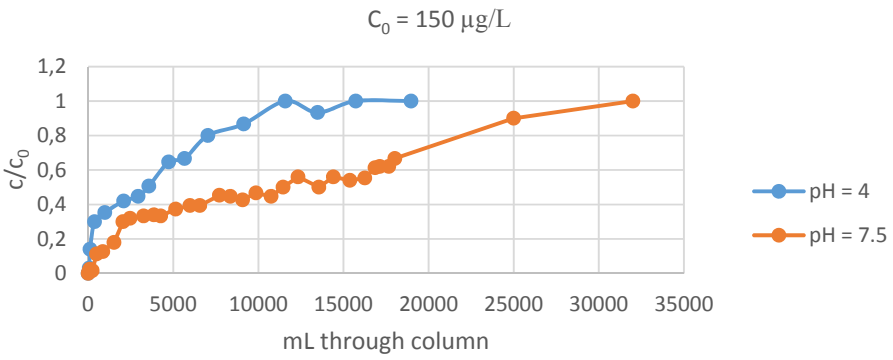

Figure 1: Saturation curves for U^{6+} sorption with DB-12P-HP at 10°C and Q = 3 mL min^{-1}

Such behavior can be explained by the species of U^{6+} in solution and the presence of other inorganic ligands such as sulphate, carbonate and phosphate [23-26]. Moreover, the competition of U^{6+} for sorption sites with SO_4^{2-} ions (from the alum shale as shown in Table 1) is higher at lower pH values. Furthermore, the formation of uranyl-sulphate complexes could potentially influence the sorption process as well at values lower than pH 7.5. This result is in accordance with the findings of Bachmaf et al. [35] for a bentonite as a sorbent were the predominant species of U^{6+} in the solution (0.01 M NaCl + 0.005 M Na_2SO_4 and [U] = 5×10^{-5} M) were UO_2OH^+ and $(UO_2)_3(OH)^{5+}$ for pH values between 4 and 5. These hydrolyzed species of U, readily form ligands with the phosphate groups fixated to the surface of DB-12P-HP.

The sorption capacity was determined by means of the fitting of the experimental data into the equilibrium isotherm models of Langmuir and Freundlich. The linearized form of both isotherms is shown in Fig. 2 and 3.

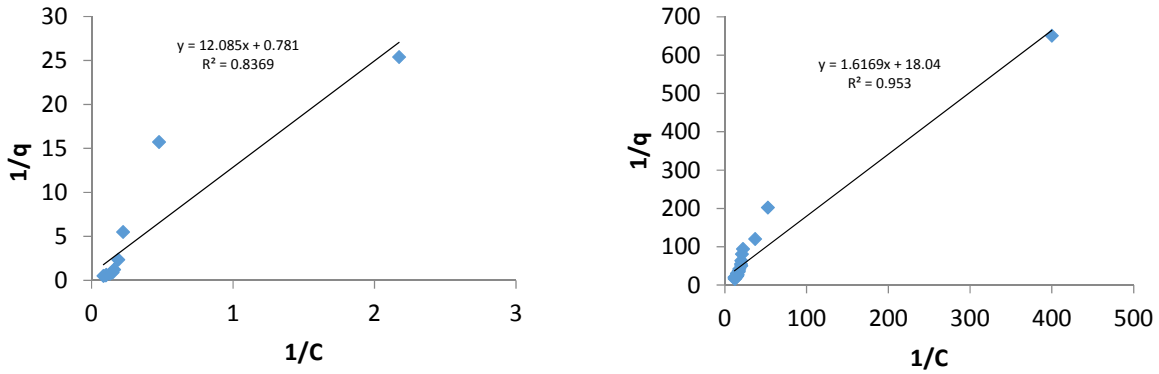

(a) (b)

Figure 2: Linearized form of the Langmuir isotherm for (a) pH = 4 and (b) pH = 7.5.

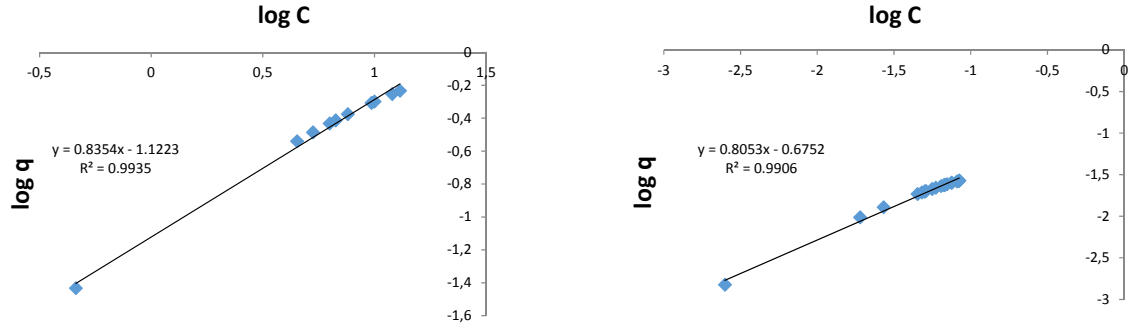

(a) (b)

Figure 3: Linearized form of the Freundlich isotherm for (a) pH = 4 and (b) pH = 7.5.

The results of K_L, K_F, n and q_0 from the linear regressions of Fig. 2 and Fig. 3 can be seen from Table 3 along with their correlation coefficients (R^2).

Table 3: Values of the constants of the Langmuir and Freundlich isotherms at the studied pH's.

pH	Langmuir			Freundlich		
	R^2	q_0	K_L,	R^2	n	K_F,
4	0.8369	1.28[a]	0.0646[c]	0.9935	1.1970	0.0755[e]
7.5	0.953	0.055[b]	11.16[d]	0.9906	1.2418	0.2113[f]

[a]: µg/g
[b]: mg/g
[c]: L/µg
[d]: L/mg
[e]: µg $L^{1/n}$/g $µg^{1/n}$
[f]: mg $L^{1/n}$/g $mg^{1/n}$

The sorption process is better described in both pH's with the Freundlich isotherm due to the higher R^2 fitting values. Moreover, there is a substantial difference in magnitude between pH 4 and pH 7. The latter showing a higher degree of sorption for U^{6+} with a sorption capacity of 30 µg g^{-1} compared to 0.6 µg g^{-1} as seen from Fig. 4 (a) and (b).

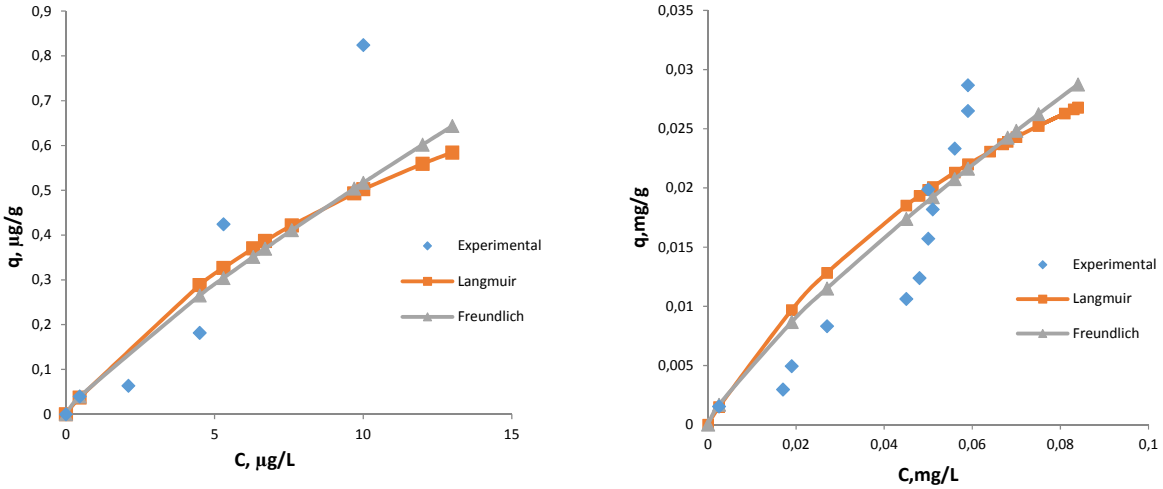

(a) (b)

Figure 4: Equilibrium isotherms for (a) pH = 4 and (b) pH = 7.5

The sorption capacity of DB-12P-HP at pH 7.5 is comparable to the one of hydrous lanthanum oxide (38 µg g^{-1}) for U removal from seawater [36]. Such sorbent represents an alternative to the expensive and freshly prepared hydrous titanium oxide, with a capacity 1550 µg g^{-1} (from sea water

as well). Khalili et al. [10] have found *q*-values as high as 62 mg g^{-1} for U^{6+} removal from a synthetic solution of U and Th with a bentonite at pH 3 and T = 25°C with a C_0 of 100 ppm. Such a broad difference in removal capacity from those studies shows clearly the effect of the competition for sorption sites on the surface of the natural bentonites in multicomponent systems as sea water or leachates for instance.

3.2 Sorption mechanism

The variation of pH in the columns (at 10°C) suggest that a cationic exchange mechanism for DB-12P-HP as seen from Fig. 5 (a) and (b). The leachate before passed through the column had a pH 4. The sorption test with NaCl 0.1 N with an initial pH of 5.5 confirms the type of mechanism. The pH inside of the column sharply decreases to a value of 2.6 as seen from Fig. 36 (a) due to the production of H^+ ions from the cation exchange. It gradually increases and it stabilizes to a value of 4 in both Fig. 5 (a) and (b) in the column. Moreover, the pH starts to change after 7000 mL in Fig. 5 (b) confirming the sorption mechanism. Therefore, the cationic exchange behavior suggest that DB-12P-HP works more efficiently over pH 7 as seen from the results from the subsection 3.1. A sorbent as DB-12P-HP would hence be more effective for removal of U^{6+} from alum shale leachate at pH values higher than 7 due to the cation exchanger nature of the sorption process and the U species in solution.

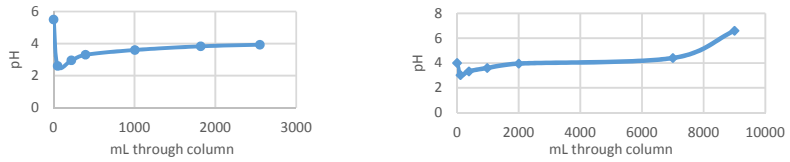

(a) (b)

Figure 5: pH variation at 10°C in the column (a) NaCl 0.1 N (b) with leachate

3.3 Regeneration process

The complete regeneration of the laboratory scale column requires 0.2 L of HCl 7.5%$_{v/v}$ as seen from Fig. 6. The desorption process occurs hence at a high rate with a low amount of acid. The power fit of the U^{6+} desorption shows how rapidly the metal can be concentrated in a small volume of acid. Moreover, the disposal of the regeneration process would be easier due to the low volumes produced by obtaining concentrated solutions of heavy metals, trace elements and radionuclides. The physical sorption of U^{6+} can therefore be reversed with a significantly low amount and concentration of mineral acid solution. In other words, the regeneration of DB-12P-HP would contribute to a cost effective design of a sorption unit for U^{6+} in a bigger scale.

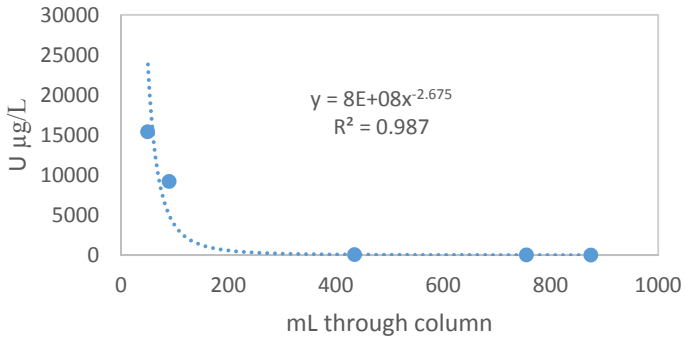

Figure 6: Desorption of U with HCl 7.5%$_{v/v}$

306 **4. Conclusions**

307 The volume of leachate treated by sorption with DB-12P-HP along with the sorption capacity were
308 drastically decreased by 50% and 98% accordingly at pH = 4 in the laboratory scale. This behavior
309 was attributed to the species of U^{6+} in solution and the high degree of competition for the sites.

310 The cationic exchange mechanism of DB-12P-HP suggest that the sorption process of U^{6+} from
311 the alum shale leachate studied is more efficient at pH values (inside of the column) over 4.

312 The regeneration of DB-12P-HP with acids occurs rapidly and with 0.08 L of HCl 7.5 $\%_{v/v}$ per g
313 of sorbent. It allows to concentrate waste (metals) easily by desorption for the further feasibility
314 estimation and design of an on-site treatment unit.

315

316 **Acknowledgment**

317 The authors of this work thank the Norwegian Public Roads Administration (Statens Vegvesen
318 Vegdirektoratet) for the funding of this work through the project "Effects and Environmental Risks
319 Associated to Interventions in Areas with Sulfide Rich Minerals (NORWAT/RV4)".

320
321
322
323
324
325
326
327
328

References

[1] A. S. Jeng, "Weathering of Some Norwegian Alum Shales I. Laboratory Simulations to Study Acid Generation and the Release of Sulphate and Metal Cations (Ca, Mg & K)," *Acta Agric. Scand.*, vol. 41, pp. 13–35, 1991.

[2] B. E. Kalinowski, A. Oskarsson, Y. Albinsson, J. Arlinger, A. Ödegaard-Jensen, T. Andlid, and K. Pedersen, "Microbial leaching of uranium and other trace elements from shale mine tailings at Ranstad," *Geoderma*, vol. 122, no. 2–4, pp. 177–194, 2004.

[3] A. Andersson and G. Siman, "Levels of Cd and Some Other Trace Elements in Soils and Crops as Influenced by Lime and Fertilizer Level," *Acta Agric. Scand.*, vol. 41, pp. 3–11, 1991.

[4] A. S. Jeng, "Weathering of Some Norwegian Alum Shales, II. Laboratory Simulations to Study the Influence of Aging, Acidification and Liming on Heavy Metal Release," *Acta Agric. Scand.*, vol. 42, pp. 76–87, 1992.

[5] N. P. Molochnikova, I. G. Tananaev, G. V. Myasoedova, and B. F. Myasoedov, "Sorption recovery of radionuclides from alkaline solutions using fibrous 'filled' sorbents," *Radiochemistry*, vol. 49, no. 1, pp. 64–66, 2007.

[6] E. S. Zakaria, I. M. Ali, H. F. Aly, N. Fuel, T. Dep, and A. E. Authority, "Adsorption Behaviour of 134 Cs and 22 Na Ions on Tin and Titanium Ferrocyanides," pp. 237–244, 2004.

[7] M. C. Duff, D. B. Hunter, D. T. Hobbs, S. D. Fink, Z. Dai, and J. P. Bradley, "Mechanisms of strontium and uranium removal from high-level radioactive waste simulant solution by the sorbent monosodium titanate," *Environ. Sci. Technol.*, vol. 38, no. 19, pp. 5201–5207, 2004.

[8] G. Gürboğa and H. Tel, "Preparation of TiO2-SiO2 mixed gel spheres for strontium adsorption," *J. Hazard. Mater.*, vol. 120, no. 1–3, pp. 135–142, 2005.

[9] S. Lahiri, K. Roy, S. Bhattacharya, S. Maji, and S. Basu, "Separation of 134Cs and 152Eu using inorganic ion exchangers, zirconium vanadate and ceric vanadate," *Appl. Radiat. Isot.*, vol. 63, no. 3, pp. 293–297, 2005.

[10] F. I. Khalili, N. H. Salameh, and M. M. Shaybe, "Sorption of Uranium (VI) and Thorium (IV) by Jordanian Bentonite," vol. 2013, 2013.

[11] K. Popa, "Sorption of uranium on lead hydroxyapatite," *J. Radioanal. Nucl. Chem.*, vol. 298, no. 3, pp. 1527–1532, 2013.

[12] Y. Wei, L. Zhang, L. Shen, and D. Hua, "Positively charged phosphonate-functionalized mesoporous silica for efficient uranium sorption from aqueous solution," *J. Mol. Liq.*, vol. In Press, 2015.

[13] B. Bilgin, G. Atun, and G. Keçeli, "Adsorption of strontium on illite," *J. Radioanal. Nucl. Chem.*, vol. 250, no. 2, pp. 323–328, 2001.

[14] S. C. Tsai, S. Ouyang, and C. N. Hsu, "Sorption and diffusion behavior of Cs and Sr on Jih-Hsing bentonite," *Appl. Radiat. Isot.*, vol. 54, no. 2, pp. 209–215, 2001.

[15] G. Atun and A. Kilislioglu, "Adsorption behavior of cesium on montmorillonite-type clay in the presence of potassium ions," *J. Radioanal. Nucl. Chem.*, vol. 258, no. 3, pp. 605–611, 2003.

[16] S. A. Stout, Y. Cho, and S. Komarneni, "Uptake of cesium and strontium cations by potassium-depleted phlogopite," *Appl. Clay Sci.*, vol. 31, no. 3–4, pp. 306–313, 2006.

[17] G. D. Turner, J. M. Zachara, J. P. McKinley, and S. C. Smith, “Surface-charge properties and UO2+\n2 adsorption of a subsurface smectite,” *Geochim. Cosmochim. Acta*, vol. 60, no. 18, pp. 3399–3414, 1996.
[18] T. Arnold, T. Zorn, G. Bernhard, and H. Nitsche, “Sorption of uranium(VI) onto phyllite,” *Chem. Geol.*, vol. 151, no. 1–4, pp. 129–141, 1998.
[19] M. H. Baik, S. P. Hyun, and P. S. Hahn, “Surface and bulk sorption of uranium (VI) onto granite rock,” *J. Anal. Nucl. Chem.*, vol. 256, no. 1, pp. 11–18, 2003.
[20] F. Z. El Aamrani, L. Duro, J. De Pablo, and J. Bruno, “Experimental study and modeling of the sorption of uranium(VI) onto olivine-rock,” *Appl. Geochemistry*, vol. 17, no. 4, pp. 399–408, 2002.
[21] L. V. A. Gurgel, R. P. de Freitas, and L. F. Gil, “Adsorption of Cu(II), Cd(II), and Pb(II) from aqueous single metal solutions by sugarcane bagasse and mercerized sugarcane bagasse chemically modified with succinic anhydride,” *Carbohydr. Polym.*, vol. 74, no. 4, pp. 922–929, 2008.
[22] P. Mondal, C. B. Majumder, and B. Mohanty, “Effects of adsorbent dose, its particle size and initial arsenic concentration on the removal of arsenic, iron and manganese from simulated ground water by Fe3+ impregnated activated carbon,” *J. Hazard. Mater.*, vol. 150, no. 3, pp. 695–702, 2008.
[23] C. Galindo, M. Del Nero, R. Barillon, E. Halter, and B. Made, “Mechanisms of uranyl and phosphate (co)sorption: Complexation and precipitation at α-Al2O3 surfaces,” *J. Colloid Interface Sci.*, vol. 347, no. 2, pp. 282–289, 2010.
[24] T. Cheng, M. O. Barnett, E. E. Roden, and J. Zhuang, “Effects of phosphate on uranium(VI) adsorption to goethite-coated sand,” *Environ. Sci. Technol.*, vol. 38, no. 22, pp. 6059–6065, 2004.
[25] A. Singh, K.-U. Ulrich, and D. E. Giammar, “Impact of phosphate on U(VI) immobilization in the presence of goethite,” *Geochim. Cosmochim. Acta*, vol. 74, no. 22, pp. 6324–6343, 2010.
[26] Z. Guo, Y. Li, and W. Wu, “Sorption of U(VI) on goethite: Effects of pH, ionic strength, phosphate, carbonate and fulvic acid,” *Appl. Radiat. Isot.*, vol. 67, no. 6, pp. 996–1000, 2009.
[27] P. M. Fox, J. A. Davis, and J. M. Zachara, “The effect of calcium on aqueous uranium(VI) speciation and adsorption to ferrihydrite and quartz,” *Geochim. Cosmochim. Acta*, vol. 70, no. 6, pp. 1379–1387, 2006.
[28] D. A. Carvajal, Y. P. Katsenovich, and L. E. Lagos, “The effects of aqueous bicarbonate and calcium ions on uranium biosorption by Arthrobacter G975 strain,” *Chem. Geol.*, vol. 330–331, no. 0, pp. 51–59, 2012.
[29] B. A. Logue, R. W. Smith, and J. C. Westall, “Role of Surface Alteration in Determining the Mobility of U (VI) in the Presence of Citrate : Implications for Extraction of U (VI) from Soils,” *Environ. Sci. Technol.*, vol. 38, no. 3, pp. 3752–3759, 2004.
[30] A. Křepelová, T. Reich, S. Sachs, J. Drebert, and G. Bernhard, “Structural characterization of U(VI) surface complexes on kaolinite in the presence of humic acid using EXAFS spectroscopy,” *J. Colloid Interface Sci.*, vol. 319, pp. 40–47, 2008.
[31] APHA, *Standard Methods for the Examination of Water and Wastewater*, 22nd ed. American Water Works Association, Clearway Logistics, 2012.
[32] S. Brunauer, P. H. Emmett, and E. Teller, “Adsorption of gases in multimolecular layers,” *J. Amer. Chem. Soc.*, vol. 60, p. 309, 1938.
[33] L. Bulgariu, M. Răţoi, D. Bulgariu, and M. Macoveanu, “Equilibrium study of Pb(II) and

421 Hg(II) sorption from aqueous solutions by moss peat," *Environ. Eng. Manag. J.*, vol. 7, no.
422 5, pp. 511–516, 2008.
423 [34] J. Bratby, "Colloids and interfaces," in *Coagulation and Flocculation in Water and*
424 *Wastewater Treatment*, 2nd ed., -, Ed. IWA Publishing, London, UK., 2006, pp. 14–17.
425 [35] S. Bachmaf, B. Planer-Friedrich, and B. J. Merkel, "Effect of sulfate, carbonate, and
426 phosphate on the uranium(VI) sorption behavior onto bentonite," *Radiochim. Acta*, vol. 96,
427 no. 6, pp. 359–366, 2008.
428 [36] S. D. Alexandratos, "Uranium Separation – Challenges and Opportunities: Recovery of
429 Uranium from Seawater with Solid Sorbents," 2010.
430

431

Appendix

Programming tools of MatLab®

Script:

```
clear all
data=xlsread('newdata.xlsx')

x=data(:,1); %Temperature (K)
y=data(:,2); %Speed (rpm)
z=data(:,3); %Torque (microNm)

% "Gjetter" på parametre - Gode startverdier her er viktig!
A = 0.5;
B = 0.5;
C = 0.5;
D = 0.5;
E = 0.5;
p0 = [A B C D E];

format long
phat = optimer( p0, x, y, z)

zhat = minfunksjon( x, y, phat);

figure(1)
plot( y, z, 'o')
xlabel('Speed (rpm)')
ylabel('Torque (microNm)')

figure(2)
plot( z, zhat, 'o', 'MarkerFaceColor', 'b' )
xlabel('z (microNm)')
ylabel('zhat (microNm)')


w1=phat(3).*exp(-5.77+1722.2./x)
w2=phat(1)
```

Function:

```
function zhat = minfunksjon( x, y, p )
   A = p(1);
   B = p(2);
   C = p(3);
   D = p(4);
   E = p(5);
   %F = p(6);
   %G = p(7);
   %H = p(8);


   zhat=A.*y.^B.*exp(-5.77+1722.2./x)+C.*y.^D;

end
```

Iteration Process:

```
function phat = optimer( p0, x, y, z )

options = optimset('MaxFunEvals',100000,'MaxIter',100000);
%options = optimset('MaxIter',10000);

phat = fminsearch( @kvadratavvik, p0, options);

   function J = kvadratavvik( p )
      zhat = minfunksjon( x, y, p );
      J = sum( (z(:) - zhat(:)).^2 );
   end

end
```

Errata List

Page 1
"wastewater treatment" added in front of its acronym "WWT" in the third paragraph. Moreover, parenthesis "(WWT)" were added to it. This is the first time the acronym is defined in Chapter 1 (Introduction).

"European Union" added in front of its acronym "EU" in the third paragraph. Moreover, parenthesis "(EU)" were added to it. This is the first time the acronym is defined in Chapter 1 (Introduction).

Page 2
"wastewater treatment plants" added in front of its acronym "WWTPs" in the second paragraph. Moreover, parenthesis "(WWTPs)" were added to it. This is the first time the acronym is defined in Chapter 1 (Introduction).

Page 3
"wastewater" added in front of its acronym "WW" in the second paragraph. Moreover, parenthesis "(WW)" were added to it. This is the first time the acronym is defined in Chapter 1 (Introduction).

Page 21
In the last paragraph of sub-section 4.6.1, "subsection 6.4.2" was replaced by "sub-section 6.4.2" to match the format selected for the document.

"in" added in front of "Oslo area" in the first paragraph of sub-section 4.6.2. It should be "in Oslo area".

Page 32
In the last paragraph, "subsection 5.2.2" was replaced by "sub-section 5.2.2" to match the format selected for the document.

Page 33
A "." was missing and added at the end of the first paragraph of sub-section 5.2.

Page 43
In the first paragraph of sub-section 6.1, "subsection 5.1.1" was replaced by "sub-section 5.1.1" to match the format selected for the document.

Page 52
"U" changed by "UT" to be consistent with Figure 31 in the second paragraph.

Page 55
Caption of Figure 33 was moved from the top of Page 56 to the bottom of Page 55 in order to place it adjacent to the Figure.

Enlargement of figures/increase in font size
The following Figures were enlarged considerably: 9, 11, 13, 16, 17, 18, 20 and 22.

The following Figures were enlarged slightly: 1, 3, 4, 6, 7, 10, 14, 15, 24, 34, 35 and 37.

The font size in the following figures was changed:

- Figure 2: White letters on colored background were increased in font size.
- Figure 12: The font size of the text for Inlet ADR, Centrate (stream sampled), and Dewatering was increased.
- Figures 23, 25, 26, 27, 28 and 30 were enlarged and the font size was increased.

Font size in equations
The font size in the following Equations was changed:

- Equation 8: A capital "C" was corrected to match the one Equation 9.
- Equation 13: The font size was increased.
- Equation 15: The font size was increased (in relation to Equation 16).
- Equation 17: The font size was increased and "Relative agronomic Efficiency" was changed by its acronym "RAE" in order to fit the format of the document.

References

Page 2
First paragraph: The citation "(Seadi et al. 2008)" was corrected in Chapter 1. It should be "(Al Seadi et al. 2008)".

Page 19
First paragraph: "Stumm and Morgan" was removed from the citation "(Stumm and Morgan 1962)" in sub-section 4.5. It should be cited as "(1962)".

Page 58
Second paragraph: ";" added in front of the citation "Galindo et al. 2010" in sub-section 6.5.1.

Page 69
The reference "(Lindsay 1979)" was misplaced in the previous reference list and it has been placed correctly by alphabetic order.

NIBIO
NORWEGIAN INSTITUTE OF
BIOECONOMY RESEARCH

Postboks 115
NO-1431 Ås, Norway
+47 40 60 41 00
www.nibio.no

Norwegian University
of Life Sciences

Postboks 5003
NO-1432 Ås, Norway
+47 67 23 00 00
www.nmbu.no